MONASH University

The Role of PRMT5 in Acute Myeloid Leukaemia

Andrej Terzic

A thesis submitted for the degree of Doctor of Philosophy at
Monash University in 2020

Central Clinical School
Australia Centre for Blood Diseases
Melbourne, Australia

Copyright notice

© Andrej Terzic (2020).

I certify that I have made all reasonable efforts to secure copyright permissions for third-party content included in this thesis and have not knowingly added copyright content to my work without the owner's permission.

Abstract

Haematopoiesis is a process that is responsible for the formation of all the various blood cells of the body. In leukaemia, there is a dysfunction in haematopoiesis that causes the accumulation of more immature, progenitor like cells in patients. Acute myeloid leukaemia (AML) is a heterogenous and devastating disease that is considered the most common haematological malignancy in adults. With the development of sophisticated sequencing techniques, we are starting to understand the genetic landscape that underpins this disease. With this understanding is a drive for researchers to find more targeted therapies against AML, as current treatments that are often associated with high toxicity and low efficacy leave much to be desired.

Protein arginine methyltransferase 5 (or PRMT5) is a methyltransferase that is responsible for methylating arginine residues on histone and non-histone proteins. Research has found that PRMT5 is crucial in a plethora of important cellular processes. It is known that PRMT5 is required for haematopoiesis, and literature also suggests that PRMT5 might be more highly expressed in stem and progenitor cells as compared to mature haematopoietic cells. PRMT5 is also known to play roles in many cancers. PRMT5 has also been implicated in AML, but more work is needed to elucidate the true role of PRMT5 in this disease.

Throughout this project, we aimed to assess the effect of enforced PRMT5 expression in haematopoiesis in an *in vivo* transgenic mouse model. We found that this endeavour was complicated, and that overexpression may rely on overexpressing the critical PRMT5 co-factor: MEP50. We also aimed to assess the functional relevance of different domains in PRMT5 through the use of PRMT5 mutants. We found that, interestingly, a mutation in the inhibitor binding pocket grants resistance abilities to cells when they are treated with a potent inhibitor of PRMT5.

The final objective of the project was to utilise the PRMT5 inhibitor in a whole genome CRISPR screen in a leukaemic cell line. This was performed with the hopes of identifying genes that may be important in resistance and sensitivity to PRMT5 inhibition. We were able to validate the screen in the context of wild type p53 cells,

and the hits that were generated by the screen allowed us to design a high throughput drug screen assay with compounds that were rationally selected. This drug screen identified a number of compounds that synergise with PRMT5 inhibition.

Ultimately, the results from this thesis demonstrate that although enforced expression of PRMT5 with the aim of understanding its role in haematopoiesis is an endeavour that requires more study, PRMT5 remains an attractive target for potential treatment in AML. Because monotherapies are often associated with low clinical efficacy, PRMT5 should be further investigated as a potential treatment in combination with other targeted therapies.

Declaration

This thesis is an original work of my research and contains no material which has been accepted for the award of any other degree or diploma at any university or equivalent institution and that, to the best of my knowledge and belief, this thesis contains no material previously published or written by another person, except where due reference is made in the text of the thesis.

Andrej Terzic

09/06/2020

Acknowledgements

To my supervisor, Prof. David Curtis, with never ending gratitude I want to thank you for taking me onboard as a bewildered Honours student in 2015. Amongst the trials and tribulations of the PhD process and whatever happens beyond, I will never underestimate the impact you had on my growing confidence in my scientific capabilities. I thank you for all the support you gave me throughout my honours and PhD studies.

To all the other lab members of the Curtis group, past and present, I consider myself lucky to be surrounded by people such as yourselves at work. You have each, in some way or another, played a pivotal part in my PhD journey. I want to especially thank Emma Toulmin, Cedric Tremblay, and Christina Makhlouf – I would be lost without your constant scientific input. To me, you three personify the finest and most exciting part of the science field, the part that thrives on collaboration and sharing.

To my close friends – thank you for supporting me and for dealing with my lack of contact over the last few months. I promise I will make up for it now that I have a chance to.

To my sister, Tijana, whom which spending time with always feels like an escape from the stress, and my nieces, Allegra and Alexia. I can only hope for more free time in order to spend it with you three. I love you three immensely.

To my parents, Ranka and Suad. I could have filled all the pages of this thesis with acknowledgments for you two. You have only ever put Tijana and I first. I cannot imagine what it would be like to migrate from a war-torn country at my age, yet you two did just that with two children in tow. It goes without saying that you two keep me afloat, and I love you dearly. Thank you for everything.

Table of Contents

List of Abbreviations

4OHT	4-hydroxytamoxifen
aDMR	Asymmetrically dimethylated arginines
AML	Acute myeloid leukaemia
ATRA	All trans retinoic acid
CRISPR	Clustered regularly interspaced palindromic repeats
dH2O	Distilled water
DMEM	Dulbecco's Modified Eagle's Medium
DMSO	Dimethyl sulfoxide
DNA	Deoxyribonucleic acid
E	Embyronic day
eGFP	Enhanced green fluorescent protein
EtOH	Ethanol
EV	Empty vector
FACS	Fluorescence activated cell sorting
FCS	Fetal calf serum
FL	Fetal liver
FSC	Forward scatter
GeCKO	Genome scale CRISPR knock out library
HSC	Haematopoietic stem cells
HSPC	Haematopoietic stem and progenitor cell
IMDM	Iscove Modified Dulbecco Media
LK	Lin- Sca1- Kit+ cells
LSC	Leukaemic stem cell
LSK	Lin- Sca1+ Kit+ cells
MaGECK	Model based analysis of genome wide CRISPR-Cas9 knockout
MDS	Myelodysplastic syndrome
MMA	Monomethyl arginine
MOI	Multiplicity of infection
MTA	Methylthioadenosine
MW	Molecular weight
NGS	Next generation sequencing
NHL	Non Hodgkin’s lymphoma
PB	Peripheral blood
PBS	Phosphate-buffered saline
PKDM	Protein lysine demethylases
PRMT	Protein arginine methyltransferase
qRT-PCR	Real time quantitative reverse transcriptase PCR
RBC	Red blood cell
RNA	Ribonucleic acid
SAM	S-adenosylmethionine
sDMR	Symmetrically dimethylated arginines
sgRNA	Single guide RNA
TPO	Thrombopoietic

ug	Microgram
uL	Microlitre
uM	Micromolar
WB	Western blot
WBC	White blood cell

Chapter 1:

Introduction

1.1 Haematopoiesis

Haematopoiesis is the process that is responsible for the formation of all haematopoietic cells of the body. The haematopoietic stem cells, or HSC, represents one of the most characterised adult stem cell, and is responsible for giving rise to all mature blood and immune cells of the body (1). Haematopoiesis is conventionally described as a hierarchical process where HSCs progressively mature through lineage restriction into distinct cell types, and this is accompanied by a loss of 'stem-cell like' properties (2). However recent literature challenges this strict hierarchical model, and haematopoietic stem and progenitor cells might display heterogeneity in their lineage potential (3). HSCs are characterised by their ability to self-renew and maintain it's population size, and although this cell type is relatively rare (1 in every 10,000 (2, 4) bone marrow cells is a HSC) they are able to generate 10^{11} – 10^{12} haematopoietic cells a day (2).

1.2 Acute Myeloid Leukaemia

Acute myeloid leukaemia, of AML, is characterised as a heterogenous, clonal disease that affects the myeloid lineage. AML involves an increase in the number of abnormal haematopoietic progenitor cells (HPCs), known as blasts, in the bone marrow (or BM) of patients. These leukaemic cells often have an underlying chromosomal translocations and/or genetic mutation/s in genes responsible for proliferation and differentiation, and this ultimately causes a differentiation block, and accumulation of these blasts. Loss of maturation potential of these HPCs is consistent with AML and typically results in some form of haematopoietic insufficiency, such as anaemia (loss of red blood cells), granulocytopenia (loss of granulocytes) and thrombocytopenia (loss of platelets) (5, 6). AML is the most common acute leukaemia in adults (7, 8). A report in 2019 that analysed cancer related statistics from 2011 – 2015 found that AML was in the top 10 cancers that presented with the worst 5-year survival rates (9). It has been reported that in Victoria, across all age groups, 5-year survival rates are 23% in men and 28% in

women (10). The median age of patients that are diagnosed with AML is between 65 – 70 years old (6, 7). A review in 2015 found that the median survival of patients >65 years, 66 – 75 and 76 – 89 was 3, 6 and 2.5 months, respectively. A mere 5% of the patients were alive 5 years after diagnosis (11).

AML is thought to arise from the clonal transformation of haematopoietic stem and progenitor cells caused by the acquisition of gene mutations and chromosomal rearrangements that ultimately lead to impairment or block of haematopoietic differentiation and a survival advantage (12, 13). A model was proposed in 2001 by Gilliland (14) in which these kinds of genetic alterations form part of a 'two-hit' model and can be clustered into two distinct groups. These are the class I mutations, which provide the proliferative and survival signals, and the class II mutations, which affect transcription factors and lead to impaired haematopoietic differentiation. To further add to the complexity of AML, massive parallel sequencing technologies have identified other groups of mutations that do not adhere to the two classes and are therefore unclassified. These mutations are thought to promote epigenetic modifications (15, 16).

1.2.1 Current and emerging treatments

Treatment options for AML have remained fairly limited over the past 50 years. The '7+3' regimen, which was initially reported in 1973 (17) which involves treatment with cytarabine for 7 days, and an anthracycline (daunorubicin for example) for 3 days, has remained the gold standard treatment over most of this period. Attempts have been made to improve this regimen. For example, alternating the dose and duration of cytarabine (18), increasing the dose of anthracycline (19) or adding agents with distinct mechanisms, such as etoposide (20). With that being said, excluding the approval of anthracycline decades ago, and all-trans retinoic acid (ATRA) for the treatment of promyelocytic leukaemia in 1995 (21), and the accelerate approval (and subsequent withdrawal 10 years later) of gemtuzumab ozogamicin in 2000 (22), no novel agents had been approved for AML.

Recently, in 2017-2018, the FDA approved 8 new drugs for AML. These are reviewed in (21) and include FLT3 inhibitors, midostaurin and venetoclax. Although these new introductions present with exciting possibilities, there are still challenges

present regarding optimal treatment sequences and drug combinations that will ensure toxicity is minimized, but efficacy is ensured.

With that being said, monotherapies are often associated with modest clinical efficacies. In cancer therapy, there is often a push for the discovery of an effective drug combination that targets multiple proteins or pathways that may be affected in the disease. This reduces the chance that a cancer will develop drug resistance when compared to treating with a monotherapy (23-25)

1.2.2 Leukaemic stem cells and downfalls of current treatments

AML is heterogenous and complex. The current standard of treatment often has very variable effects depending on the subtype of AML that the patient is suffering from. Prognostically, resistance to treatment is often correlated to the blast cytogenetics that a patient presents with. Cytogenetic studies allow the patients risk to be categorised into three categories – favourable, intermediate, or adverse. Generally, patients aged between 18 – 60 who have favourable or intermediate cytogenetic profiles achieve complete remission rates between 70 - 80% following induction therapy (26). Even with such promising statistics, only 20 – 30% of patients achieve long-term disease-free survival, and majority of the patients will die from persistent or relapsed AML.

The current therapies for AML are targeted against blast cells. These are cells that are characterised by their rapid cell cycle activity. The presence of relapse in AML is thought to be caused by the rare, but present, leukaemic stem cell (LSC) population. In order to be considered an LSC, the leukaemic cell must: a) be capable of initiating disease when transplanted into immunodeficient mice, b) be capable of self-renewal and c) can partly differentiate into non-LSC blasts that are a reflection of the original disease. The first *in vivo* identification of LSCs was reported by John Dicks group more than two decades ago (27). The group described their identification of a population of stem cells, which we know refer to as the LSC, that was able to initiate human AML in SCID mice. They identified this cell type by segregating AML cells since their expression of CD34 and CD38. Transplantation of cells from the CD34+CD38- quadrant, and only this quadrant, was able to reinitiate leukaemia, so they concluded that this quadrant must contain the LSC population. However, John

Dick and colleagues published a subsequent article in 2016 that described the detection of LSCs in all fractions of the CD34/CD38 phenotype, highlighting the need of further characterisation to determine LSC activity in specific cell marker phenotypes (28).

Although the identification of the exact origins of the LSC is still unknown, the LSC model highlights an important clinical perspective. To ensure that we treat AML effectively with the aim of preventing relapse, we have to utilise treatments that will eradicate this LSC population (29). We now know that LSCs are able to self-renew, are quiescent, have the capability to resist apoptosis and have a higher level of drug efflux. All of this combined, even though current treatments are effective at targeting bulk blast populations, they are simply ineffective against targeting LSCs (30).

DNA methylation profiling has shed light on the potential role that the epigenetic landscape may have in AML (31). This has led to the to the identification of haematopoietic stem cells (HSCs) that are considered ‘pre-leukaemic’. These cells do not have the capacity to generate leukaemia *in vivo*, but commonly contain mutations in epigenetic regulator genes that may behave like early driver mutations (32, 33). This raises the question of whether we should be directing our research towards therapies that will target these epigenetic regulators, as it may eradicate this pre-leukaemic population of cells before they acquire additional mutations and subsequently cause leukaemia.

1.2.3 Genetic landscape of AML

Before the introduction of next-generation sequencing (NGS), much of the pathogenesis of AML was studied by cytogenetic analysis (34). This presented with its limitations, as more than half of AML patients presented with normal karyotypes (31). Due to the emergence of these new sequencing technologies, work has been conducted to try and map the AML genome in larger scale cohorts of patients (31, 35). What these studies have uncovered, is that AML is genetically heterogenous. It was found that only 23 genes were commonly mutated across the spectrum of samples that were sequenced (31, 35, 36). Because of these studies, common occurring mutations have now been described and are used as markers of AML both prognostically and diagnostically. These include markers such as FLT3, NPM1,

RUNX1, TP53 etc.). Collectively, the use of NGS and the uncovering of the genetic landscape of AML has increased our understanding of the pathogenesis of the disease.

1.3 Epigenetics

Epigenetics was first described in 1939 by C.H. Waddington (37) and explains how monozygotic twins or cloned animals can have different phenotypes despite carrying identical DNA sequences (38, 39). Epigenetic changes are heritable and reversible changes that affect gene expression that occur independently to alterations in DNA sequence. Epigenetic mechanisms play crucial roles in both physiological processes in normal cells, as well as cells in a cancerous state. These changes are modulated by common epigenetic processes such as DNA modification, histone modification, non-coding RNA regulation, chromatin remodelling and RNA modification. Some of the physiological processes that epigenetics plays a crucial role in includes imprinting, cellular differentiation and large scale silencing (such as X inactivation)(40).

1.3.1 Chromatin Remodelling and Gene Expression

Within an organism, DNA is processed and expressed differentially between different cell types that contain identical genomic DNA. This is driven by a nucleosome – a molecular scaffold that consists of DNA and protein. Within individual nucleosomes, 147 base pairs of DNA wrap around 8 positively charged proteins, known as histones. Within each histone exists two copies of histone proteins H2A, H2B, H3 and H4. These nucleosomes are further condensed into higher-order structures referred to as chromatin (41). Epigenetic events play a very key role in regulating the condensation state of chromatin. DNA is normally tightly condensed around histones and forms what is known as heterochromatin. Genes are transcriptionally inactive in this state. When gene expression needs to take place, chromatin ‘opens’ to form euchromatin, and this chromatin remodelling can occur at a local level (affecting the expression of a single gene) and a more global level (this can affect the accessibility of whole chromosome domains) (42). Chromatin can be remodelled by a number of epigenetic events, including DNA

methylation and post-translational modification of histone proteins (43). Histones an be modified on their free N-terminal tails through chemical modifications, including methylation (methylation is further discussed in section 1.4.3)(44).

1.3.2 The Relationship Between Epigenetics and AML

The sequencing of AML patients has revealed that, in a large proportion of AML patients, there are recurrent mutations that are present in genes that are involved in epigenetic regulation. However, literature has shown that, within AML, epigenetic dysregulation cannot be explained by recurrent somatic mutations alone. A good example to highlight this is that genome wide patterns of DNA methylation that are dysregulated can be present in AML cases that do not correlate with somatic mutations in known epigenetic modifiers (45). Furthermore, there have been reports of alterations in enhancer elements that have been shown to perturb normal gene expression regulation (46). A review by Wouters et al. (47) describes the role of epigenetics, and how this can be used in various epigenetic therapies in AML. Interestingly, as most epigenetic modifications are reversible, epigenetic pathways that are functionally aberrant in AML can potentially make for attractive therapeutic targets. Specific inhibitors already exist that can target proteins that drive/maintain DNA methylation and inhibitors of histone-modifying proteins and more. As research has shown that mutations and alterations of epigenetic genes are usually not enough to cause overt acute leukaemia, but may contribute to a pre-leukaemic cell state, this may suggest that these underlying mutations/alterations are present in early clones and supports the targeting of these abnormalities in the hopes of circumventing disease (48).

1.3.3 Post-translational modifications

Protein-protein interactions can be controlled by various means, for example by gene transcription, translation or by the structure of the protein itself that is determined primarily by its underlying gene sequence. Another way in which these interactions can be controlled is via post-translational modifications (or PTMs). Several common PTMs include methylation, phosphorylation, ubiquitination, acetylation and glycosylation. Our understanding of the epigenetic landscape has

increased over the last decade, and research has shown that the proteome – or the total collection of proteins with a cell (49) – is heavily regulated by PTMs. PTMs can cause several changes to a protein, such as cleavage of the backbone, modification of amino acids or the addition of chemical groups. These modifications can ultimately cause a change in where the protein is localised in a cell, its structure, or how a protein will interact with other proteins. These processes mean that a relatively small collection of proteins within a cell can elicit a much greater number of functions due to PTMs. Essentially this acts to increase the proteomes functional capabilities.

15 amino acids are capable of being modified, and these modifications occur by enzymatic reactions. There are several enzymes that are capable of causing modifications to the proteome, and this can be driven by the addition or removal of functional groups. These groups are defined in relation to the partner substrate or enzyme that they rely on: methylation relies on S-adenosylmethionine (SAM), phosphorylation relies on ATP and acetylation relies on acetyl CoA (50). Importantly, removal of functional groups allows PTMs to display reversibility. This results in an added layer of complexity to the proteome, as this PTM plasticity allows for the rapid response to specific stimuli. For example, PTM reversibility can assist in the formation or dissociation of protein complexes (51).

1.3.4 Methylation

Methylation has been recognised as a widespread PTM that plays a role in many cellular processes. Two residues that are common methylated include arginine (Arg) and lysine (Lys) residues (52). Methylation of lysine residues is driven by protein lysine methyltransferases (of PKMTs). The majority of these PKMTs possess a conserved catalytic domain, known as the SET domain (53). Within the lysine methylation system, different PKMTs can drive the mono-, di- or tri-methylation of lysine residues on various histone and non-histone targets (54). Conversely, methylation of arginine residues is driven by protein arginine methyltransferases (or PRMTs), and arginine residues on histone and non-histone proteins can drive mono-, asymmetric di- or symmetric di-methylation of arginine residues (55). It is well known that methylation of lysine and arginine residues by these methyltransferases is important for physiological processes (56, 57), but research is starting the roles

that PKMTs and PRMTs might have in disease, as they have been found to be associated with various diseases, including cancer (58).

As mentioned in the previous section, methylation is a reversible modification. In the case of PKMTs, this lysine demethylation is driven by protein lysine demethylases (PKDMs). The first reported histone PKDM was lysine specific demethylase 1 (LSD1), however, it was found that this demethylase could only demethylate mono- or di-methylated lysines (59). A second family of enzymes was subsequently discovered, known as the Jumonji C-domain containing proteins (JmjC), and it was found that this family was capable of demethylation of mono-, di- and tri-methylated lysines (60). In the case of the reversal of arginine methylation (via PRMTs), until recently, it was unknown whether methylated arginine residues could be demethylated (61). In 2016, a study published by Walport et al. (62) reported that, other than being able to act as a lysine demethylase, a subset of the JmjC PKDMs (including KDM3A, KDM4E and KDM5C) could also cause the demethylation of mono-, symmetric di- and asymmetric di-methyl arginine residues. Because the literature suggests that the enzymatic events that underlie demethylation are similar to lysine demethylation, it would suggest that other JmjC proteins could also demethylate methylarginines. However, as this is a recently new discovery, more research is needed to functionally understand these dual PKDM/PRDM *in vivo*, and whether there is any interplay between their activities (63).

1.3.5 Arginine methylation

Out of all the amino acids, arginine is known to have the longest side chain which contains a positively charged guanidinium group, and therefore, carries a net positive charge. This side chain contains two hydrogen bond donors that allow arginine to interact with hydrogen bond acceptor molecules and that have a negative charge. This can include DNA, RNA and proteins (64). When an arginine is methylated, methyl groups replace the available hydrogen atoms, and results in the removal of a potential hydrogen bond donor (65). As mentioned in the previous section, these methyl groups can be incorporated in three different ways. Monomethyl arginine, or MMA, is the result of one methyl group being added to one of the terminal nitrogen atoms or the arginine. Dimethyl arginine can be formed in either a symmetric or asymmetric function. In symmetric dimethylated arginines

(sDMR), there is a methyl group placed on each of the nitrogen atoms present on the terminal end of the arginine; and in asymmetric dimethyl arginines (aDMR), there are two methyl groups that are both present on only one of the nitrogen atoms (57). All 3 of these forms are catalysed by PRMTs (Fig 1.1).

1.3.6 Protein arginine methyltransferases (PRMTs)

As mentioned previously, PRMTs are responsible for a common PTM that involves the addition of a methyl group onto arginine residues of a protein or histone. They do this by transferring a methyl group from a SAM co-factor to the guanidinium group of the side chain present on the arginine (66). Generally, it is believed that there are 9 human PRMTs that are able to methylate the guanidine nitrogen atoms on arginine residues, however, as literature suggests that there may be a number of putative methyltransferases, this number may increase (66, 67). The commonly described PRMTs can be divided into three distinct families based on how they catalyse the addition of the methyl groups on the arginine residues. Type I, II and III. All types are able to catalyse monomethylation of arginine residues, with the following representing the differences between the families:

- Type I PRMTs, which include PRMT1 (the major Type I enzyme), PRMT2, PRMT3, PRMT4 (also referred to as CARM1), PRMT6 and PRMT8 can additionally asymmetrically dimethylate the arginine residues on their targets.

- The major type II PRMT, known as PRMT5, can additionally symmetrically dimethylate arginine residues. Recently PRMT9, somewhat controversially, has been described as having symmetric dimethylation capabilities alongside PRMT5 (68, 69). However, it is important to note that although PRMT9 has been identified as being able to catalyse sDMR methylation marks, majority of the sDMR modifications that are deposited on target histones and proteins is elicited by PRMT5 (69). Research over the last few years has only identified a couple of targets of PRMT9, including splicing factors SAP145 (68) and SF3B2 (69) and further research is needed to elicit to what extent it is considered a type II PRMT. The diverse number of PRMT5 targets that exist, and the importance of the protein in development and in haematopoiesis will be described in subsequent sections.

- The remaining PRMT, PRMT7, was thought to have type II enzymatic activity, however recent data has concluded that PRMT7 is a type III PRMT and is only able to catalyse monomethyl arginine residues (70).

In terms of sequence, all PRMTs contain a highly conserved core region that elicits catalytic activity. These core regions contain the signature methyltransferase motifs I, post-I, II and III. Motif I is responsible for facilitating SAM binding, and it contains the double-E loop, which consists of two glutamate residues. The location of the sulphur atom of SAM and this pair of invariant glutamate residues constitutes the active site of PRMT5 (71). At the C-terminus of the core region exists the threonine-histidine-tryptophan (or THW) loop. This loop contains the most highly conserved sequence of the domain. These sequences are responsible for arranging the methyltransferase active site in all the PRMTs (57). It is important to note that the structure of the catalytic core also shows a high level of conservation, particularly between PRMT1, PRMT3, PRMT4 and PRMT5 (71-76) (Fig. 1.2).

PRMTs have gained significant traction in recent literature due to the discovery of their complex roles in signal transduction, both activation and repression of several transcriptional processes, embryonic development, and differentiation. They have also been shown to be deregulated in multiple human diseases, with different PRMT family members being reported as playing roles in several cancer types (61).

1.4 Protein Arginine Methyltransferase 5 (PRMT5)

As mentioned, PRMT5 is the major type II methyltransferase. It was described two decades ago as a protein that interacted with the chloride conductance regulatory protein, known as pICln (77). In 1999, PRMT5 was described as a Jak2 binding protein. Furthermore, it was found to have methyltransferase functionality, and three of its substrates were identified – histone H4, histone H2A and myelin basic protein (MBP) (78). Branscombe et al. (79) subsequently published the finding that, through biochemical characterisation, PRMT5 could enzymatically form sDMR. PRMT5 was now described as the first enzyme of this type. Interestingly, it is believed that PRMT5 has a critical role in biology, as it's protein has been conserved all the way from yeast to humans throughout speciation (77, 79, 80). PRMT5 has a critical co-factor known as the methylosome protein 50 (or MEP50) that is absolutely

required for methyltransferase activity, and these proteins are found in complex, the structure of which will be described in the next section [72]. PRMT5 is responsible for the symmetric dimethylation of arginine residues on many substrates, of which two important ones are histone H4 arginine 3 (H4R3) and histone H3 arginine 8 (H4R8) (81).

1.4.1 PRMT5 structure

The domain architecture of human PRMTs has been described. All human PRMTs contain a catalytic core, that is composed of a Rossman fold (conserved of consecutive alternating β-strands and α β-sheet with one or two layers of α-helices)(82). Cofactor binding - and in the case of PRMT5, specifically SAM – occurs in this domain. PRMTs also contain a β-barrel, and this is conversely where substrate binding occurs (66).

In 2011, Sun et al. aimed to elucidate the enzymatic mechanisms by which sDMR and aDMR modifications differed, as they were isometric, but were thought to be functionally contradictory to each other. Determining the crystal structure of PRMT5 from *C. elegans,* the group found that PRMT5 dimerization was driven by domains that were found between the TIM-barrel and the β-barrel (71). The group suggested that human PRMT5 would also dimerize for three reasons: (i) there was extensive conservation of amino acids between human and *C. elegans* PRMT5, (ii) a previous study that had described not only dimeric, but also oligomeric forms of human PRMT5 (83) and (iii) the fact that all previous arginine methyltransferase structure studies had found that the respective methyltransferase dimerized via a 'dimerization-arm' (75, 76, 84).

However, limited information existed on PRMT5's structural interaction with MEP50. This was the focus of a study published in 2012 by Antomysamy et al. (85). Utilising chromatography, sedimentation analysis, enzymology and X-ray crystallography, the group was able to structurally characterise the PRMT5:MEP50 complex, along with the complex bound to an AdoMet analogue and a histone H4 substrate. Contrary to the *C. elegans* PRMT5 data that was published in the study mentioned above, it was found that PRMT5 binds MEP50 to form a $(PRMT5)_4(MEP50)_4$ hetero-octameric complex (Figure 1.3) (85). The group concluded that this $(PRMT5)_4(MEP50)_4$

component was likely to represent the main structural unit that interacted with the various partner proteins to form the numerous complexes that are associated with different biological functions.

1.4.2 Mutant PRMT5 – A Tool for Studying Domain Function

Over the years, mutational studies have identified important features in the sequence of the PRMT5, some of which will be described in this section. One of the first mutant PRMT5s to be reported on was a PRMT5 mutant that was catalytically inactive. That is, it was unable to catalyse sDMR marks on its substrates. Pal et al. published the results of a study that utilised a mutant form of PRMT5 that contained 2 amino acid changes. G367A and R368A. They found that this mutant PRMT5 was not able to methylate H3 and H4 histones (86). The specifics of how this occur are unclear in the literature, but based on the domain structure of PRMT5, this mutation would occur in the catalytic Rossman fold. Considering that the double-E loop is found in positions 435 and 444, the mutations responsible for the methylation dead mutant might confer a conformational change in this domain that prevents PRMT5 from eliciting it's function.

Another mutant that has recently been properly described is a mutant PRMT5 that is able to catalyse both sDMR and aDMR marks (and therefore act as a dual type I and II PRMT). The mutation that is responsible for this gain of function is a point mutation in the phenylalanine at position 327 being converted to a methionine (F327M). This mutant PRMT5 was found to be able to symmetrically and asymmetrically dimethylate H4R3, and it was proposed that this was due to the methionine resulting in more conformational flexibility, which had been seen in PRMT1 and PRMT4 (both type I PRMTs) (71).

1.4.3 Major roles of PRMT5

As the major type II enzyme that can catalyse sDMR marks on arginine residues, PRMT5 has a myriad of targets, and therefore functions, within the cell. PRMT5 can methylate both histone (H4, H3 and H2A) and non-histone proteins. Some of its non-histone substrates include ribosomal nucloelin, p53, NF-kB, p65, HOXA9, E2F1, MBD2, EGFR, CRAF, SREBP1a and many more (reviewed in (85)).

In terms of biological processes, PRMT5 is involved in transcriptional regulation (87), mRNA splicing (88), ribosomal biogenesis (89), the formation of the Golgi apparatus (90) and more. PRMT5 has been shown to be important in development and haematopoiesis and has been implicated as a potential oncogenic influence in both solid and haematological cancers.

1.4.4 PRMT5 in Development

PRMT5 has been shown to be important in both early and late development pathways. It is well known that *Prmt5-/-* murine embryos are unable to produce embryonic stem (or ES) cells and suffer early embryonic lethality. Furthermore, RNAi against PRMT5 in ES cells has shown that, following knockdown of PRMT5, there is an up-regulation of differentiation associated genes (91). This supports the consensus that PRMT5 is required in stem cells for the maintenance of a stem-cell like phenotype. PRMT5 is also known to play a role in primordial germ cell differentiation, as it's known to methylates Piwi proteins. Piwi proteins interact with small-non coding RNAs, known as piRNAs, of which the downstream effect is gene silencing – a process that is required for normal gametogenesis (92). It is also known that PRMT5 is an important player in keratinocyte differentiation. Gene expression of involucrin is partially controlled by the suppression of PRMT5 (by PKC- δ)(93).

1.4.5 PRMT5 in Haematopoiesis

When interrogating mRNA expression data in normal haematopoiesis on Bloodspot, stem and progenitor cells appear to have higher expression levels of PRMT5. These expression levels reduce as cells mature (Fig. 1.4) (94).

In 2016, Liu et al. published the results of a study that assessed the importance of PRMT5 in normal adult haematopoiesis, an area which had not been studied. They found that *Prmt5* mRNA was relatively unchanged between the different subsets of stem and progenitor cells but appeared to be reduced in more mature cells (except for B cells). Interestingly, at the protein level, all mature cell types, including B cells, presented with 5 – 24% of the PRMT5 protein as compared to the stem and progenitor cells. This suggested that there were important post translational mechanisms that controlled the expression of PRMT5 in these cells (95).

Having confirmed that stem and progenitor cells in haematopoiesis seemed to rely on PRMT5 protein, the group developed a murine MxCre conditional knockout model of *Prmt5*. They showed that in MxCre^{+} PRMT5$^{fl/fl}$ mice that were treated with poly(I:C) and found the complete loss of methyltransferase activity 7 days after the induction of Cre. Most of the mice presented with anaemia and had to be culled just 2 weeks after Cre induction. Analysis of the mice found that the peripheral blood results reflected pancytopenia. There was a 5-fold decrease in the red blood cells, more than a 10-fold decrease in the white blood cells and platelets were down more than 100-fold compared to normal mice. 7 days post Cre induction, the bone marrow cellularity of the mice had reduced to half, and by day 15, there was only 5% of normal cellularity. The mice also presented with aberrant erythroid differentiation. Interestingly, in terms of the haematopoietic stem and progenitor cells, initially there was an increase in the progenitor populations in mice 7 days after Cre induction, however further analysis (utilising secondary transplant experiments) found that these HSPCs were non-functional. By day 9, even the levels of the HSPCs were dramatically reduced (95).

As a result of this study, some light has been shed on the potential role of PRMT5 in haematopoiesis, and more importantly, in stem cells. However, these findings are still preliminary, and raise some mechanistic question. The study showed that HSCs deficient in PRMT5 showed an increase in proliferation, alongside an increase in p53 activity. The group has shown in the past that p53 is required for stem cells to maintain quiescence (96). This suggests that there are other, more influential pathways that are responsible for driving the HSCs into the cell cycle. Conversely, more mature progenitor cells presented with the inverse outcome, where deletion of PRMT5 caused an impairment of proliferation in these cells. The group conclude that this opposite effect could be due to the fact that PRMT5 can be found in multiple different complexes and in different subcellular locations, and that this pleiotropic effect might be cell specific, however, more research is needed to understand the mechanistic details underlying these responses.

1.4.6 PRMT5 in Cancer

PRMT5 overexpression is thought to be associated with many different types of cancer. In terms of solid cancer, PRMT5 overexpression has been described in gastric cancer (97), gliomas (98), ovarian cancer (99) and lung cancer (100) to name a few. The studies have found that this overexpression is associated with promoted tumour growth and poor prognosis. Literature has suggested ways in which PRMT5 can be upregulated in a cancer state. One of the mechanisms might involve the nuclear transcription factor Y, or NF-Y, which is responsible for the upregulation of oncogenes in several cancer. It is believed that NF-Y is capable of binding to the proximal promoter of PRMT5 (101). Another potential mechanism of PRMT5 overexpression might be driven through the proto-oncogene Myc. Myc has been shown to upregulate PRMT5 and core small nuclear ribonucleoprotein transcriptional activity – these are both implicated in pre-mRNA splicing. PRMT5 is downregulated alongside Myc downregulation, and this leads to aberrant splicing. This causes an increase in apoptosis and reduced tumorigenic potential in haematological malignancies. Although this has been shown in lymphomagenesis (102), the findings may represent a more overall dysfunction of PRMT5 regulation due to overexpression of Myc, as Myc is found in many different cancer types (103).

1.4.7 PRMT5 in Haematological Malignancies

PRMT5 has been found to be involved in several haematological malignancies (104). One of the first studies that looked focused on lymphomagenesis. It was found that PRMT5 protein levels are upregulated in B-cell chronic lymphoid leukaemia (B-CLL) cell lines, as well as in primary lymphoma patient samples (105). It was proposed that this was due to a dysfunction in the physiological regulation of PRMT5 by various miRNAs (106).

A study in 2015 described PRMT5 as being required for lymphomagenesis that is driven by multiple oncogenic drivers. Two key pieces of evidence supported this idea: a) that the expression of oncogenic drivers Notch1, MLL-AF9 and Myc resulted in an upregulation of PRMT5 and b) that transplant experiments utilising *Prmt5* knockdown or deletion suggested that there was a strong selective pressure for the maintenance of cells that did not undergo knockdown or deletion of PRMT5.

Furthermore, the results of a study that assessed the clinical potential of a PRMT5 inhibitor in mantle cell lymphoma (MCL) supported the idea that PRMT5 is important in lymphomagenesis (107).

Although the role of PRMT5 was extensively studied in the context of lymphomagenesis, it wasn't until recently that research was published in relation to the role of PRMT5 in myeloid malignancies. It was found that in chronic myelogenous leukaemia (or CML), *Prmt5* mRNA and protein levels were found to also be elevated in CD34+ cells harvested from CML patient samples as opposed to normal bone marrow controls samples. This result paved the way for also assessing a PRMT5 inhibitor in the context of CML (108).

1.4.8 PRMT5 in AML

The potential contribution of PRMT5 to AML leukaemogenesis is still unclear. To date, only a handful of publications have focused on elucidating the role of PRMT5 in AML. In 2016, Tarighat et al. (109) published the results of a study that found that PRMT5 could contribute to AML through a complex miRNA-protein regulatory network that controls both gene activation and repression. Mice that were injected with THP-1 cells – a human acute monocytic leukaemia cell line (110) - that lentivirally overexpressed PRMT5 displayed promoted leukaemogenesis (including shorter time of onset) as compared to controls, providing evidence that PRMT5 overexpression could potentially promote leukaemia. The group further described potential mechanisms behind this promoted leukaemogenesis and concluded that increased PRMT5 levels were able to suppress miR-29b expression via methylation of H4R3 histones at it's promoter region. This in turn caused an upregulation in downstream *Sp1* - a zinc finger transcription factor that recognises GC-rich motifs in many promoters (111) - that led to an increase in the transcriptional activity of Sp1 at the FLT3 promoter and 3-fold increase in FLT3 expression. As a result, this led to enhanced growth and survival of cells (109).

A 2018 publication by Serio et al. (112) focused on the regulation of the *Prmt5* gene by the PAF complex in MLL fusion leukaemias. Previous literature has shown that the polymerase-associated factor complex (or PAFc) is essential for proliferation in AML (mainly focusing on MLL-translocation associated AML (113)) and other

cancers (114, 115) The group performed RNA-sequencing on murine derived MLL-AF9 cells that harboured a conditional knockout of a critical subunit of PAFc (known as *Cdc73*) and compared it to control MLL-AF9 cells. Their results implicated the *Prmt5* gene, along with other PRMTs, as direct transcriptional targets of PAFc, and found that knocking out *Cdc73* caused a significant downregulation of *Prmt5*. Importantly, they also found that almost all *Prmt* genes were upregulated in murine MLL-AF9 cells (as compared to normal murine lin^- $c\text{-}kit^+$ progenitor bone marrow cells), and *Prmt5* showed the greatest increase in leukaemic cells (almost a 2-fold increase in *Prmt5* RPKM)(112).

Kaushik et al. (116) also published a paper in 2018 that aimed to assess the clinical potential of a small molecule inhibitor of PRMT5 in MLL-rearranged AML. Aside from the clinical assessment of the inhibitor, the group performed an experiment that involved MLL-AF9 cells harbouring a conditional knockout of *Prmt5*. Sub-lethally irradiated recipient mice were injected with fetal liver cells harvested from either $Mx1Cre^-$ $PRMT5^{fl/fl}$ control or $Mx1Cre^+$ $PRMT5^{fl/fl}$ mice (conditional knockout is driven by treatment with polyinosinic:polycyctidylic acid – or poly:IC), both of which were transduced with *MLL-AF9*. The mice in the control group died of AML in less than 90 days. However, the mice that received the leukaemic cells that contained a knockout of *Prmt5* showed a significantly prolonged leukaemia onset. The group suggested that the leukaemia that did develop in the latter mice were due to leukaemic cells that failed to delete PRMT5 and concluded that PRMT5 was required for the initiation and maintenance of MLL-rearranged leukaemias.

In light of a number of publications over the last few years, the importance of PRMT5 in AML has become clearer. However, whether the protein can behave as a driver of AML in and of itself or in partnership with other oncogenes, or whether it is simply a reflection of the disease state is still relatively unknown.

1.5 Clinical Potential of PRMT5 Inhibition

As PRMT5 (as well as other PRMTs) has been implicated in various cancers to date, interest in developing inhibitors against PRMT5 has significantly increased in the last several years, with several inhibitors already developed. Within the solid cancer field, assessing PRMT5 as a candidate therapeutic target has been assessed

in cancer such as lung cancer (117, 118), breast cancer (119), colorectal cancer (120), gastric cancer (121), glioblastoma (122) and neuroblastoma (123), and has shown that inhibition presents with some clinical efficacy.

1.5.2 PRMT5 Inhibition in Haematological Malignancies

The clinical potential of PRMT5 inhibition has also been somewhat studied within haematological malignancies. This includes studies both focusing on knockdown and chemical inhibition of PRMT5 with a small molecule inhibitor. In 2013, a publication by Chung et al. (124) found that, in models of lymphoma, shRNA mediated PRMT5 knockdown was shown to lead to RB1 reactivation, which caused an inhibition of downstream PRC2 and subsequent upregulation (through a derepression mechanism) of its downstream target gene, many of which are involved in pro-apoptotic processes. This knockdown was conducted *in vitro* in Non-Hodgkin's lymphoma cell lines and in murine lymphoma primary cell samples and resulted in an inhibition of cell growth and the induction of cell death (124).

In 2015, Chan-Penebre et al. published one of the first publications that employed the use of a cell potent (that is, an IC_{50} in the nanomolar range), orally bioavailable small molecule inhibitor of PRMT5. To date, most publications that had published results using PRMT5 inhibitor compounds had failed to correlate a phenotypic result to a reduction in a PRMT5 specific methyl mark (such as H4R3me2s). The group showed that you could induce antitumour activity in MCL cell lines and xenograft models with oral dosing of a PRMT5 inhibitor known as EPZ015666, and they could correlate this result to a dose-dependent decrease in levels of symmetrically dimethylated PRMT5 substrates following treatment (such as SmD3me2s) (107)

The efficacy of PRMT5 inhibition in CML was also interrogated in a publication by Jin et al. in 2016 (108). The group utilised both a PRMT5 knockdown approach as well as the use of a small molecule inhibitor, and found that in both cases, PRMT5 inhibition could cause an induction of apoptosis in CML cells both *in vitro* and *in vivo* models of CML. They also analysed the effect that PRMT5 knockdown had on the LSC repopulation capability by performing secondary transplants into irradiated mice, and found that knockdown of PRMT5 led to prolonged survival, providing

evidence that PRMT5 inhibition may be effective strategy for targeting leukaemia stem cells (108).

In AML, the results of several studies also seem to suggest that PRMT5 may be a good treatment target. As mentioned previously, Targihat et al. not only interrogated the role of PRMT5 in leukaemogenesis, but they also found treatment of AML cell lines – MV4-11 and THP-1 – and primary patient samples with a PRMT5 inhibitor led to a decrease in cell growth and viability, however this was achieved at less than ideal micromolar ranges (the IC_{50} was calculated as being as low as 7.21μM in cell lines and 3.98μM for patient blasts) of the compound that they utilised called HLCL-61 (109). Serio et al. (112)also performed inhibitor studies using EPZ015666. *In vitro*, they demonstrated that multiple human leukaemic cell lines – U937, NB4 and MonoMac6 – were sensitive to treatment with the PRMT5 inhibitor, highlighted by a dose-dependent decrease in cell number and symmetrically dimethylated H4R3. In a mouse model of MLL-AF9, treatment with EPZ015666 compound for two weeks prolonged survival by a modest, but significant, 4.5 days. Lastly, as mentioned in the previous section, the publication by Kaushik et al. also aimed to address whether PRMT5 is required to control the differentiation block that is associated with MLL-fusion driven leukaemias. Their EPZ015666 inhibitor experiments found that if you treat mice that were transplanted with MLL-ENL/$Nras^{G12D}$ cells, leukaemia onset was once again significantly delayed, but median survival differed between the control and treatment group by only about 7 days (116).

Literature seems to suggest that PRMT5 inhibition may present as an effective target in leukaemia, including AML. However, only a handful of publications to date have aimed to address this. Many of the studies in AML have focused on MLL-fusion leukaemia's - a particularly rare subset of AMLs with a very short leukemic latency - and have found modest effects with *in vivo* treatment using a PRMT5 inhibitor. As is common with leukaemia treatment strategies, combination treatment might address this issue, as combining a PRMT5 inhibitor with another drug in a synergistic fashion may present with more desired outcomes. More work is needed to elucidate if there are other AML subtypes that may respond more favourably to PRMT5 inhibition.

With that being said, two PRMT5 inhibitors, GSK3326595 and JNJ-64619178, are currently undergoing clinical trials. GSK3326595 is undergoing a phase I clinical trial to assess its safety through a dose-escalation study. GSK3326595 is undergoing another phase II clinical trial to determine its efficacy as an oral treatment for patients with relapsed and refractory MDS, chronic myelomonocytic leukaemia and hyperproliferative AML. JNJ-64619178 is undergoing a phase I clinical trial to identify the maximum tolerated dose in subjects with relapsed/refractory B cell non-Hodgkin's lymphoma (NHL) or advanced solid tumours (125).

1.6 Project Rationale and Aims

Although data suggests that PRMT5 may be more highly expressed in primary AML bone marrow samples as compared to healthy control patients, the role that PRMT5 plays in haematopoiesis and leukaemia is uncertain. That is, whether overexpression of the protein promotes leukaemogenesis, or whether the expression is purely a reflection of the more immature cell types that are associated with the diseases. In order to address this question, this thesis will utilise mouse models of PRMT5 overexpression to view the effects that overexpression has on haematopoiesis.

Furthermore, PRMT5 is not only required for development, but is also required for sustaining adult haematopoiesis. This thesis will look to assess whether PRMT5 overexpression can rescue a knockout phenotype of PRMT5 deletion. Coupled with this, mutant variants of PRMT5 will be utilised to assess the structure-function of PRMT5 and how mutant forms of PRMT5 response to inhibition, and whether these mutant forms are also able to rescue the deletion phenotype.

Finally, *in vitro* and *in vivo* data suggests that PRMT5 inhibition may be an effective strategy in treating certain subtypes of AML. The clinical efficacy of a PRMT5 inhibition has presented with mixed results *in vivo*, and therefore combination strategies might present with better outcomes. This thesis will utilise a CRISPR knockout library with the hopes of identifying pathways that may be involved in resistance, and pathways that may cause sensitisation to treatment with a potent PRMT5 inhibitor. This data was utilised in order to perform drug combination studies.

In summary, this thesis examines the following questions:

Chapter 3: Determining the effects of PRMT5 overexpression in haematopoiesis.

Chapter 4: Examining the structure-function of key residues of PRMT5.

Chapter 5: Identifying mechanisms that confer sensitivity and resistance to PRMT5 inhibitors.

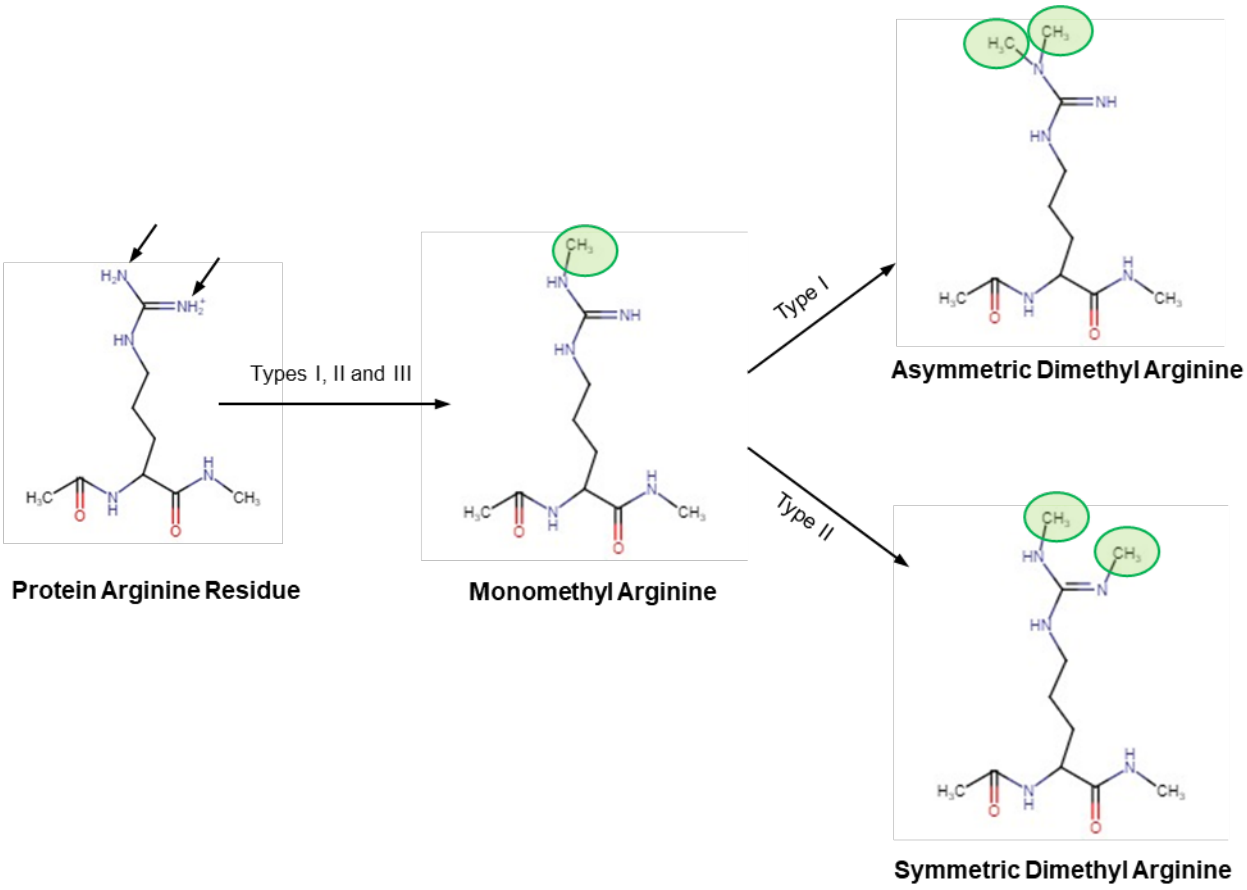

Figure 1.1 Types of mammalian protein arginine methylation. This can be categorised into type I, II and III PRMTs. All types can form monomethylate arginines, while type I can also asymmetrically dimethylate arginines, while type II can also symmetrically dimethylate arginines. Adapted from (126)

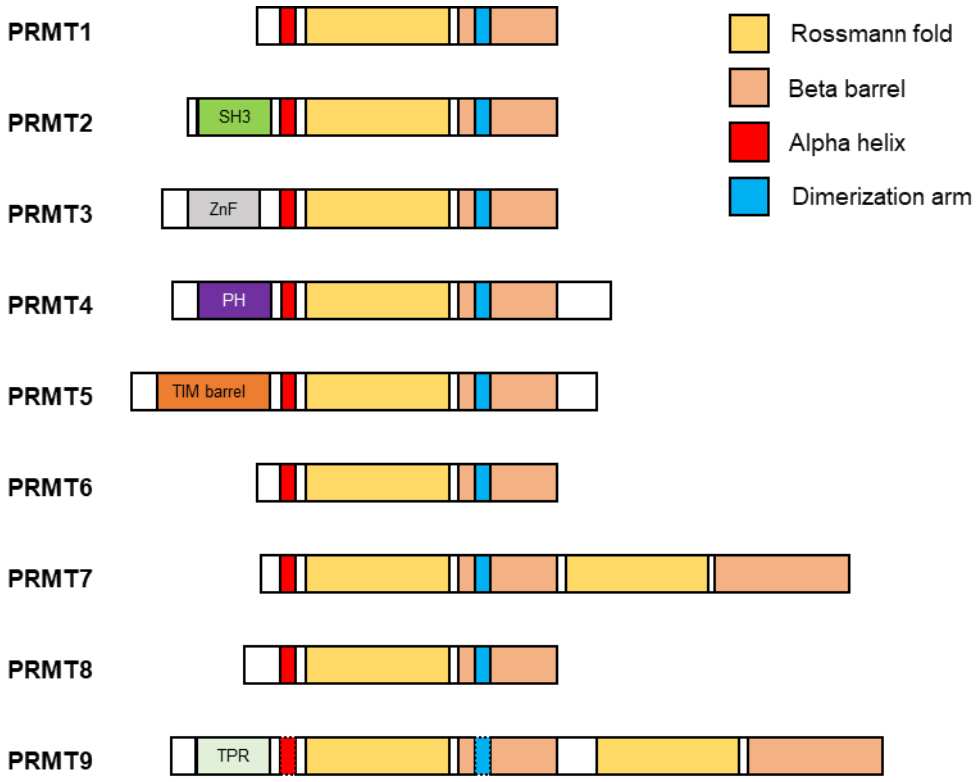

Figure 1.2 Members of the protein arginine methyltransferase family. Domains are assigned based on protein alignments within the PRMT5 family members. SH3 – SRC homology 3 domain; ZnF – Zinc finger domain; PH – Pleckstrin homology domain; TPR – Tetratricopeptide repeat. Domains that have dashed outlines in PRMT9 are based on protein alignment alone as crystal structure data is unavailable. Adapted from (127)

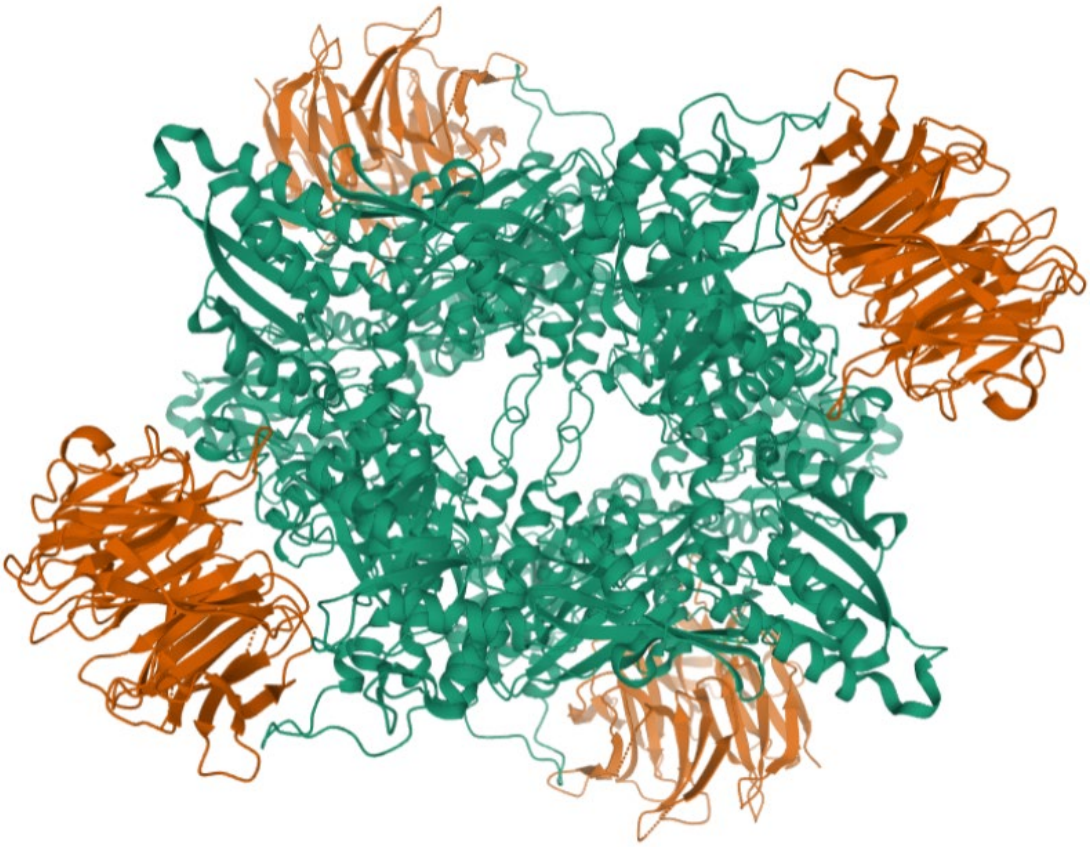

Figure 1.3 Crystal structure of PRMT5 in complex with MEP50. PRMT5 binds MEP50 to form a hetero-octomeric complex. This complex represents the main structural unit. PRMT5 is coloured green, and MEP50 is coloured orange. Figure was generated on PDB (128).

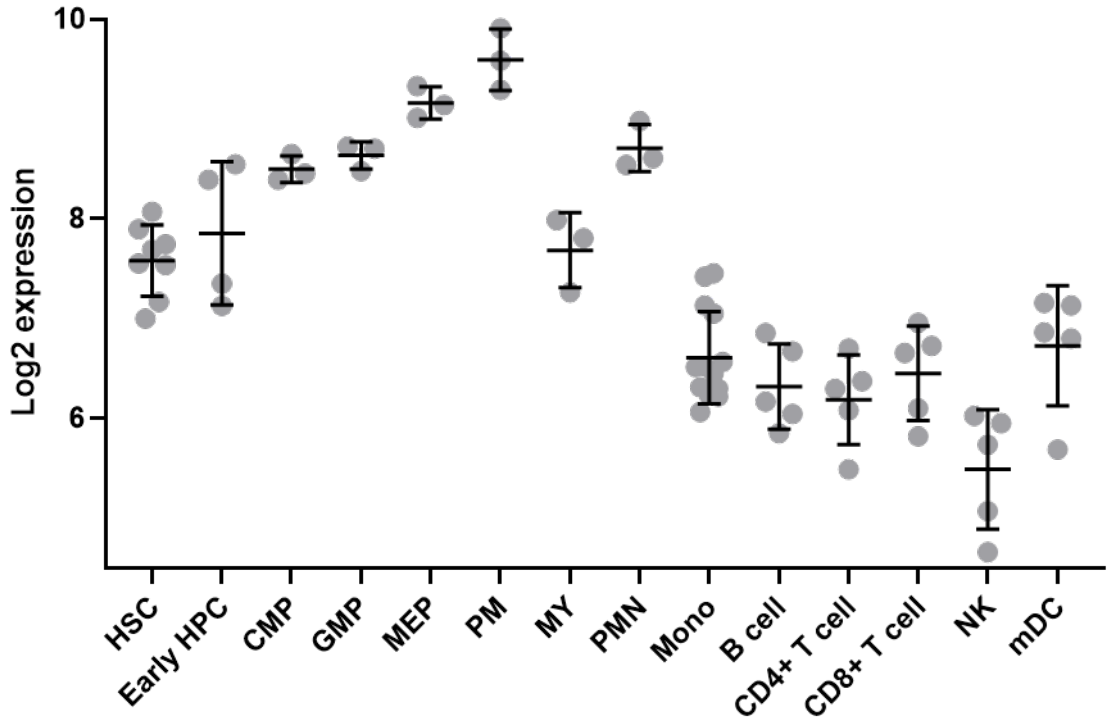

Figure 1.4 mRNA expression of PRMT5 in normal haematopoiesis. PRMT5 expression levels in different populations of cells. Generated using data from Bloodspot (94). Data is represented as mean ± SD of 3 – 14 samples. HSC – Haematopoietic stem cell, HPS – Haematopoietic progenitor cell, CMP – Common myeloid progenitor, GMP – Granulocyte monocyte progenitor, MEP – Megakaryocyte-erythroid progenitor, PM – Promyelocyte, MY – Myelocyte, PMN – Polymorphonuclear cells, NK – Natural killed cells, mDC – myeloid dendritic cells.

Chapter 2:

Methods

2.1 *In vitro* cell culture conditions

Fetal liver cells harvested from mice were cultured in StemPro34 (Gibco) with the provided supplement and 1x L-glutamine (Gibco) as well as 1% penicillin-streptomycin (Gibco). This media was also supplemented with cytokines – 10ng/mL mIL-3, 10ng/mL mIL-6, 50ng/ml hFLT-3, 50ng/mL mSCF and 50ng/mL TPO (all cytokines from PeproTech). Cells were incubated at 37°C, 10% CO_2.
MLL-ENL cells (both p53 wild type and p53 null) were cultured in Iscove's Modified Dulbecco's Medium (IMDM) (Gibco) with 10% Fetal Calf Serum (FCS) (Sigma-Aldrich), 1% penicillin-streptomycin (Gibco) and 10ng/mL mIL-3 (PeproTech). Cells were incubated at 37°C, 5% CO_2.
293T cells were cultured in Dulbecco's Modified Eagle Medium (DMEM) (Gibco) with 10% FCS (Sigma-Aldrich) and 1% penicillin-streptomycin. Cells were incubated at 37°C, 10% CO_2.

2.2 Molecular biology techniques

2.2.1 RNA extraction

5 x 10^5 – 1 x 10^6 cells were harvested, depending on the experiment. Cells were pelleted, supernatant was removed, and cells were resuspended in 1mL of TRIZOL reagent (Invitrogen). In order to extract the RNA, the samples were thawed at room temperature, and 200uL of chloroform was added to the samples. These samples were shaken vigorously for 15 seconds and were allowed to incubate at room temperature for 2-3 minutes. Samples were centrifuged (12,000 x g/15 mins/4°C) to separate the RNA into a clear aqueous phase. This aqueous phase was transferred into a fresh microcentrifuge tube containing 500uL of isopropanol and 2uL of glycogen. The contents of the tube were mixed by inversion and incubated (10 mins at room temp). The samples were centrifuged (12,000 x g/10 mins/4°C) and the supernatant was aspirated. To clean the RNA pellet, 1mL of 75% ethanol was added and the sample was vortexed to dislodge the pellet. The sample was centrifuged

(7,700 x g/5 mins/4°C). The supernatant was aspirated, and the RNA pellet was allowed to air dry at room temperature before it was resuspended in 20uL of RNase free water.

2.2.2 cDNA synthesis

To convert RNA into cDNA, the First Strand cDNA Synthesis Kit (Roche) was utilised. Using PCR tubes, 2μL of RNA was added to 1μL of 50μM anchored oligo(dT)18 primer and 10μL of RNase free H2O. This mixture was heated in a to 65°C for 5 mins and the incubated at 4OC for 1 min. To each PCR tube, 4μL 5x Transcriptor Reverse Transcriptase Reaction Buffer, 0.5μL of Protector RNase inhibitor (40U/μL), 2μL of deoxynucleotide mix (10mM each of dATP, dCTP, dGTP and dTTP) and 0.5μL of Transcriptor Reverse Transcriptase 24 (20U/μL) was added. The contents were mixed by gentle pipetting. The PCR tubes were heated to 50°C for 60 mins to maximize the activity of the reverse transcriptase, and then the enzyme was deactivated by heating the samples to 85°C for 5 mins. The cDNA was stored at -20°C.

2.2.3 Plasmid harvest

Colonies are picked and places in 3mL LB broth supplemented with ampicillin. These were incubated at 37°C overnight with gentle rocking. The next day, bacterial DNA was extracted using Qiagen QIAprep miniprep kit.

2.2.5 qRT-PCR

Analysis of mRNA expression was performed via qRT-PCR for PRMT5 cDNA was amplified from cells of interest, and then RT-PCR was performed on a Roche LightCycler 480 thermocycler. HPRT was incorporated as the housekeeping control gene. Sequence of primers is listed in Table 2.1 This was done using the TaqMan (Thermo Fisher) gene expression assay primer mix, and the reaction was set up as follows: 1uL cDNA, 1uL of primer mix, 5uL of TAQman universal PCR master mix reagent (Thermo Fisher) and 4uL of nuclease free H_2O. The RT-PCR reaction was set up according to the manufacturer's instructions – pre-incubation for 50°C for 2 minutes, denaturation at 95°C for 10 minutes, 45 amplification cycles that consist of denaturation at 95°C for 15 seconds, followed by an annealing and elongation at 60°C for 1 minute. The final extension step was 37°C for 30 seconds.

Relative transcript quantification was deduced from ΔΔCt method:

- Average Ct (PRMT5) – Average Ct (HPRT) = ΔCT
- ΔCt (test sample) – ΔCt (control sample) = ΔΔCt
- $2^{-\Delta\Delta Ct}$ = Fold change gene expression.

2.2.5 Western blot

Protein samples were prepared by washing cells twice in PBS followed by centrifugation (300 x g/5 min/room temp). Cell were lysed by adding 200uL of 1x SLAB buffer and boiling for 10 minutes. Proteins within the sample were stratified according to size using a dodecyl sulfate polyacrylamide gel electrophoresis (SDS-PAGE). This involved casting a gel that consisted of a stacking zone and a separating zone, both consisting of 10% acrylamide. First, a separating gel was cast. This was composed of 7.2mL of milli-Q H2O, 3.8mLs of separating gel buffer (375mM Tris HCL pH 8.8, 0.1% SDS), 3.76mL 40% acrylamide and 224µL 10% ammonium persulfate (APS). To induce polymerisation reaction, 10µL of tetramethylethylenediamine (TEMED) (Sigma-Aldrich) was added. This gel was then quickly poured into a 1.5mm gel plate (BIO-RAD) before setting occurred, and a thin layer of isopropanol (roughly 500µL) was added to remove any air bubbles. The gel was allowed to set for 30 mins, and then the isopropanol was washed off using distilled water (dH2O). Any excess water on the margin of the gel was soaked up using absorbent paper. A stacking gel was then prepared, consisting of 2.15mL of milli-Q H2O, 888µL of stacking gel buffer (125mM Tris HCl pH 6.8, 0.1% SDS), 450µL 40% acrylamide and 35µL 10% APS. As before, 10µL of TEMED was added to the mixture to cause polymerisation and this was poured on top of the separating gel. In order to create the wells within the stacking gel, a 1.5mm comb (BIO-RAD) was inserted directly into the gel. This was allowed to set for 30 mins.
The comb was removed from the set gel, and the gel was placed into a mini-PROTEAN tetra cell (BIO-RAD). This tank is filled with Western blot running buffer. 20uL of protein lysate is loaded into the wells and 130V is applied to the tank and the sample is allowed to run through the gel until the loading dye reaches the bottom of the gel. The gel is removed, and a transfer system is set up. This involved activating a polyvinylidene difluoride (PVDF) membrane (GE Healthcare Life Sciences) in methanol. The protein gel is transferred onto the PVDF membrane surrounded by blotting paper and sponges in a gel tank filled with Western blot transfer buffer

(voltage is run through the tank at 100V for 2 hours at 4°C). Following transfer, the membrane was removed from the transfer system, and is incubated with 5% skim milk for 60 minutes at room temp. The membrane was then washed with TBST and is then incubated with the primary antibody (diluted in TBST + 2% BSA) and is incubated overnight at 4°C.

The following day, the primary antibody solution is removed, and the blot is washed with TBST 6 times for a total of 30 minutes. The membrane is then incubated with secondary antibody (1:1000) for 60 minutes at room temp. The membranes were washed again for TBST 6 times for a total of 30 minutes, and are then incubated with 1mL of SignalFire ECL reagent (CST) for 1 minute. The membranes were then dried, and where images with the ChemiDoc imaging system (Bio-Rad).

A table of primary and secondary antibodies used throughout this chapter is provided in Table 2.2

2.3 Dose-response assays

For three-day drug treatment, MLL-ENL cells were seeded at 1 x 10^4 cells/mL. Cells were cultured in 48 well plates in a total volume of 0.5mL per replicate/dose in desired concentration of inhibitor. For 72-hour assay, cells are cultured without splitting for three days, and at 72 hours, either a cell count is obtained, or a cell death FACS is performed to quantify the proportion of live cells.

In the context of 5 days drug assays, like the ones performed when validating the CRISPR screen results, cells are seeded at 3 x 10^4 cells/mL. The cells were split at day 2 of treatment into fresh media with drug and were allowed to culture for a further 3 days. When calculating the viable cell number at the end of the experiment, the concentration of cells was multiplied by the factor of the split.

For two-week treatment, as required for 4OHT treatment in the ERT2Cre PRMT5$^{fl/fl}$ cell line, cells were split every 2 days and resuspended in fresh media.

2.4 FACS analysis and sorting

2 x 10^6 cells were washed, and aliquoted into 96 well V-bottom plates and were incubated with 10uL of FACS block (made up of 10uL of rat IgG at 1ug/uL concentration) as well as 30uL of the FACS staining solution containing the antibodies of interest. For each experiment, a unstained and a single antibody

control were utilised to ensure proper compensation on the FACS machine. Samples were incubated in the antibody solution for 25 minutes at 4°C in the dark, and where then washed twice with 150uL MT-PBS + 2% FCS and were centrifuged at 350 x g/5 mins/4°C. Samples were analysed on the LSRII. Antibodies used in FACS analysis are listed in Table 2.3.

For cell sorting, cell in suspension were pelleted and washed twice with PBS + 2% FCS. The cells were then resuspended and passed through a 70uM mesh cap provided in 3mL polystyrene tubes (Falcon). These cells were centrifuged once more and resuspended in the appropriate live/dead the sort at a concentration of no more than 10 x 10^6 cells/mL FACS sorted cells were collected in 5mL FACS tubes containing 3mL of the respective cell media.

For single cell sorting, cells were sorted on the BD influx (BD) cell sorter into a 96 well-plate with 100uL of media.

2.5 Retroviral infection of cells

2.5.1 293T transfection and virus harvest

To generate virus, 293T cells were seeded at 5 x 10^6 cells per well in a 6 well plate. These cells were allowed to incubate overnight to ensure around 80% confluency the next day. Prior to transfection, the media is replaced with fresh media. In a tube, 150uL of DMEM (with no supplements) was combined with 7uL of Lipofectamine 3000 (Thermo Fisher). In another tube, in 150uL of uncomplemented DMEM, 1 ug of the vector of interest was added to 2.4ug of GAG-POL vector and 1.2ug CAG-ECO vector. This was then combined with the tube containing the Lipofectamine 3000, and the solution was allowed to incubate for 10-20 mins at room temperature. After incubation, the 300uL was taken up into a pipette and was dispensed drop wise onto the 293T cells without agitation.

293T cells were allowed to incubate for 24 – 48 hours, and then virus is harvested by filtering supernatant through a 0.45um Minisart syringe filter. This removed debris from the virus.

2.5.2 Retrovirus infection of cells

The day before the infection, the number of required wells in non TC-coated 24 well plates (Corning) were coated with retronectin diluted in MT-PBS at a final concentration of 32ug/mL These plates were incubated (without movement) overnight.

On the day of infection, the retronectin matrix was removed from the plates. Wells were blocked with 1mL 2% BSA diluted in MT-PBS for 30 mins at room temperature. Next, virus was dispensed into the well, and plates were spun at 1000 x g/1 hour/4°C. The viral media is removed from the wells, and cells are resuspended in the wells in 1mL of appropriate media. Cells were incubated overnight at 37°C and infection efficiency was checked the next day via FACS.

2.6 CRISPR experiments

2.6.1 Generation of a Cas9 expressing cell line

Cas9 virus was kindly provided by the MHTP platform (Monash). To generate a Cas9 expressing cell line, 1 x 10^5 cells were seeded into a 6 well plate. Anywhere from 100uL – 1mL of virus was used, depending on the instruction of the platform, and cells were centrifuged at 1,070 x g/30 mins/room temp. After the spin, cells were put into the incubator overnight. 24-hour post infection, the media was removed from the well and replaced with fresh media with a pre-determined concentration of blasticidin (Gibco) – this is to ensure selection of Cas9 infected cells. Cells were observed over the 4 or more days to look at cell death effects and outgrowth of infected cells.

Because we have had problems with blasticidin selection in the past, we opted to further conduct single cell sorting on these cells to ensure that we could screen for Cas9 expression (via Western blot) in clonal populations of cells that either do or do not express Cas9.

2.9.2 Validation of Cas9 activity

To ensure that Cas9 is active within these cells, another infection is conducted using the BRD011 vector. This vector drives the expression of GFP while also expressing a sgRNA that targets GFP. Cells are selected with puromycin (Gibco) following

infection, and the proportion of GFP positive cells vs GFP negative cells is analysed over the next 4 days via GFP. If Cas9 is active, you should see over 90% loss of GFP expressing cells by day 4.

2.6.3 Infection with the CRISPR 'brie' library

Infection of Cas9 expressing cells with the GeCKO library was conducted at the MHTP functional genomics lab.

2.6.4 Treating cells post incorporation of the sgRNA library

In order to maintain representation of the pool of sgRNAs, for the duration of the screen we maintained cells at no less than 80 x 10^6 cells. This ensured that there was always, proportionally, 1,000 cells per sgRNA that existed in the library. MLL-ENL Cas9+ expressing cells were cultured in numerous T175 culture flasks with either DMSO or the determined concentration of PRMT5i. Every 2-3 days, a cell count was obtained for each treatment group to analyse the effects that treatment had on proliferation. 80 x 10^6 cells were collected and were split into fresh media either containing DMSO or PRMT5i. All the remaining cells on these days were harvested for DNA collection.

2.6.5 NGS analysis

All NGS sequencing during the CRISPR screen was conducted at the MHTP functional genomics lab. An overview of the NGS process is provided (129).

2.7 Generation of knockout clones for CRISPR validation

2.7.1 Oligo cloning of sgRNA

Utilising a lenti-guide vector, known as BRD003, we created several individual sgRNA lentiviral vectors in order to validate the hits from the CRISPR screen in a drug assay. The BRD003 vector was digested with BsmBI in the following reaction: 10ug of circular vector, 5uL of 10X fast digest buffer, 2uL of BsmBI and adjust to 50uL with dH_2O. This reaction was incubated at 37°C overnight. The next day, the digested vector was purified in a PCR purification column (Qiagen) and eluted with 2 x 20uL of EB buffer. The vector was recut by adding 5uL of the 10X fast digest buffer and 3uL of the BsmBI to the 40uL elution containing the vector. This was incubated

at 37°C for 3 hours. The vector was run on a 1% agarose gel and purified with a gel purification column (Qiagen). This was eluted in 2 x 25uL of EB buffer. Specific oligos were ordered from IDT (listed in table 2.4) that ultimately targeted the genes we wanted to validate. Oligos were resuspended to a final concentration of 100uM, and in an Eppendorf tube, 1.5uL of forward and 1.5uL of respective reverse oligos were added. This was combined with 5uL of NEB buffer 3.1 and dH_2O made the solution up to 50uL. This was incubated for 4 mins at 95°C on a heat block, and then the plug was pulled out of the heat block to allow for gradual cooling of the sample. For the ligation step, the following reaction was created: 1uL of the oligo mix, around 20ng of the precut open vector, 10X ligase buffer, 15uL of dH_2O and 1uL of T4 DNA ligase (NEB). Ligation proceeded at 16°C for 3-4 hours. This ligation mix was transformed into competent E. Coli by adding 2uL of the ligation mix to 25uL of chemically competent cells. These cells were incubated on ice for 10 mins and were then heat shocked for 30 seconds at 42°C. This was followed by an incubation on ice for 2 mins. 400uL of SOC media was added to the cells, and this was incubated at 37°C for 1 hour with shaking. 150uL of the transformants were plated onto agar dishes that contained 100ug/mL of Ampicillin. These plates were incubated, upside down, overnight at 37°C. The next day, 2-4 colonies were picked, and plasmid was harvested as per section 2.2.3).
These minipreps were sequenced using the sequencing primer indicated in Table 2.4 by Micromon (Monash).

2.7.2 Lentivirus production

0.5 x 10^6 cells were seeded into a 6 well plate in 3 mLs of media, and were allowed to grow overnight in culture. The next day, the following transfection mix was prepared: 250ng VSV-G plasmid, 1250ng psPAX2 plasmid and 1250ng of the lentivector. This was brought up to 75uL with supplement free DMEM. In another tube, 8.25uL of Fugene was resuspended in 75uL supplement free DMEM. The DNA mix and the Fugene were combined and incubated at room temperature for 20 – 30 mins. 1mL of media was removed from the cultured cells and was replaced with fresh media. The transfection mix was dispensed drop wise onto the cells. The cells were allowed to culture for 48 hours, and then the viral supernatant was harvested and passed through a 0.4um filter.

The same protocol as listed in section 2.9.1 was used to infect MLL-ENL cells with the vectors targeting individual genes.

2.8 High throughput drug screen

Once we had a list of candidate drugs that we wanted to test as single agent and in combination with the PRMT5i, through the use of Compounds Australia (Griffith University) 140 compounds were incorporated into 384 well plates. The setup of the plates was duplicated so that one set would be seeded with MLL-ENL cells that were pre-treated with DMSO vehicle, and one set would be seeded with MLL-ENL cells that were pre-treated with the PRMT5i. Cells were seeded at 0.3 x 10^6 cells/mL in 3mLs of media with respective drug, and were pre-treated for 48 hours. The cells were split 1:60 and resuspended in fresh media (including either DMSO or PRMT5i), and then 62.5uL of this cell solution was aliquoted into the 384 well plates. The cells were incubated for a further 3 days. Plates were analysed on the BD Canto II, and propidium iodide was used a live/dead marker to look for the proportion of live cells in the cell death assay.

2.9 Mouse experimentation

2.9.1 Mouse models

Vav-iCre-PRMT5 mouse: Transgenic mouse that contains the cDNA sequence for PRMT5 3' of a splice acceptor in the *Rosa26* locus between exons 1 and 2. Cre-mediated deletion of the STOP cassette enables the transcription of the *Rosa26* exon1-PRMT5-FLAG-IRES-eGFP bicistronic mRNA only in cells that express *vav*. This restricts enforced PRMT5 expression to most blood cells (with the exception of more mature erythrocytes).

ERT2Cre PRMT5$^{fl/fl}$ mouse: This mouse was used to assess the effects of PRMT5 deletion in the blood system of mice. Treatment with tamoxifen results in expression of cre in all cell types, and subsequent deletion of PRMT5.

2.9.2 Mice euthanasia and tissue harvesting

At experimental end-point, mice were euthanised via CO_2 gas asphyxiation, followed by cervical dislocation as a secondary measure.

To harvest bone marrow, the hind limb long bones were dissected from mice. The muscle and connective tissue were removed from the bone, the condyles and epiphysis was removed to expose the metaphysis of the bone. Using an 18G needle filled with PBS + 2% FCS, the bone marrow is flushed from the metaphysis of the bone into a tube willed with PBS + 2% FCS. This cell mixture is passed up and down through a needle and syringe to homogenise the sample into single cells.

To harvest thymocytes, the thymus was dissected from the mice. The organ was filtered through a 50uM nylon cell strained (Falcon) using PBS and the blunt end of a plastic 3mL syringe (Falcon).

2.9.3 Red blood cell lysis

To perform FACS analysis on bone marrow cells, red blood cell lysis was performed to remove erythrocytes from the sample. To do this, 20uL of collected PB was suspended in 3mLs of 1x RBC lysis buffer.

2.9.4 Fetal liver transplant

E13.5 fetal liver (FL) cells were thawed and allowed to recover overnight. The cells are Ter119 depleted and undergo infection (as per section 2.8). On the day of transplant, the cells are counted, and 1 x 10^6 cells are harvested per mouse and resuspended in a final injection volume of 200uL PBS + 2% FCS. Mice were sublethally irradiated and were allowed to recover for a period of 3 hours. The cells were then injected into recipient mice through intravenous tail vein injection.

2.9.5 Competitive transplant

To conduct the competitive transplant assay, bone marrow cells were harvested from ERT2Cre PRMT5$^{fl/fl}$ mice alongside cre controls, as well as from Ly5.1 mice (these cells would act as competitor cells) . These cells were counted, and Ly5.2 and 5.1 cells were mixed at a 1:1 ratio in a max volume of 200uL PBS + 2% FCS/mouse that was being transplanted. Ly5.1 recipient mice underwent lethal irradiation, with 2

doses administered 3 hours apart to allow for recovery. Mice were then transplanted with the cell mixture through a tail vein injection. These mice were allowed to recover for 4 weeks before they were administered with Tamoxifen in order to delete PRMT5 in the ERT2Cre cells.

2.9.6. Tamoxifen administration through gavage

To induce deletion of PRMT5 in cells from our ERT2Cre mouse model, mice had to undergo tamoxifen administration through oral gavage. Tamoxifen (Sigma) was diluted in 90% peanut oil (Sigma) and 10% ethanol. The tamoxifen was dissolved by placing the solution in a water bath at 50°C with frequent vertexing. Mice were administered with 50mg/kg of tamoxifen in a max. volume of 150uL through oral gavage. Tamoxifen was administered daily for 3 days to ensure deletion of PRMT5.

2.10 Statistical analysis

2.10.1 MAGeCK analysis of the CRISPR screen

In order to generate p-values corresponding to the Log_2FC differences in the genes that were included in our screen, MAGeCK analysis (MAGeCK stands for Model-based Analysis of Genome-wide CRISPR/Cas9 Knockout) was performed by A/Prof. Joseph Rosenbluh (MHTP; Monash). The principles of MAGeCK analysis can be found in an article by Li et al. (130). In short, read counts from different samples are first median-normalised to adjust for the effect of library size and read count distribution. The variance of this read count is estimated by sharing information across features, and a negative binomial (NB) model is used to test whether sgRNA abundance differs significantly between treatment and controls. This model is meant to perform better as compared to existing models, and is capable of identifying positively and negatively selected genes simultaneously.

2.11 Buffers and solutions

Mouse tonicity phosphate-buffered saline (MT-PBS) (10x): 57g $Na_2HPO_4.2H_2O$, 11.03g $NaH2PO_4.1H_2O$, 174g NaCl. Add up to 2L dH_2O and mix.
SDS solution (20% w/v): SDS powder 100g, fill up to 500mL with dH_2O with gentle heating and mixing.

SLAB buffer (5X): 150mM Tris HCl pH 6.8m 20% SDSm 25% glycerol, 12.5% beta-mercaptoethanol, Bromophenol blue

Western blot running buffer: 150g Tris, 720g glycine, 250mL 20% SDS, fill up to 4.5L with dH_2O, mix with magnetic stirrer until it is dissolved. Fill up to 5L.

Western blot transfer buffer: 144g glycine, 31.3g Tris, 5mL 20% SDS, 2L methanol, fill up to 10L with dH_2O.

TBS buffer (10X): 48.4g Tris, 160g NaCl, adjust pH to 7.6 with HCl, fill up to 2L with dH_2O. Dilute to 1X prior to use and add 1mL of Tween 20 per 1L of buffer.

Red blood cell lysis buffer: 8.34g NH_4Cl dissolved in 1L of dH_2O, pH 7.6.

Table 2.1 Antibodies used for Western blot

Target	Supplier	Cat no.	Species	Dilution	MW (kDa)
PRMT5	Abcam	Ab109451	Rabbit	1:1000	73
FLAG	Sigma-Aldrich	F3165	Mouse	1:1000	~73
H4R3me2s	Merck	N/A	Rabbit	1:50	11
MEP50	CST	2823	Rabbit	1:1000	42
sDMR	CST	13222	Rabbit	1:1000	Multiple
aDMR	CST	13522	Rabbit	1:1000	Multiple
Cas9	CST	14697	Mouse	1:1000	160
Actin-HRP	CST	5125	Rabbit	1:1000	45

Table 2.2 Primers used for qRT-PCR

Gene of interest	F sequence	R sequence
PRMT5	CAGCATACAGCTTTATCCGCCG	CTAGACCGAGTACCAGAAGAGG
HPRT	CCTCCTCAGACCGCTTTTT	AACCTGGTTCATCATCGCTAA

Table 2.3 Antibodies and viability dyes used for flow cytometry

Antigen	Clone	Conjugate	Supplier	Dilution
Ter119	Ter119	BV605/APC	BD	1/500
CD3	17A2	BV605/PE	BD	1/500
Gr-1	RB608C5	BV605/PeCy7	BD	1/1000
Mac1	M1/70	BV605/V450	BD	1/250
CD19	1D3	APCCy7	BD	1/500
B220	RA3-6B2	BV605	BD	1/500
C-kit	ACK45	APC	BD	1/100
Sca-1	12-1581-82	PeCy7	BD	1/100
Thy1.2	53-2.1	V500	BD	1/500
CD4	GK1.5	AlexaF700	BD	1/500
CD8	53-6.7	Pacific blue	BD	1/500
CD71	C2	PE	BD	1/500
Ly5.1	A20	AF700	BD	1/100
Ly5.2	104	BV605	BD	1/100
SytoxBlue			Thermo	1/1000
Propridium Iodide			BD	1/1000

Table 2.4 Oligos used for generation of knock-out clones for CRISPR validation

Oligo name	Forward sequence	Reverse sequence
WT_Trp53_1	CACCGGAAGTCACAGCACATGACGG	AAACCCGTCATGTGCTGTGACTTCC
WT_Trp53_2	CACCGGTGTAATAGCTCCTGCATGG	CACCGGTGTAATAGCTCCTGCATGG
WT_Gata2_1	CACCGCCTGGGCTGTGCAACAAGTG	AAACCACTTGTTGCACAGCCCAGGC
WT_Gata2_2	CACCGACAGCTGCTGCCTCCCGACG	AAACCGTCGGGAGGCAGCAGCTGTC
WTp53ko_Calr_1	CACCGCAAGAATGTGCTGATCAACA	AAACTGTTGATCAGCACATTCTTGC
WTp53ko_Calr_2	CACCGGCGGCCAGACAACACCTATG	AAACCATAGGTGTTGTCTGGCCGCC
WT_PTEN_1	CACCGCCTCCAATTCAGGACCCACG	AAACCGTGGGTCCTGAATTGGAGGC
WT_PTEN_2	CACCGACTATTCCAATGTTCAGTGG	AAACCCACTGAACATTGGAATAGTC
WT_MTAP_1	CACCGGGACAATAGTCACAATTGAG	AAACCTCAATTGTGACTATTGTCCC
WT_MTAP_2	CACCGGCCTTCAAAAGTCAACTACC	AAACGGTAGTTGACTTTTGAAGGCC
WT_Uchl5_1	CACCGAAAGACACCAGCCAAAGAGG	AAACCCTCTTTGGCTGGTGTCTTTC
WT_Uchl5_2	CACCGTAATAATGCTTGTGCCACTC	AAACGAGTGGCACAAGCATTATTAC
p53ko_Svyn_1	CACCGTCAGGATGCTGTGATAAGCG	AAACCGCTTATCACAGCATCCTGAC
p53ko_Svyn_2	CACCGAAGGGCCACTTACAATTAGG	AAACCCTAATTGTAAGTGGCCCTTC
p53ko_Cic_1	CACCGGAAGCAGAAATACCACGACC	AAACGGTCGTGGTATTTCTGCTTCC
p53ko_Cic_2	CACCGCACTAAACTGACACCCATTG	AAACCAATGGGTGTCAGTTTAGTGC
p53ko_EZH2_1	CACCGTATCGTAGTAAGTACCAATG	AAACCATTGGTACTTACTACGATAC
p53ko_EZH2_2	CACCGGACACCACCTAAACGCCCAG	AAACCTGGGCGTTTAGGTGGTGTCC
p53ko_Suz12_1	CACCGAGGAGCTGTAGACTTATCGT	AAACACGATAAGTCTACAGCTCCTC
p53ko_Suz12_2	CACCGCTGTTTAGAGTAACTCGTCC	AAACGGACGAGTTACTCTAAACAGC
p53ko_Ino80_1	CACCGGGGTTGCGGAATATCCTCAC	AAACGTGAGGATATTCCGCAACCCC
p53ko_Ino80_2	CACCGTGCCCATCAATGCATGAAGG	AAACCCTTCATGCATTGATGGGCAC
BRD003_Seq	GACTATCATATGCTTACCGT	

Chapter 3:

PRMT5 overexpression in haematopoiesis

3.1 Introduction

What role PRMT5 expression levels play in haematopoiesis and leukaemic development are still relatively unknown. Although it is generally believed that PRMT5 expression levels are higher in more stem and progenitor like haematopoietic cells as opposed to their mature counterparts, how or why this occurs, and what effect enforced expression of PRMT5 has on blood cells still needs to be further elucidated.

A study by Liu et al. (95) showed that, at the protein level, PRTM5 was more highly expressed in HSPCs. This would support the gene expression data (generated by Bloodspot) presented in chapter 1 of this thesis. In terms of leukemogenesis, it has been shown that lentiviral overexpression of PRMT5 could promote leukaemia, however this was shown in a leukaemic model that was already primed for leukaemia onset. Overexpression was associated with a shorter onset of leukemogenesis (109). What effect PRMT5 overexpression has on normal haematopoiesis is still unknown.

This chapter describes the generation and characterisation of a mouse model of PRMT5 overexpression. Gain-of-function mouse models have been mainly generated by pro-nuclear microinjection and random integration of the transgene into the genome. The downfall of this method is that is often results in unpredictable expression profiles, variable copy numbers and sometimes gene-silencing effects. Single-copy transgene transgenesis utilising the well-defined Rosa26 locus is thought to overcome these problems (131) and this model will be used throughout the chapter. As an alternative strategy, we describe the effects of retroviral overexpression of PRMT5 in fetal liver cells in a transplant setting.

3.2 Generation of a mouse model of enforced PRMT5 expression: The VaviCre-PRMT5 model

To allow us to address the effects of enforced PRMT5 expression in haematopoiesis, a mouse model, known as the VaviCre-PRMT5 model was generated. In this model, PRMT5 expression is driven by the *Rosa*26 locus in a cre-dependant manner. To generate this model, a gateway ROSA26 destination vector (pROSA26-DV1) operated as a substrate for the insertion of murine *Prmt5* cDNA containing a FLAG tag sequence incorporated in a Gateway entry clone. The *Prmt5* cDNA was introduced 3' of a splice acceptor (SA) followed by a LoxP flanked PGK-neo-3xpA (STOP cassette) and 5' of an IRES-eGFP reporter. LR reactions resulted in a pROSA25-DV1 derived expression vector (Fig 3.1A). Through recombination of our targeting vector and the wild type *Rosa26* allele (Fig 3.2B), as well as previously described methods for identifying correct *Rosa26* locus targeting (132), the targeting vector was used for ES cell electroporation into G4 ES cells (method described in (133). These ES cells were used to generate transgenic mice with knock in alleles in the *Rosa26* locus that contain our *Prmt5* cDNA sequence, of which transcription is inhibited by the STOP cassette. This cassette ultimately contains a multimerized polyadenylation sequence (3xpA) which efficiently stops transcription initiated by the *Rosa26* promoter (134)(Fig 3.1C). These mice were crossed with Vav-iCre mice in order to restrict cre expression to the haematopoietic compartment, thus ensuring only haematopoietic cells express the transgene (135). Cre-mediated deletion of the STOP cassette enables the transcription of the *Rosa26* exon1-*Prmt5*-FLAG-IRES-eGFP bi-cistronic mRNA (Figure 3.1D). This enabled a two-way verification of transgene expression – via eGFP expression which could be analysed by FACS, or by Western blot analysis of protein samples utilising an α-FLAG antibody.

3.3 Transgene expression was observed in almost all haematopoietic lineages

In order to determine what haematopoietic cell types were expressing the transgene, peripheral blood, bone marrow and spleen cells were harvested from mice of at least 8 weeks of age, and FACS analysis was conducted to analyse eGFP expression in the various haematopoietic compartments. Within the bone marrow, we were able to separate the cells into their respective lineages. The antibody panel allowed us to analyse T cells (CD3+), B cells (CD19+, B220+), mature myeloid cells (Gr-1+, Mac-1+) and immature myeloid cells (Gr-1-, Mac-1+) (FACS gating strategy shown in Fig

3.2A). When comparing the transgenic mice to the cre control mice, it was found that all populations had an eGFP expression of at least 92% (Fig 3.2B). As PRMT5 is expressed at higher levels in stem cells, another population of interest within the bone marrow were the stem and progenitor cells. In order to analyse these cells, we used an antibody panel to isolate the LK (Lin-, Sca-1-, C-kit+) and the LSK (Lin-, Sca-1+, C-kit+) cells (FACS gating strategy shown in Fig 3.2C). It was also found in these populations in the transgenic mice, that at least 90% of cells were expressing eGFP (Fig. 3.2D). To further analyse the T cell populations, a more extensive FACS analysis was performed on spleen cells harvested from control and transgenic mice. Using the thymus cell antigen 1 marker (Thy1) as a pan-T cell marker, we were able to analyse the double positive, or DP (CD4+, CD8+); the double negative, or DN (CD4-, CD8-); CD4 T cells, or SP4 (CD4+, CD8-) and CD8 T cells or SP8 T cells (CD4-, CD8+) (FACS gating strategy shown in Fig 3.2E). Within these populations, in the transgenic mice, it was found that at least 93% of cells were expressing eGFP (Fig 3.2F).

Although high eGFP expression was observed in the above-mentioned populations, we also analysed expression in the erythrocyte populations of the peripheral blood. Previous literature that has utilised the VaviCre mouse model has reported a lack of expression in the more mature erythrocyte populations in the blood (136, 137). In order to separate the E1 – E4 erythroid progenitors, CD71 and Ter119 antibodies were used, as cells will increase expression of Ter119 and decrease expression of CD71 as they progress through maturation (FACS gating strategy shown in Fig 3.2G). When analysing the erythroid progenitor populations, eGFP expression is highest in the E1 population (58.50% ± 2.3%). As erythroid maturation progresses, the proportion of eGFP expressing cells reduces until there is virtually no eGFP expression in the E4 cell population (0.55% ± 0.05%).
It was found that there was robust transgene expression in the haematopoietic system of our VaviCre-PRMT5 transgenic mice, with >90% of cells expressing relatively high levels of eGFP. The erythroid cell population was the exception to this, as FACS analysis revealed a loss of transgene expression in more mature erythroid cell types. eGFP expression in the various populations is summarised in Fig. 3.2I.

3.4 There was no increase in PRMT5 protein expression over baseline in the VaviCre-PRMT5 model

To determine whether transgene expression resulted in an increased level of PRMT5, we analysed PRMT5 expression at the RNA and protein level. Bone marrow cells were harvested from cre control and transgenic mice of at least 8 weeks of age. qRT-PCR was performed on the bone marrow cells, and it was found that *Prmt5* mRNA was significantly overexpressed in transgenic mice compared to controls (fold increase of 4.586 ± 0.7197, P<0.001)(Fig 3.3A). To confirm whether PRMT5 protein levels were increased, Western blots were conducted on bone marrow samples, and although we confirmed expression of FLAG tagged PRMT5, there was no increase in total PRMT5 protein in the transgenic model (Fig 3.3B). In order to corroborate this finding, we developed a FACS based approach for quantifying protein levels of PRMT5. This allowed us to utilise a secondary antibody (Alexa Fluor 546 – or AF546) bound to the α-PRMT5 protein that was used for Western blot to compare the antibody MFI in our transgenic mice as compared to our controls (representative FACS plots are shown in figure Fig 3.3C). This provided us with a robust readout of protein expression (about 20 fold increase in MFI in our control mice compared to either our isotype of secondary antibody negative controls), and confirmed that there was no significant increase in PRMT5 protein expression in either the bone marrow (MFI of 8,268.8 ± 930.8 in control vs 10,354.5 ± 874.7 in transgenic, P=0.32) or thymus of transgenic mice (MFI of 7,741.5 ± 1,429.5 in control vs 10,152.3 ± 2,313.9 in transgenic, P=0.07) despite increased mRNA expression (Fig. 3.3D).

3.5 Transgenic expression resulted in no phenotypic difference in haematopoiesis

FACS analysis was conducted on all the haematopoietic compartments in our transgenic mice to assess whether there was any difference in phenotype in transgenic mice (the same FACS antibody panel and gating strategy was used as highlighted in Fig 3.2). Two populations that were of interest were the stem and progenitor cell compartment and the myeloid cell compartment, as these populations are known to express higher levels of PRMT5. When analysing stem and progenitor cells we found no significant difference in the proportions and overall numbers of LK or LSK cells (Fig 3.4A). When analysing the different lineages in the blood, we found

no difference in the absolute numbers or proportions of the different lineages, including mature and immature myeloid cells (Fig 3.4B). Lastly, when analysing the splenocytes of control mice as compared to transgenic, there was no difference in T cell subpopulation proportions as well as absolute numbers (Fig 3.4C).

3.6 Retroviral overexpression of PRMT5 *in vivo*

As PRMT5 protein was not significantly expressed over baseline levels in our transgenic mouse model, we aimed to overexpress PRMT5 retrovirally (this retroviral system is more thoroughly discussed in chapter 4). Briefly, frozen E14 fetal liver cells were infected with an MSCV vector that resulted in a bicistronic expression of FLAG-tagged PRMT5 as well as mCherry (in order to be able to assess engraftment via FACS). We confirmed that, compared to uninfected cells, infection levels were 42% in fetal liver cells infected with MSCV empty vector, and 28% in cells infected with our MSCV-PRMT5 construct (Fig. 3.5A). We sought to confirm protein overexpression by analysing protein lysates of pooled fetal liver cells, containing a mixture of uninfected and infected cells. Western blot confirmed that there was enforced expression of PRMT5 in the fetal liver cells infected with MSCV-PRMT5 (this was absent in our empty vector infected cells). This is evident in the blot by the presence of a slightly heavier band when probing for PRMT5 – this represents our FLAG-tagged PRMT5 (Fig. 3.5 B; top panel). It appears that the intensity of both the PRMT5 and PRMT5-FLAG band are similar. Considering that only 28% of the cells that were processed in this lysate would represent MSCV-PRMT5 infected cells, this would suggest that our retroviral vector was driving around 4x increased expression of PRMT5. To determine whether this overexpression of PRMT5 would drive a more stem cell like state in the cells, and therefore improve engraftment as compared to our empty vector controls, these fetal liver cells were transplanted into 8 week old mice that were sublethally irradiated. Every 4 weeks, the mice were bled, and the peripheral blood was analysed via FACS to confirm the percentage of infected cells by analysing mCherry expression. Although there appeared to be initial engraftment of our infected cells (16.25% ± 2.02% in empty vector and 16.22 ± 2.60% in MSCV-PRMT5 infected cells), the percentage of mCherry cells decreased over time, whereby the percentage of mCherry positive cells was less than 2% in both groups by week 12 post-transplant.

3.7 Discussion

3.7.1 Overcoming the modest PRMT5 protein increase in the Rosa26 driven VaviCre model

Increased PRMT5 expression has been linked to many forms of cancer, including haematological malignancies. This chapter aimed at utilising a transgenic mouse model with the hopes of generating a consistent model of PRMT5 overexpression, as retroviral overexpression systems are often associated with variable expression levels that are often considerably higher than baseline expression. There are several advantages to using the Rosa26 locus as a targeting site to introduce cDNAs. One strength is centred on the efficiency of germline transgene transmission from the founder males to the first litter being relatively high. This reduces the number of chimeras that must be analysed, therefore decreasing model generation waiting times. Furthermore, these mice can be bred to any cre line of interest (138). Most importantly, even though the Rosa26 model results in lower expression levels than found in other conventional gain-of-function transgenics, this is touted as being physiologically relevant, and may more accurately mimic human disease (139). This method of gain-of-function has been utilised in a study to overexpress Snail protein – a family of transcription factors that play a role in epithelial to mesenchymal transition (EMT) processes (140). Using this model, they were able to achieve an mRNA increase of up to four-fold for Snai1 and Snai2 expression. In the case of Snai2 overexpression, this overexpression has the potential to cause embryonic lethality (138). Although we also achieved a moderate increase in mRNA expression of PRMT5, this did not translate at the protein level. This may be due to some post translational effect and would have to be interrogated further. Another potential explanation for the lack of PRMT5 protein could be due to the idea that PRMT5 protein expression is controlled by the expression of MEP50, and this is discussed in section 3.7.3).

We saw no phenotypic differences in our transgenic mice, which could be attributed to the observation that there was no significant upregulation of PRMT5 protein. This is something that we want to address in future experiments. There are two ways that the flaws in the model might be overcome: to use an improved Rosa26 mouse line,

or to simultaneously overexpress PRMT5's critical binding partner, MEP50.

3.7.2 Utilising a modified Rosa26 mouse model with higher expression levels

The conventional Rosa26 mouse model might not be suitable for high expression levels. As a means to overcome this modest increase in expression, an improved model, coined modRosa26 ("mod" for modified) has been generated (131). As with the model used in this chapter, targeted transgenesis utilising random mediated cassette exchange (RMCE) by cre recombinase can be combined with activity from exogenous promoters. Within the modRosa26 model, the endogenous Rosa26 promoter is silenced and replaced with a CAGG promoter. Reports have shown that this modification is able to increase expression 8-10 fold over a Rosa26-promoter based model (138).

If we simply need to increase expression levels of PRMT5 in our overexpression system to see an effect on phenotype, this model will allow us to achieve that. However, considering that our results show a decent increase in PRMT5 at the mRNA level, it could be that there is a limiting factor that is responsible for no difference in PRMT5 protein. One of those factors could be the expression levels of MEP50. The studies conducted by Jin et. al. observed that CD34+ cells from CML patient samples had a close to 2-fold increase in PRMT5 protein levels (108). Future overexpression studies will hopefully be able to achieve at least double the expression of PRMT5 protein.

3.7.3 Simultaneous overexpression of MEP50 may be required for increased PRMT5 activity

As described in Chapter 1, MEP50 is an essential co-factor of PRMT5. It is known that MEP50 binding to PRMT5 stabilises and increases its activity, and is also able to function to recruit substrate proteins for methylation Data in subsequent chapters shows that PRMT5 deletion also results in a downregulation of MEP50 protein. This highlights the importance of the interaction that exists between these two proteins in maintenance and/or stability or both members. Data also suggests that PRMT5 is

unable to positively regulate MEP50, in that PRMT5 overexpression does not result in MEP50 overexpression (discussed in further detail in Chapter 4). Therefore, one of the reasons we are unable to achieve PRMT5 overexpression in the VaviCre-PRMT5 model may be since we were not overexpressing MEP50. The use of a bicistronic design may overcome this downfall (discussed in Chapter 4). However, retroviral infection of fetal liver cells resulted in considerable expression of ectopic PRMT5-FLAG protein, as evident by Western blot. This may suggest that the association is not so clear cut. It may in fact be that PRMT5 protein can be overexpressed but does not result in an increase in overall PRMT5 methyltransferase activity due to the limiting conditions of MEP50 expression (which ultimately controls the amount of achievable PRMT5 activity). With that being said, there is value in assessing the effects of PRMT5 and MEP50 co-overexpression *in vivo* in a transgenic mouse model.

3.7.4 PRMT5 protein expression in haematopoiesis

We were able to develop a FACS based method for determining PRMT5 expression in both cells from the bone marrow and thymus. This was achieved using the same antibody that was used to probe PRMT5 in Western blots. This method provided us with a robust readout of protein expression that was, in comparison, almost absent in both the secondary antibody and isotype controls. In chapter 4, there is also FACS based protein expression data from *in vitro* overexpression lines that shows even greater increases in MFI compared to controls. The benefit of this system is that is allows us to accurately quantitate protein expression level, overcoming the semi-quantitative nature of Western blots. Although we associate higher expression levels of PRMT5 with HSPCs, a lot of the supporting data focuses on mRNA expression in the various cell types. A study found that mRNA and protein levels did not necessarily correlate, as although B cells had quite high mRNA expression of PRMT5 (similar expression levels as found in HSPCs), this was not reflected at the protein level. However, this was done using a Western blot method where cells had to be sorted prior to making up the protein lysate (95). Generally, more extensive PRMT5 protein expression data remains sparse in the literature. It is often difficult to single cell sort adequate numbers of the various stem and progenitor lineages to generate a good quality protein lysate for Western blot analysis, so a method that

does not involve pre-sorting would be ideal. This FACS based method could be utilised with various antibody panels to overcome this. Cells could be simultaneously stained with subpopulation markers as well as the PRMT5 antibody conjugated to an appropriate secondary antibody. This would allow for quantitative analysis of PRMT5 expression levels (as represented by MFI) and a true comparison of protein expression differences between various haematopoietic subpopulations. Why downregulation occurs as cells mature is still relatively unknown and generating robust haematopoietic subpopulation protein profiles may assist in answering this question.

3.7.5 PRMT5 overexpressing fetal liver cells were unable to engraft

Our results found that retroviral overexpression of PRMT5 in fetal liver cells conferred no advantage in terms of engraftment and repopulation in recipient mice. Although there was a transient presence of infected cells in the peripheral blood at week 4, this tapered off until there was virtually no mCherry expression by week 16. There were a few experimental details that may have led to this result. Firstly, the fetal liver cells that were used for infection and subsequent transplant were previously frozen. Using fresh fetal liver cells may have resulted in better repopulating capacity of the fetal liver cells. Furthermore, the recipient mice were only sub lethally irradiated prior to transplantation (this was done to ensure that mice would survive if reconstitution did not occur). As mice were healthy throughout the experiment, it would suggest that there was an overgrowth of uninfected cells. Some would argue that bone marrow would be more appropriate, as an adequate number of cells is easier to obtain from less mice required for transplantation. With that being said, the use of fetal liver material over bone marrow is a justifiable choice. Various publications have reported the benefit of using fetal liver cells in not only short-term, but particularly long-term engraftment. Fetal liver cells have been shown to be superior in long-term reconstitution ability as compared to bone marrow, with fetal liver cells being 5 fold more effective in competitive transplant assays as compared to bone marrow (85, 141).

To assess the true reconstitution potential of cells infected with our PRMT5 retrovirus, competitive transplant assays should be done utilising Ly5.1 recipient

mice that have been lethally irradiated. These mice should be transplanted with a mixture of Ly5.1 uninfected cells, and Ly5.2 cells infected with our retrovirus. This will allow us to assess the reconstitution capability of PRMT5 overexpressing cells in a competitive manner.

Furthermore, and related to the previous sections on MEP50s role in PRMT5 activity, this assay could be utilised with a co-overexpression system, and fetal liver cells could be infected to overexpress PRMT5 and MEP50 simultaneously. This would address the question of whether more PRMT5 activity (through overexpression of MEP50) is enough to enhance engraftment in a transplant assay setting.

3.7.6 Conclusion

To summarize, the VaviCre-PRMT5 mouse model was developed to overcome various downfalls of pronuclear microinjection methods related to gain-of-function experiments by utilising the Rosa26 locus. Characterisation of the model found that, although our transgene was expressed in almost all haematopoietic lineages (with the exception of more mature erythroid cell types), this did not correlate with overexpression of total PRMT5 protein in both the bone marrow and thymus of transgenic mice. Unsurprisingly, transgene expression was not associated with any phenotypic differences when analysing the various hematopoietic subpopulations via FACS. Furthermore, when a retroviral overexpression system was harnessed to try and overcome the issue of overexpression, we found that fetal liver cells were unable to engraft in recipient mice in a transplant setting. The findings from this chapter raise a few questions - whether the Rosa26 model that we utilised is just not suitable for high level PRMT5 overexpression, or whether we need to overexpress MEP50 alongside PRMT5 remains an important one. The results from Chapter 3 prompted us to develop an *in vitro* retroviral overexpression system to try and generate data relating to true PRMT5 protein overexpression and the possible importance of MEP50 (discussed further in Chapter 4).

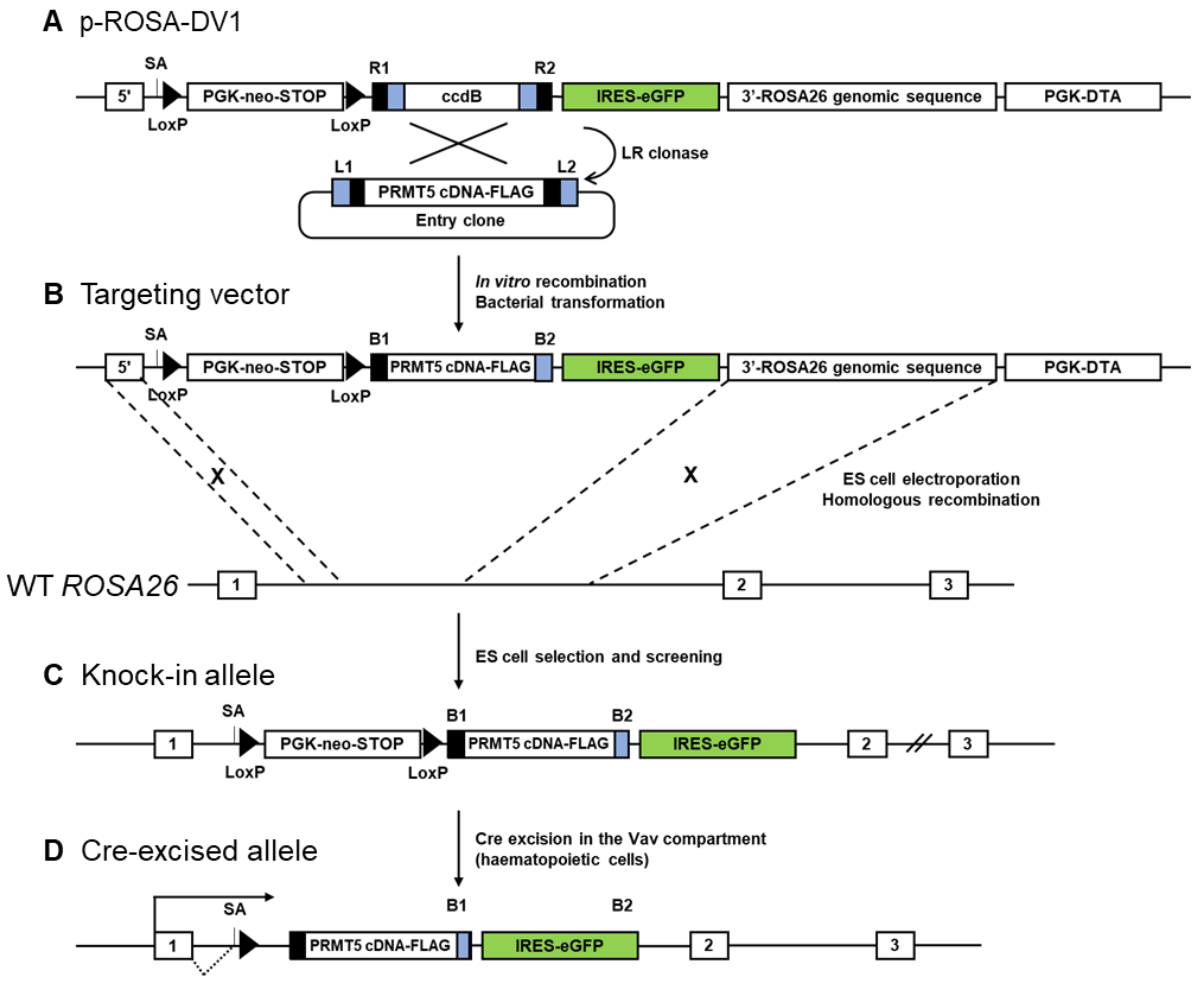

Figure 3.1. Generation of the VaviCre-PRMT5 mouse model
(A) LR reaction performed between the pROSA26DV-1 vector and the entry clone containing cDNA for *Prmt5*. **(B)** *Rosa26* targeting vector containing the PGK-neo-3xpA (STOP) cassette flanked by LoxP sites. **(C)** Knock-in allele incorporated between exons 1 and 2 in the *Rosa26* allele. **(D)** Cre-mediated deletion of the LoxP flanked STOP cassette occurs in the vav compartment and results in the expression of an exon1-*Prmt5*-eGFP bi-cistronic fusion transcript. SA: Splice acceptor.

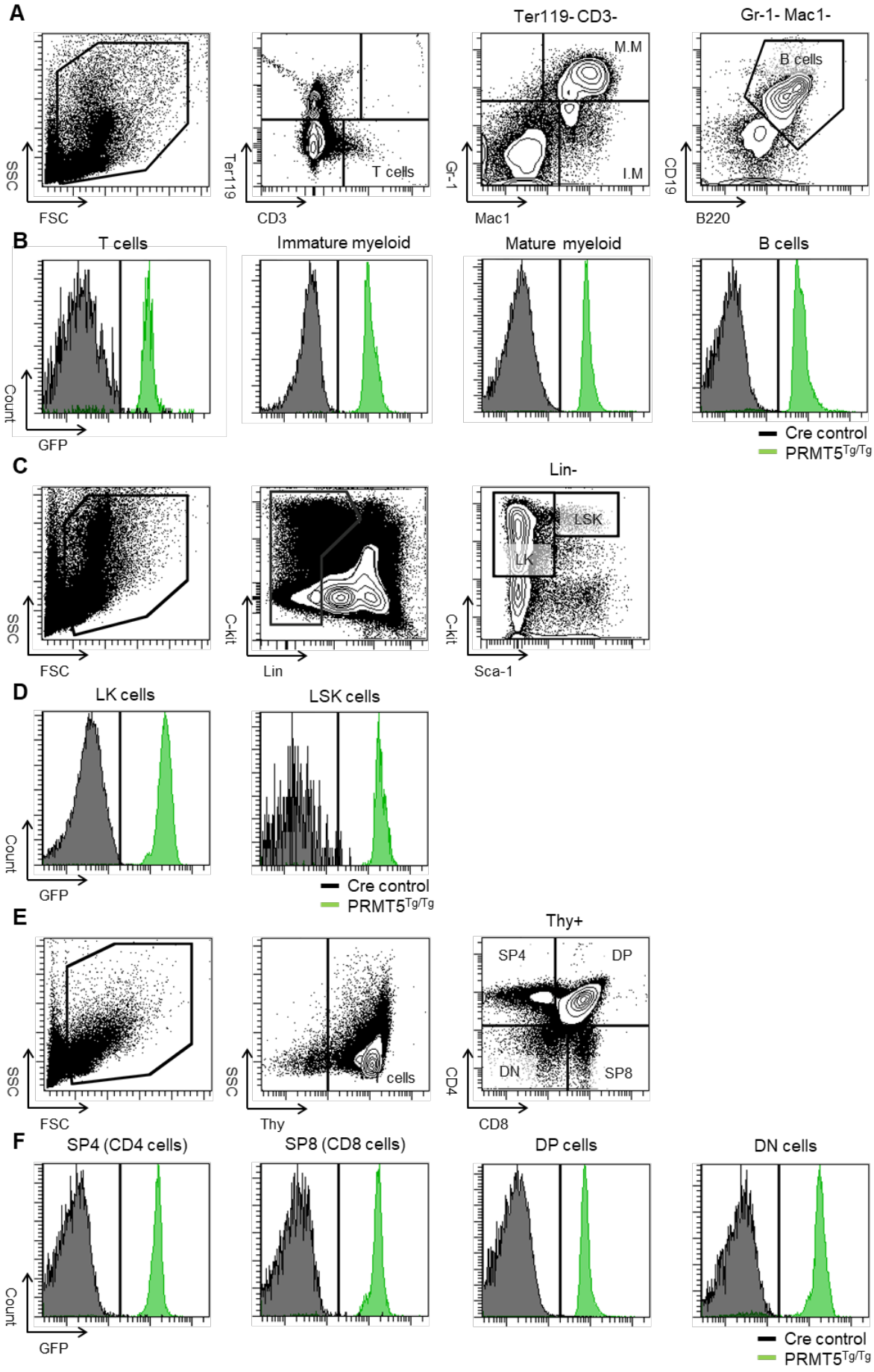
A
SSC
FSC
Ter119
CD3
T cells
Ter119- CD3-
M.M
I.M
Gr-1
Mac1
Gr-1- Mac1-
B cells
CD19
B220
B
T cells
Immature myeloid
Mature myeloid
B cells
Count
GFP
Cre control
PRMT5Tg/Tg
C
Lin-
LSK
LK
C-kit
Lin
Sca-1
D
LK cells
LSK cells
Count
GFP
Cre control
PRMT5Tg/Tg
E
Thy+
SP4
DP
DN
SP8
SSC
FSC
cells
Thy
CD4
CD8
F
SP4 (CD4 cells)
SP8 (CD8 cells)
DP cells
DN cells
Count
GFP
Cre control
PRMT5Tg/Tg

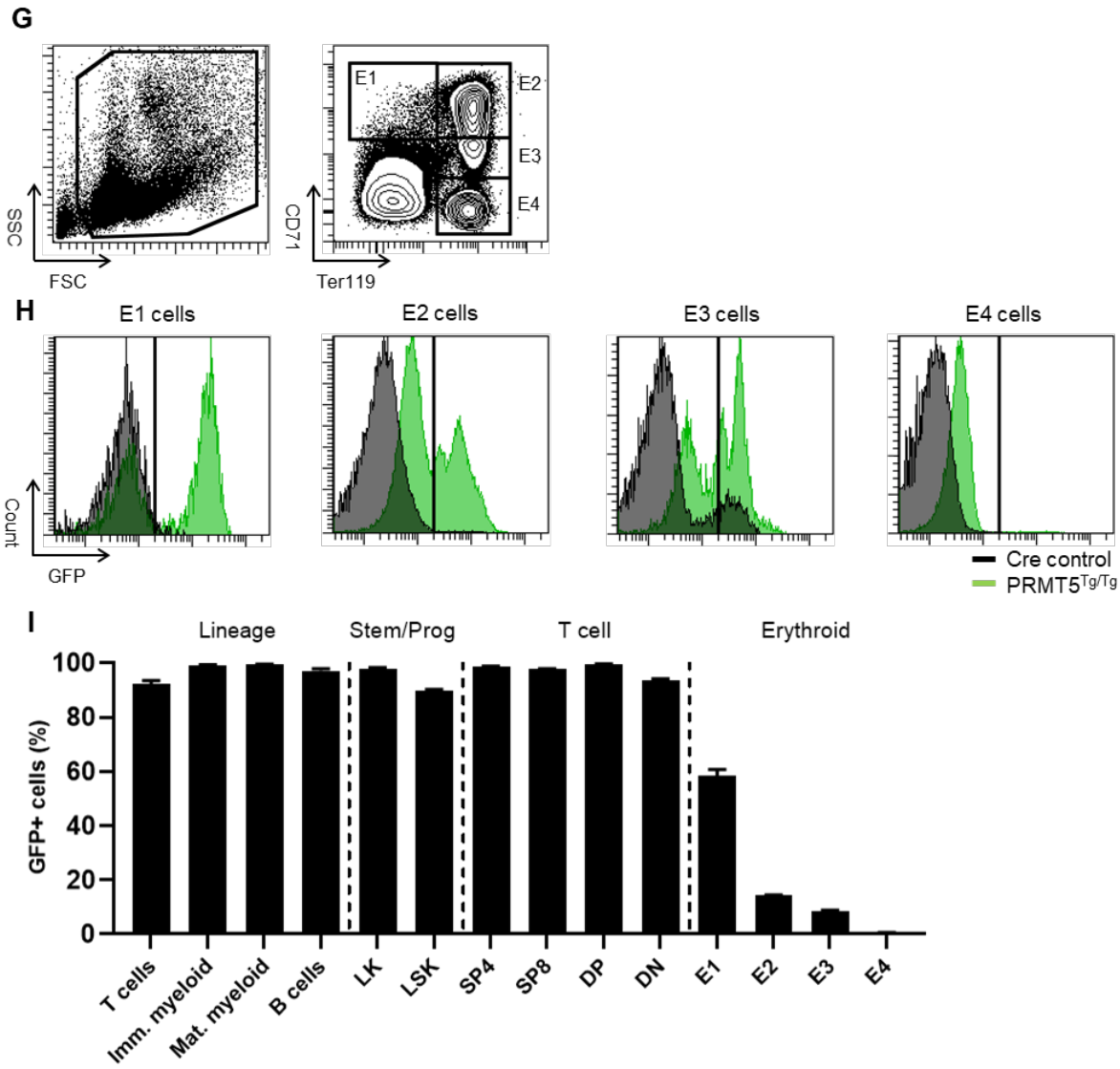

Figure 3.2. Transgene expression in haematopoietic compartments
(A) Haematopoietic lineage, **(C)** stem and progenitor cell, **(E)** T cell subpopulations and **(G)** erythroid progenitor FASC gating strategy, with associated histograms of eGFP expression levels **(B, D, F, H respectively)**. **(I)** summary quantification of eGFP expression levels in the various lineages. Mean +/- SEM are shown, n=4-6.

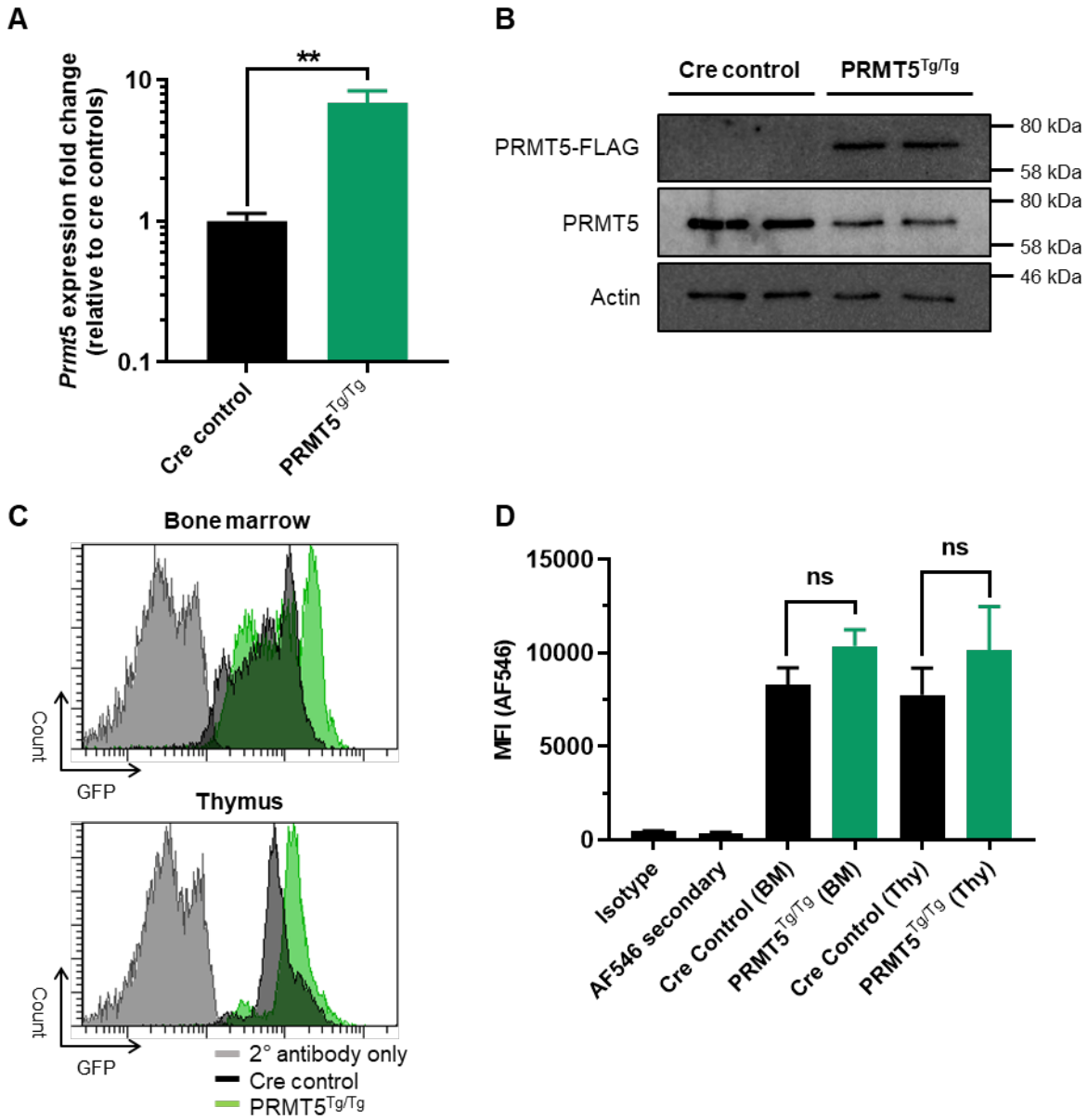

Figure 3.3. PRMT5 expression in the VaviCre-PRMT5 mouse model
(A) RT-PCR of *Prmt5* mRNA expression in bone marrow cells from transgenic mice vs cre controls, values are mean+/- SEM, n=5. **(B)** Western blot of bone marrow lysates analysing levels of PRMT5 and transgene associated FLAG. Actin was used as loading control. **(C)** Representative histograms of AF546 expression corresponding to PRMT5 protein levels in the bone marrow of control and transgenic mice as compared to the negative isotype control. **(D)** MFI (associated with PRMT5 expression) of control and transgenic mice. Mean +/- SEM are shown, n=4. *P<0.05, **P=<0.01, ***P<0.001, students t-test as compared to cre control.

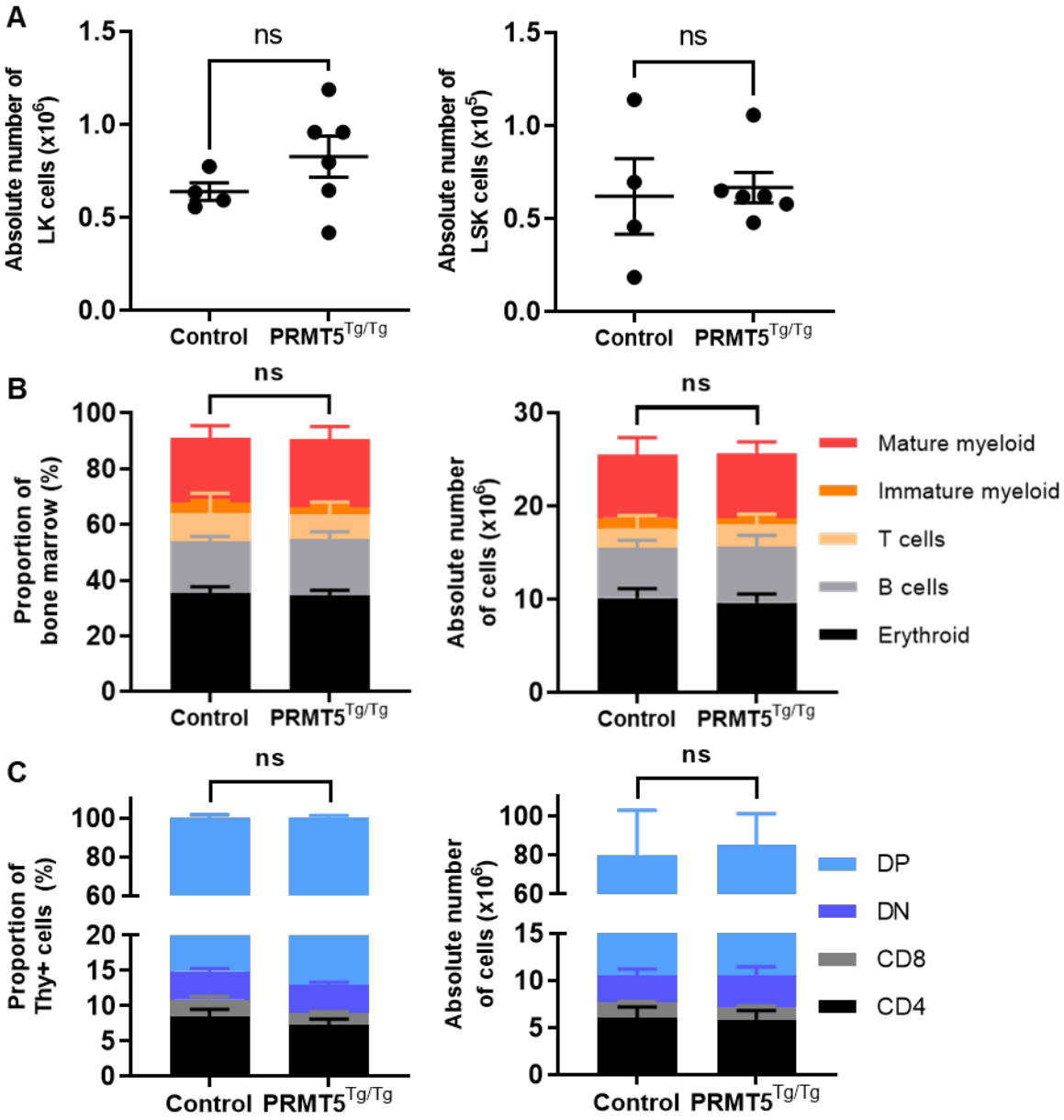

Figure 3.4. Haematopoietic subpopulation phenotypes

(A) Absolute number of LK and LSK cells in the bone marrow. **(B)** Proportion and absolute number of cells in the different lineages in the bone marrow. **(C)** Proportion and absolute number of T cell subpopulations in the thymus of mice. Mean +/- SEM are shown, n=4-6.

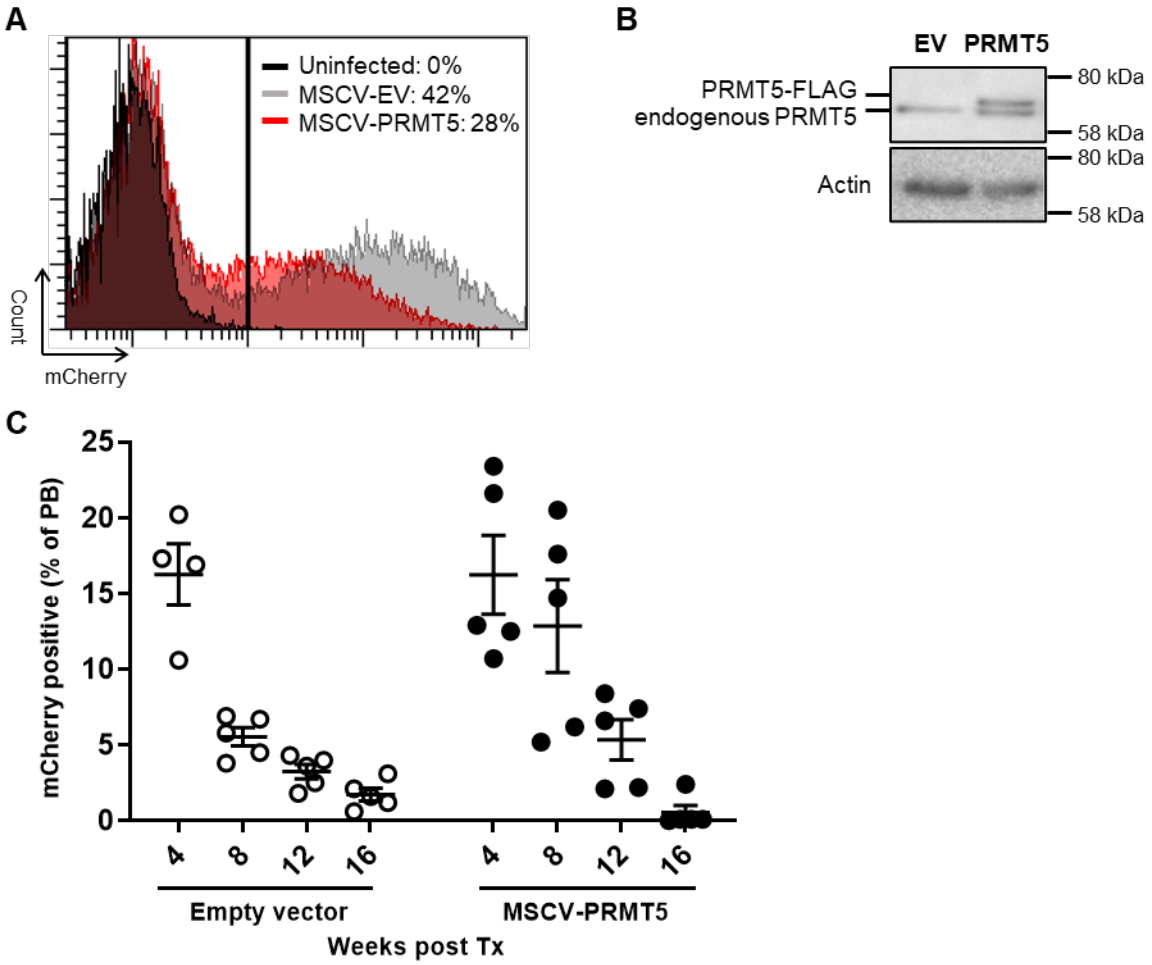

Figure 3.5. Retroviral overexpression of PRMT5 in fetal liver cells
(A) Infection efficiency of fetal liver cells (represented as eGFP expression) infected with empty vector (MSCV-EV) and a PRMT5 overexpressing construct (MSCV-PRMT5) as compared to uninfected cells. **(B)** Western blot analysis of pooled fetal liver cells post infection, analysing levels of PRMT5 and retrovirally expressed FLAG-tagged PRMT5 (band associated with a higher kDa). Actin was used as the loading control. **(C)** Engraftment analysis of fetal liver cells post retroviral infection with either MSCV-EV or MSCV-PRMT5 over a 12 week period. Engraftment is represented by expression of mCherry. Mean % of mCherry expressing cells +/- SEM are shown. n=4-5.

Chapter 4:

Structure-function of PRMT5

4.1 Introduction

Due to the modest overexpression levels achieved by the Rosa26 mouse model from the previous chapter, we wanted to employ an MSCV retroviral overexpression system with the aim of driving higher expression of exogenous PRMT5 levels. This system was used throughout this chapter.

Deletion studies have shown that PRMT5 is critical for haematopoiesis. One major study, which utilised Mx1Cre^{+}PRMT5$^{fl/fl}$ mice, found that even though PRMT5 depletion led to BM failure and HSPC dysfunction, this was associated with Flt3 and c-kit downregulation in HSPCs (95). However, studies have shown that Flt3 is generally absent from HSCs (142), and that this trend of c-kit downregulation might be a general refection of preferential apoptosis that seems to be geared towards c-kit^{high} HSCs (143). A recent study by Tan et al. aimed at elucidating the cellular processes that are responsible for PRMT5 dependency in HSCs. The emphasis of the study primarily focuses on PRMT5-mediated splicing, as there is evidence in the literature that supports the idea that PRMT5 depletion affects mRNA splicing in both murine (88, 102) and human cell line models (107, 144). Their study concluded that PRMT5 depletion led to a rapid loss of the HSC compartment due to endogenous DNA damage that resulted in p53 activation. PRMT5 was reported to be important in maintaining HSC integrity by modulating splicing and expression of the *Fanc* family of genes (genes that are involved in DNA repair) and underpinned the importance of PRMT5 activity in HSC maintenance (145). Throughout this chapter, we aim to corroborate this deletion phenotype in an ERT2Cre system, both *in vitro* and *in vivo*. Combining these deletion models with retroviral infection to drive exogenous PRMT5 expression, we aim to assess whether we can rescue the phenotype observed with deletion.

Furthermore, although the crystal structure of PRMT5 has been described fairly extensively (85), the functional relevance of the different domains of PRMT5 remains fairly unclear. We aim to employ two different mutant forms of PRMT5 within this

chapter. One mutant, known as the asymmetric dimethyl mutant – or aDMR mutant - contains an F327M mutation, and has been described as being able to perform both symmetric and asymmetric dimethylation (71). The second mutant, which is often used as a control, is known as the methylation dead mutant – or md mutant. This mutant contains G367A and R368A mutations, and functions as a catalytically inactive form of PRMT5 that is unable to catalyse sDMR marks on its substrates (106). Domain specific effects will be assessed throughout the following experiments in this chapter, with particularly interesting results surrounding how these mutant forms respond to PRMT5 inhibition.

4.2 Deletion of PRMT5 in an ERT2Cre deletion system leads to loss of haematopoiesis

Utilising an ERT2Cre model of PRMT5 deletion, we first analysed the effects of PRMT5 deletion on haematopoiesis. To achieve this, bone marrow was harvested from ERT2Cre$^{Tg/Tg}$ PRMT5$^{fl/fl}$ and their respective ERT2Cre$^{Tg/Tg}$ PRMT5$^{+/+}$ cre control mice. For brevity, the ERT2Cre$^{Tg/Tg}$ PRMT5$^{+/+}$ mice will be referred to as ‘cre control’, and the ERT2Cre$^{Tg/Tg}$ PRMT5$^{fl/fl}$ mice will be referred to as ‘PRMT5$^{fl/fl}$’ for the remainder of the chapter. A competitive transplant assay was performed in which Ly5.2 donor cre control or PRMT5$^{fl/fl}$ cells were mixed in a 1:1 ratio with Ly5.1 bone marrow cells. These cells were transplanted into a lethally irradiated Ly5.1 recipient. Following a 4-week recovery, the recipient mice received 3 daily doses of Tamoxifen to induce expression of Cre. To assess the effects of cre expression and subsequent PRMT5 deletion, peripheral blood (PB) was harvested at weeks 2, 4 and 8 post tamoxifen treatment, and a cull was conducted at week 10, in which bone marrow and thymus was harvested for analysis (Fig. 4.1A).

The competitive nature of the transplant allowed us to analyse the contribution that donor cells (Ly5.2) were having to haematopoiesis vs. the competitor cells (Ly5.2). These cells were clearly distinguishable by FACS when staining the cells with Ly5.1 and Ly5.2 antibodies. When combined with other markers for various haematopoietic lineages – Mac1+ for myeloid cells, B220+ for B cells and CD4+ or CD8+ for T cells

– this could further be stratified into the Ly5.1/5.2 contributions in these specific populations (representative FACS plots shown in Fig. 4.1B).
The first analysis was conducted at 2 weeks post-transplant and tamoxifen treatment, and there was a significant difference in the PB Ly5.2 contribution when comparing the cre control cells to PRMT5$^{fl/fl}$ (29.56 ± 2.64% vs 21.77 ± 2.09%, respectively, $p<0.05$). Although the contribution remained consistent in the context of the cre control setting, Ly5.2 contribution progressively declined in the PRMT5$^{fl/fl}$ cells. By week 8, PRMT5$^{fl/fl}$ donor cells made up less than 4% of the blood (Fig. 4.1C).

Mice were culled at week 10, and FACS was performed on the PB, bone marrow and thymus to look at Ly5.2 contributions to the specific lineages. When analysing the PB (Fig. 4.1D), PRMT5 deletion affected all analysed lineages, and when comparing PRMT5$^{fl/fl}$ Ly5.2 cells to the cre controls, there was a marked reduction observed in myeloid cells (43.10 ± 5% reduction, p=0.013), B cells (42.31 ± 1.38% reduction, p = 0.001) and T cells (19.14 ± 1.50% reduction, p=0.006). This was also confirmed when analysing the bone marrow and thymus (Fig. 4.1E), where the PRMT5$^{fl/fl}$ Ly5.2 contribution was significantly reduced in the myeloid (64.85 ± 14.50% reduction, p=0.047) and B cell (55.75% ± 4.07% reduction, p=0.005) populations in the bone marrow, and in the T cells (61.22 ± 8.49% reduction, p=0.019) of the thymus.

4.3 Generation of an *in vitro* model of PRMT5 deletion in a leukaemic cell line

To assess whether deletion of PRMT5 leads to cellular death *in vitro*, we sought to generate a leukaemic cell line in which we were able to delete PRMT5. To do this, ERT2Cre$^{Tg/Tg}$ PRMT5$^{fl/fl}$ and respective cre control mice were transplanted with fetal liver cells that had been infected with the MLL-ENL oncogene construct that contains an eGFP reporter. Once leukaemia development was confirmed in the blood of mice (by analysing eGFP levels via FACS), the mice were culled, and their spleens were harvested. The splenocytes were adapted to IL-3 *in vitro* to generate a cell line (Fig 4.2A). Two cell lines were generated; an MLL-ENL PRMT5$^{fl/fl}$ line in which genetic deletion could be induced with 4OHT treatment, and an MLL-ENL Cre control line

where although cells would express cre following treatment with 4OHT, there would be no PRMT5 deletion. To confirm that this was the case, growth assays were conducted with the two cell lines treated with 4OHT over a 2 week period. In the context of $^{PRMT5fl/fl}$, at the lower dose of 3nM 4OHT, by day 4 cell growth is impacted and by day 8, the number of total cells was only 4% of that obtained in the vehicle (EtOH) control group. This effect was even more pronounced when treating with a higher dose of 10nM 4OHT. In this situation, total cell numbers started to show a reduction by as early as day 6 and cell numbers continued to progressively decline over the last 8 days (Fig 4.2B; right panel). We confirmed this was due to PRMT5 deletion in three ways. Firstly, we treated our cre control line with 4OHT and found that cells treated with 10nM 4OHT continued to expand, and there was only a slight impact on cell growth over the two week period (Fig 4.2B; left panel). Furthermore, protein was harvested at day 4 of treatment and analysed via Western blot. The results confirmed that there was a loss PRMT5 protein that was only observed in the $PRMT5^{fl/fl}$ line (Fig 4.2B). Lastly, as another control to ensure the effect we were seeing on cell growth was not due to 4OHT toxicity, we treated parental MLL-ENL cells with 100nM 4OHT (10x the highest dose used in the $PRMT5^{fl/fl}$ line). There was no difference in cell growth at this dose when comparing to vehicle treated cells (Fig 4.2C).

4.4 Achieving enforced PRMT5 expression *in vitro* in the MLL-ENL line

To be able to elucidate whether enforced expression of exogenous PRMT5 can rescue the phenotype we observed in the above experiments, we utilised an MSCV retroviral construct. This retroviral construct, which contains the PRMT5-FLAG sequence and an IRES-driven mCherry was used to infect MLL-ENL cells. Infection was confirmed by assessing mCherry levels via FACS, and cells were single cell sorted to obtain a pure population of cells that were enforcing expression of PRMT5 (Fig 4.3A). To analyse the effects that various mutations have on PRMT5 activity and its ability to rescue, we utilised three different constructs. A construct that contained wild type PRMT5 (referred to as WT), one with a mutant that is believed to also be able to asymmetrically dimethylate due to a F327M mutation (71) – referred to as aDMR - and a third mutant that lacks methylation capabilities due to H367A and R368A mutations (86) - referred to as md (Fig 4.3B). Crystal structure analysis

revealed that the aDMR mutation was found in the pocket where PRMT5 binds to substrate. Although relatively close to the aDMR mutation, the md mutant appeared to be associated with the region where PRMT5 interacts with SAM (Fig. 4.3C). Protein was harvested from the different mutant populations, and Western blot analysis was conducted to assess the effects that the retroviruses had on PRMT5 levels and other associated proteins. Most importantly, PRMT5-FLAG looked to be exogenously expressed in all lines except for our empty vector control. This can be seen by binding of the α-FLAG antibody in these lines, and by the presence of a heavier band when the blot is probed with α-PRMT5. Based on visual inspection of the fluorescence intensities, exogenous PRMT5 is expressed at higher levels than endogenous in the WT and aDMR mutants, and there seems to be a downregulation in endogenous PRMT5. This can be seen by comparing the intensity of the bottom band when probing for PRMT5 to the endogenous PRMT5 band in the EV control. Although there is certainly exogenous expression of PRMT5 in the md mutant, the exogenous expression levels do not appear to be as high as our WT and aDMR mutant lines. Furthermore, there is no suppression of endogenous PRMT5 in the md line. Although we achieved enforced PRMT5 expression, this did not affect MEP50 protein levels or the H4R3me2s methylation mark, which remained consistent between all lines. Furthermore, probing with α-sDMR and α-aDMR antibodies revealed no clear distinction between our lines (Fig. 4.3D).

To generate a more quantitative measure regarding how much enforced expression was achieved, we analysed *Prmt5* mRNA expression and protein levels via FACS, utilising the same FACS-based strategy introduced in chapter 3. qRT-PCR analysis of RNA harvested from the lines confirmed that PRMT5 was significantly overexpressed in all three lines when compared to the EV control. Higher overexpression was seen in the WT mutant (fold increase of 31.4 ± 3.8, P=0.001) and the aDMR mutant (fold increase of 29.8 ± 3.8, P=0.002), but overexpression was half as pronounced in the md mutant (fold increase of 16 ± 2.8, P=0.006)(Fig 4.3E). When comparing the MFI of the AF488 secondary antibody bound to the α-PRMT5 antibody via FACS as a measure of protein level, we found that PRMT5 protein was overexpressed at similar levels in all three PRMT5 overexpressing lines [WT: 4.4 ± 0.7 fold increase, P=0.02; aDMR: 4.8 ± 0.8 fold increase, P=0.021; md: 3.9 ± 0.1 fold increase, P=0.002) when compared to EV (Fig. 4.3F).

To determine whether there was a growth advantage in the generated cell lines, a cell growth assay was performed. To do this, cells were counted every second day over a period of 6 days. It was found that overexpression of either one of the constructs did not result in a higher proliferation rate in either one of the cell lines compared to the EV controls (Fig. 4.3G).

4.5 Mutations in PRMT5 can alter response to PRMT5 inhibition

As PRMT5 inhibition is known to influence cell growth in the MLL-ENL cell line, we sought to determine whether different mutations of PRMT5 may alter the response to inhibition. To do this, we conducted a 6-point cell death dose response assay in our generated lines, where cells were treated for 72 hours with a PRMT5 inhibitor (PRMT5i). Although there are confidentiality agreements surrounding the inhibitor, and therefore there are restrictions to the amount of information that can be presented in this thesis, this particular inhibitor has been shown to be a potent and very selective inhibitor of PRMT5. Cell death was measured via FACS using SytoxBlue, and growth curves were generated that allowed us to analyse the response we saw in our various PRMT5 overexpressing lines as compared to the EV control (Fig 4.4A). An LD50 was calculated for each of the lines. In our WT line, the LD50 was found to be significantly higher (375.1nM ± 26.6nM) when compared to EV (178nM ± 28.9nM, P=0.003). In contrast, in the md mutant the LD50 was found to be significantly reduced (96.3nM ± 17nM, P=0.05). Interestingly, we were unable to generate an LD50 value for the aDMR mutant, as the highest dose of the inhibitor that was utilised in the assay (1uM) did not result in 50% cell death. In fact, at the highest dose, over 98% of the cells were found to be viable when normalised to the vehicle treated group. For this reason, the LD50 is reported as being >1uM (Fig. 4.4B).

It is important to note that the inhibitor that was used in this experiment is known to strongly bind to the substrate binding pocket of PRMT5 in a competitive fashion. We therefore aimed to analyse whether this response could be linked to the binding property of the specific inhibitor.

4.6 Response to inhibition depends on specific drug interaction

To confirm whether this resistance response that was seen in the aDMR line is specific to substrate competitive PRMT5 inhibitors, we treated our EV and aDMR lines with three different PRMT5 inhibitors (overview schematic of binding profiles of the inhibitors is summarised in Fig 4.5C). When treating the lines with a second inhibitor (PRMT5i-2) that is substrate competitive, we again found that the LD50 values was over 1uM. We confirmed that, when compared to the LD50 of EV (167.7nM ± 19.2nM), the aDMR line was resistant to treatment with this inhibitor (LD50 reported as <1000nM, $P<0.0001$). This response was found to be specific to the type of inhibitor that was used. When utilising a SAM competitive PRMT5 inhibitor (PRMT5i-3), compared to the EV line, the aDMR line was found to have no significant difference in LD50 (3.6nM ± 0.3nM vs. 3.3nM ± 0.4nM, respectively, $P=0.56$). Furthermore, when treating cells with an inhibitor that is able to competitively bind to both the substrate binding and SAM interacting pockets (dual inhibitor – “PRMT5i-4”), there was no difference in LD50 when comparing the EV and aDMR lines (7.4nM ± .5nM vs. 12.3nM ± 2.7nM, respectively, $P=0.15$)(Growth curves in Fig. 4.5A and LD50 overview in Fig. 4.5B).

4.7 Resistance to inhibition is sustained long-term

A cell death resistance response was observed in the aDMR line when treated with substrate competitive PRMT5 inhibitors. However, it was still unclear what the cytostatic effects of the drug were, or whether this cell death resistance was reflective of a delayed response as the cell death assays were run over a 72 hour period. To address this, the EV, WT and aDMR lines were treated with 4 doses of PRMT5i for a period of 10 days in a cell growth assay. Cell counts were obtained every second day and growth curves were generated to assess the long-term effects of PRMT5 inhibition on the cell growth abilities of the various lines.
In the context of EV, by day 4 cell growth had been affected by PRMT5 inhibition. There was a complete loss of cells at the 1uM dose, and there was 24% the number of cells at the 100nM dose compared to the vehicle (Fig. 4.6A). This response was less pronounced in the WT cells, and the same response took another 2 days to

achieve. At the 6-day time-point in these cells, there was 23% the number of cells at the 100nM dose as compared to vehicle, and like in the EV cell line, all the cells had died at the highest dose of inhibitor used (Fig. 4.6B). In the aDMR line, over the length of the 10-day assay, cells continued to grow at the 1uM dose of inhibitor. As a comparison, at the 100nM dose at the 6-day time-point, there was still 65% the number of cells as compared to vehicle. This suggests that the resistance response in the aDMR line is maintained long-term.

4.8 Exogenous PRMT5 expression in an *in vitro* PRMT5 deletion model

As we confirmed that PRMT5 deletion is detrimental to cells *in vitro*, we next generated a model that would allow us to determine whether enforced expression of PRMT5 would rescue the cells from this observed phenotype. The functional relevance of the different domains of PRMT5 could also be assessed by enforcing expression of our aDMR and md mutants. To do this, the MLL-ENL cell lines that we generated and validated from the ERT2Cre transgenic mice (section 4.3) were infected with our various MSCV constructs, and 8 cell lines were generated. 4 lines (representing EV, WT, aDMR and md infected lines) both within our Cre control and $PRMT5^{fl/fl}$ cell lines (Fig. 4.7A).
Protein was harvested from these cell lines, and a Western blot was conducted to assess whether there was enforced expression of PRMT5 protein post infection and single cell sorting of mCherry positive cells (Fig. 4.7B). When cells were infected with the EV, there was no enforced expression, as visible by the absence of a band when probing with an α-FLAG antibody. However, when cells were infected with the other 3 constructs, FLAG protein was detected alongside a slightly heavier band when probing for PRMT5 (indicative of our PRMT5-FLAG protein).

4.9 There was a failure to rescue the phenotype associated with PRMT5 deletion

The generation of the above-mentioned cell lines allowed us to assess the rescue capabilities of enforcing exogenous, retroviral expression of PRMT5. To do this, the cell lines were treated with 4OHT at a dose of 10nM to delete endogenous levels of

PRMT5, and cell growth was assessed over a period of 2-weeks by counting cells every other day. In the Cre control cell lines, across all the different vector variants, 4OHT had a similar effect on cell growth as observed when validating these cell lines (Fig 4.2B: left panel) and cells continued to proliferate across the 14 days (Fig. 4.8A: filled circles). However, 4OHT treatment in the PRMT5$^{fl/fl}$ cell lines resulted in an eventual loss of cell proliferation across all the vector variants. This response was comparable in the EV, WT and md variants, where cell growth was impacted from day 4-6, and there was a progressive decline in cell numbers from day 8 – 10. In the PRMT5$^{fl/fl}$ aDMR line, although initially there seemed to be a rescue of the phenotype in the first 8 days of the assay, by day 10 there is a reduction in cell growth and cells stopped proliferating by day 14 (Fig. 4.8: empty circles).

Protein was harvested at day 4 of the assay and was analysed by Western blot to confirm whether there was deletion of endogenous PRMT5, as well as check the effect that PRMT5 depletion had on methylation (with the sDMR and H4R3me2s antibodies). No deletion of endogenous PRMT5 was observed in the cre control lines. In the PRMT5$^{fl/fl}$ lines, deletion of endogenous PRMT5 was observed, however this was only restricted to the EV, WT and md lines at this time-point. In the context of the PRMT5$^{fl/fl}$ cells infected with EV, this depletion led to a loss of sDMR and a reduction in H4R3me2s. What is also important to note, is that PRMT5 deletion also lead to a reduction in the levels of MEP50 protein. In the WT and md setting, there was a reduction or complete loss of the sDMR and H4R3me2s proteins by day 4 of 4OHT treatment, which supports the phenotype observed in the cell growth assay. In the PRMT5$^{fl/fl}$ aDMR cell line, however, endogenous PRMT5 was not deleted by day 4 of the assay (Fig. 4.8B). Although no protein was harvested at the later time points for analysis, the cell growth data (and the loss of proliferation after 14 days in the PRMT5$^{fl/fl}$ aDMR cell line) would suggest that deletion was delayed in this particular cell line.

4.10 Discussion

4.10.1 Using an MSCV retrovirus to drive exogenous PRMT5 protein expression

The use of a retroviral system seemed to overcome the modest overexpression levels we observed in chapter 3. However, like the Rosa26 model in the previous chapter, although we achieved high overexpression of PRMT5 at the mRNA level of around 30-fold, this still only translated to 4-5-fold increase in protein level. As we also confirmed that enforced expression of PRMT5 did not result in an increase in MEP50, this brings to question whether higher MEP50 levels are required for even higher levels of exogenous PRMT5 expression and activity. To our knowledge, there are no reports of the effects of simultaneously exogenously expressing both PRMT5 and MEP50. This could be achieved in the MSCV-PRMT5 retroviral system used in this chapter by incorporating the MEP50 sequence after PRMT5 with a P2A self-cleaving peptide in between. This bicistronic design would ensure that PRMT5 and MEP50 would be expressed in a 1:1 ratio.

Another potentially interesting, albeit inconclusive finding, is that exogenous PRMT5 might potentially be responsible for downregulating endogenous PRMT5. This finding will need to be confirmed at the RNA level, by comparing the contribution of endogenous vs. exogenous PRMT5 mRNA.

4.10.2 Resistance to substrate binding PRMT5 inhibitors in our aDMR mutant

We achieved long-term resistance to PRMT5 inhibition in our aDMR mutant line. However, this was only restricted to PRMT5 inhibitors that bound to the substrate binding pocket of PRMT5. As the F327M mutation is found inside the substrate binding pocket, it would suggest that the mutation might make substrate competitive inhibitors unable to bind to the aDMR mutant PRMT5. There is a lack of literature on this mutant form of PRMT5, with a paper by Sun et al. providing the main description (71). It has been suggested that this change from a phenylalanine to a methionine might make the site more ‘flexible’ and makes the protein conformationally resemble PRMT1. To address the question of whether the inhibitor can bind the mutant form, the deletion cell line could be utilised to deplete endogenous PRMT5. Using the

substrate competitive inhibitor, conjugated to a magnetic particle, cells could be treated and protein could be harvested to perform a co-immunoprecipitation (co-IP). This technique would allow for the analysis of whether there is any drug-mutant protein interaction occurring.

Although this mutant form is reported as being functionally capable of catalysing symmetric and asymmetric dimethylation, the only evidence provided in the literature that we are aware of is based on Western blot data. Through our experience, Western blot did not reveal any clear differences in levels of sDMR vs. aDMR in any of the lines. The use of the commercially available antibodies often gave varied results, with different band patterns being observed. From our knowledge, there has been no clear validation of any of the antibody targets.

4.10.3 Further mutational and binding partner studies

As mentioned, the link between the F327M mutation and gain of function asymmetric capabilities of PRMT5 is weak. Further studies are required to delineate the requirements for symmetric vs. asymmetric dimethylation. Traditional global mutagenesis studies utilising radiation or chemically induced DNA damage presents with downfalls. Because most mutations are located outside the target of interest, there is a requirement to generate and maintain a large number of cells. Other methods involving plasmid libraries can often result in inappropriate expression or regulation of the target protein, and the libraries are often limited in diversity and length. One way to overcome this, and to generate a diverse library of mutants in their native context is to utilise CRISPRx (146). This is a technology that harnesses the power of activation-induced cytidine deaminase (AID) that is responsible for the process of somatic hypermutation that B cells undergo to introduce point mutations in the immunoglobulin (147). By utilising a catalytically inactive form of Cas9, this method can be used to target AID to induce a diverse range of localised point mutations, as active Cas9 is known to induce mutations via insertions and deletions. This technique could be used to target PRMT5, and to generate a spread of point mutations within the protein. The resistance phenotype of F327M could be confirmed, but CRISPRx might also provide some insight regarding the structural requirements responsible for aDMR vs. sDMR outside of this specific point mutation.

Furthermore, whether there are any binding partner differences between wild type PRMT5 and the aDMR mutant form is unknown. As PRMT5 plays a role in many major biological processes (involving both histone and non-histone substrates), work has been done to try and characterise changes in methylation, particularly in the context of inhibition as PRMT5 inhibitors gain traction as anticancer compounds (148). Advances in technology have overcome some of the challenges associated with analysing protein methylation (a particularly challenging posttranslational modification to characterise). Antibody-based methods can now be employed for the enrichment of arginine methyl peptides (149). When this affinity enrichment is combined with stable isotope labelling with amino acids in cell culture (or SILAC for short), MS can be performed to generate a comprehensive profile of the arginine methyl proteome. This could be harnessed with the use of the aDMR mutant as compared to wild type PRMT5, as these methyl proteomes can be generated to include accurate measures of both sDMR and aDMR and could offer insight as to the functional differences between the PRMT5 variants.

4.10.4 PRMT5 deletion phenotype could not be rescued with exogenous retroviral expression of PRMT5

Although we were able to confirm that PRMT5 deletion is detrimental to cells in our ERT2Cre *in vivo* and *in vitro* models, we were unable to rescue the phenotype with exogenous expression of PRMT5. It brings to question whether the exogenous PRMT5 expressed by our retrovirus is functional.

Although the data is not shown, we generated primers that spanned the whole length of the PRMT5 sequence, and we confirmed that the sequence in the vectors was indeed correct, with the appropriate mutations only existing in the mutant forms of the vectors. The lack of rescue was not due to sequence errors. The results obtained from the inhibitor experiments would suggest that the protein is functional. Although the WT and md cell lines both expressed PRMT5 protein at comparable levels (about 4 fold over EV control), the WT cell line showed slight resistance to the inhibitor, while the md line showed increased sensitivity. If both the WT and md overexpressed proteins were non-functional, we would expect that the response

would be quite similar between the two lines. This, however, would need to be corroborated with *in vitro* methylation assays that confirm that the exogenously expressed PRMT5 is in fact functionally active, and the md variant would act as a catalytically inactive control. Another potential area of clarification revolves around whether the incorporated FLAG tag interferes with the integration of the ectopic PRMT5 into a functional PRMT5 complex. If this is the case, there is a possibility that the non-functional FLAG-tagged protein reduces the effectiveness of the inhibitor if the ectopic protein is still able to interact with the drug.

There is literature that has found that enforced PRMT5 expression only partially rescues the deletion phenotype following endogenous depletion. This was done in the context of colony forming capability where cells generated from ERT2Cre $PRMT5^{fl/fl}$ mice were also used (150). Why this is the case is unclear. The above mentioned bicistronic retroviral system could be employed to assess whether enforced MEP50 is also required to ensure rescue in the deletion setting.

4.10.5 PRMT5 deletion and its complex roles in splicing defects and DNA damage

As PRMT5 is known to be a regulator of RNA splicing, it is unsurprising that deletion of PRMT5 has been reported to alter the splicing of many different proteins. Studies have shown that PRMT5 deletion leads to reduced methylation, aberrant constitutive splicing and alternate splicing of specific mRNAs with weak 5' donor sites (88). These events can lead to altered cell-cycle progression and apoptosis and may contribute to the cell death phenotype observed following depletion of PRMT5.
One protein that has been reported to be affected by splicing defects is *Mdm4*, a key p53 activator. It is suggested that cells can 'sense' these splicing defects by an increase in the expression of a shorter, less stable isoform known as MDM4S. This increase leads to the activation of the p53 transcriptional program (88). Another example includes an increase in the exon skipping events observed in the mRNA of eIF4E (involved in directing ribosomes to the cap structures of mRNAs) which is a rate limiting component in the translation process. These exon skipping events are thought to affect genes involved in apoptosis and cell cycle arrest (88, 151).

Another effect of PRMT5 deletion that has been reported is the induction of DNA damage and genomic instability. This DNA damage response includes the phosphorylation of histone H2AX. This generation of H2AX in the regions surrounds the DNA break sites, together with other histone modifications, leads to the recruitment of proteins that are involved in non-homologous end joining (NHEJ) or homologous recombination (HR) DNA repair. In deletion studies, loss of PRMT5 is thought to cause defective HR based repair, which leads to the activation of p53. This leads to cell cycle arrest or death (150).

It would be informative to analyse the contribution that the splicing machinery defect and the DNA damage response has on the phenotype of future deletion experiments. This would allow us to observe whether there is any partial rescue or alleviation in either pathway with exogenous expression of PRMT5. As p53 seems to be a key mediator of cell death in many of these complex processes, it would also be interesting to look at the rescue capability of exogenous PRMT5 in a p53 null background, as cell death is eventually seen with PRMT5 deletion even in the p53 null setting, albeit the response has been reported to be delayed (145).

4.10.6 Conclusion

In summary, a retroviral system was utilised to enforce expression of exogenous wild type PRMT5 and two other mutant variants. Although PRMT5 deletion leads to a loss of cells both *in vitro* and *in vivo* in the ERT2Cre PRMT5$^{fl/fl}$ background, we were unable to rescue this phenotype with exogenous expression of PRMT5. Experiments utilising the vectors infected into MLL-ENL cells suggest that the protein is in fact functional, as there was a resistance associated with exogenous expression of wild type PRMT5, and sensitivity associated with exogenous expression of catalytically inactive PRMT5. Interestingly, cells that enforced expression of aDMR mutant PRMT5 were found to be resistance to PRMT5 inhibition both in a cell death and cell growth assay, and this response was maintained long-term. However, this was restricted to substrate competitive PRMT5 inhibitors that bound to the substrate binding pocket, and not inhibitors that were SAM competitive, or dual-competitive. Generating a bicistronic vector that would allow us to co-express MEP50 would allow us to assess the effects of MEP50 overexpression alongside PRMT5, and whether this allows the deletion phenotype to be rescued. Future studies should also analyse any methylosome profile differences between wild type PRMT5 and the asymmetric dimethyl mutant, which might provide insights into the structural relevance of this mutation.

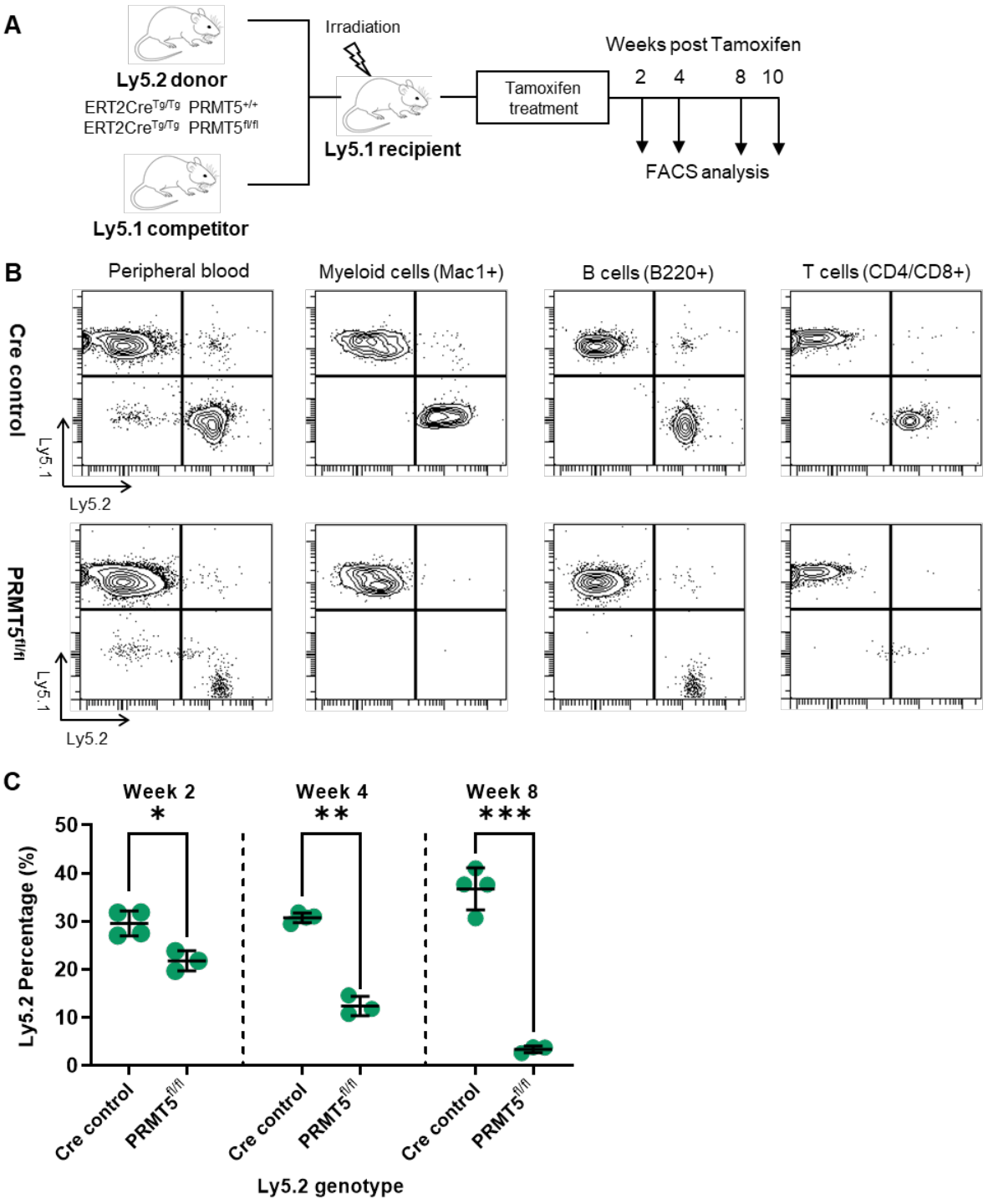
A
Ly5.2 donor
ERT2Cre^Tg/Tg PRMT5^+/+
ERT2Cre^Tg/Tg PRMT5^fl/fl
Ly5.1 competitor
Irradiation
Ly5.1 recipient
Tamoxifen treatment
Weeks post Tamoxifen
2 4 8 10
FACS analysis
B
Peripheral blood
Myeloid cells (Mac1+)
B cells (B220+)
T cells (CD4/CD8+)
Cre control
PRMT5fl/fl
Ly5.1
Ly5.2
C
Week 2
Week 4
Week 8
*
**
***
Ly5.2 Percentage (%)
50
40
30
20
10
0
Cre control
PRMT5fl/fl
Ly5.2 genotype

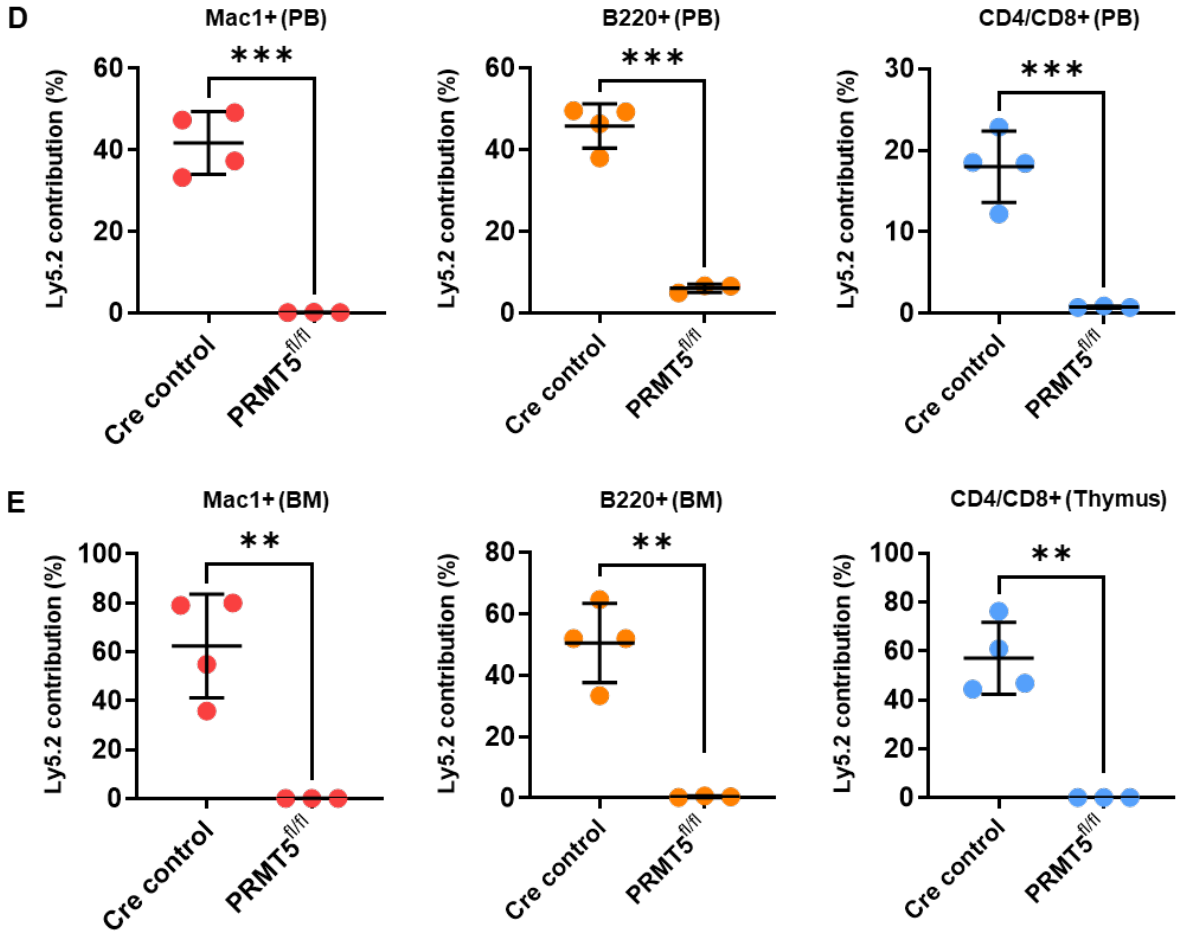

Figure 4.1 Effects of PRMT5 deletion *in vivo* on haematopoiesis.
(A) Experimental design of competitive transplant assay conducted to assess the effects of PRMT5 deletion following treatment with tamoxifen. **(B)** Representative Ly5.1/Ly5.2 separation FACS gating strategy of myeloid cells (Mac1+), B cells (B220+) and T cells (CD4/CD8+) of peripheral blood 8 weeks after tamoxifen treatment. **(C)** Changes in Ly5.2 donor proportions over an 8 week period following tamoxifen treatment. Mice were culled at 10 weeks post tamoxifen, and the myeloid, B cell and T cell contribution of the Ly5.2 donor cells were analysed in either the **(D)** peripheral blood (PB), **(E)** Bone marrow (BM) or thymus. All analysis was performed comparing ERT2Cre$^{Tg/Tg}$PRMT5$^{fl/fl}$ mice to cre controls. Mean ± SEM of n=3-4 are shown. *P<0.05, **P=<0.01, ***P<0.001, student's t-test as compared to cre controls.

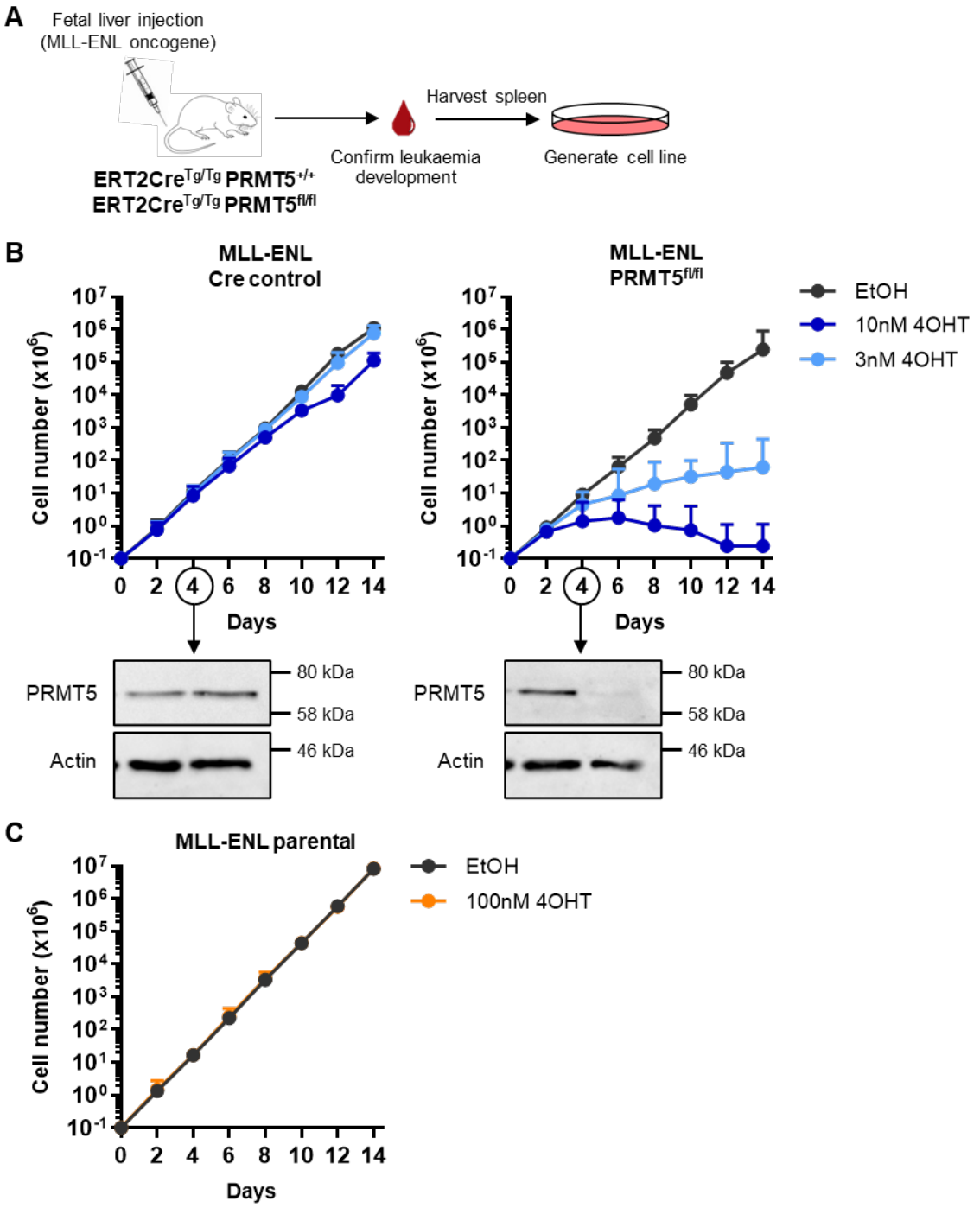

Figure 4.2 Generating an *in vitro* PRMT5 deletion model.
(A) Schematic of generation of leukaemic cell line in which PRMT5 is deleted with 4OHT. **(B)** Growth curves generated over a 2 week period after treatment with 2 doses of 4OHT in MLL-ENL PRMT5$^{fl/fl}$ and a cre control cell lines. Mean ± SEM of three independent experiments is shown. Protein harvested at day 4 was analysed via Western blot for levels of PRMT5, and the representative results are shown below the growth curves. Actin was used as the loading control. **(C)** Growth curves of parental MLL-ENL cells treated with a higher dose of 4OHT over a two week period. Mean ± SEM of three independent experiments is shown.

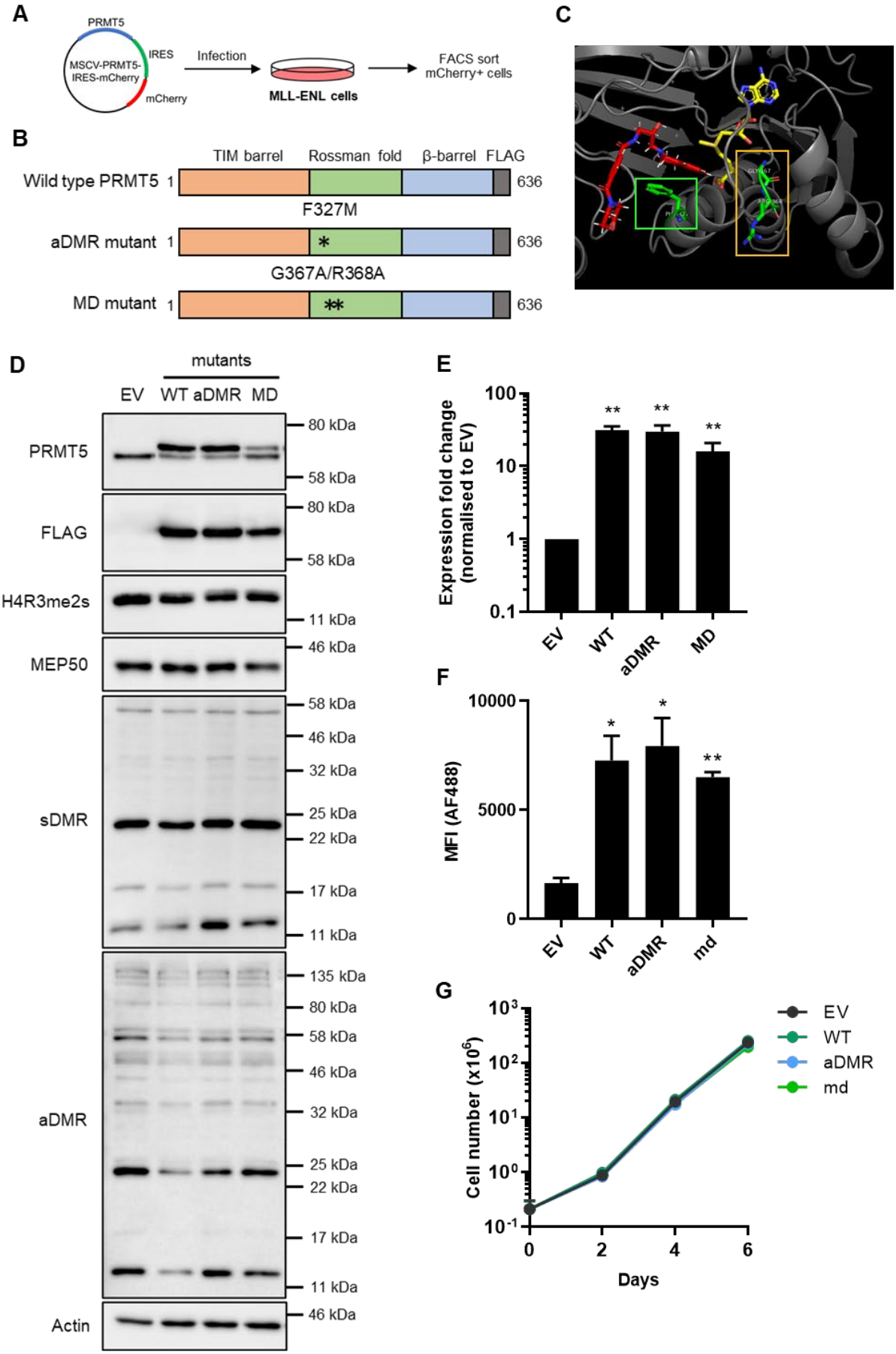
A
PRMT5
IRES
MSCV-PRMT5-IRES-mCherry
mCherry
Infection
MLL-ENL cells
FACS sort mCherry+ cells
B
TIM barrel
Rossman fold
β-barrel
FLAG
Wild type PRMT5
1
636
F327M
aDMR mutant
*
G367A/R368A
MD mutant
**
C
D
mutants
EV
WT
aDMR
MD
PRMT5
FLAG
H4R3me2s
MEP50
sDMR
aDMR
Actin
80 kDa
58 kDa
46 kDa
32 kDa
25 kDa
22 kDa
17 kDa
11 kDa
135 kDa
E
Expression fold change (normalised to EV)
100
10
1
0.1
EV
WT
aDMR
MD
F
MFI (AF488)
10000
5000
0
md
G
Cell number (x10^6)
Days
EV
WT
aDMR
md

Figure 4.3 Retroviral overexpression of PRMT5 in MLL-ENL cells
(A) Schematic of MSCV vector infected into MLL-ENL cells to enforce PRMT5 expression. **(B)** Various PRMT5 constructs with * donating mutation locations. **(C)** Crystal structure of PRMT5 substrate binding pocket. Arginine substrate and SAM are coloured red and yellow, respectively. Green box denotes location of F327 mutation and orange box denotes location of G367A/R368A mutation. **(D)** Western blot analysis of the various PRMT5 overexpressing cell lines, probed for PRMT5 (total), PRMT5-FLAG, H4R3me2s mark, MEP50, sDMR and aDMR. Actin was used as the loading control. **(E)** RT-PCR of *Prmt5* mRNA expression, **(F)** MFI (associated with PRMT5 protein expression) and **(G)** growth kinetics (over a 6 day period) of the various cell lines. Mean ± SEM of 3 independent experiments are shown. *P<0.05, **P=<0.01, ***P<0.001, student's t-test comparing the overexpressing cell lines to the empty vector (EV) control.

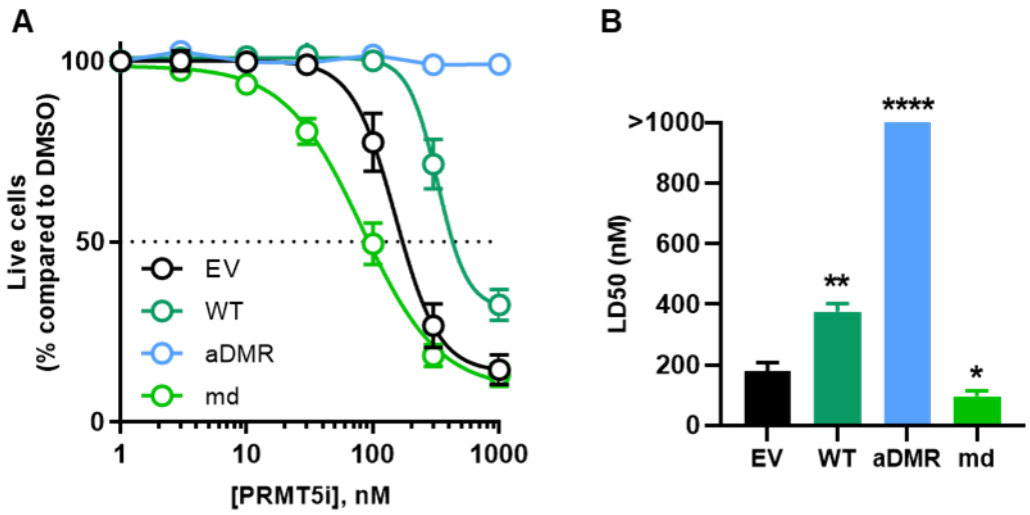

Figure 4.4 PRMT5 inhibition in overexpressing cell lines
(A) Growth curves following a 72 hour cell growth assay in various cell lines with enforced PRMT5 expression treated with a PRMT5 inhibitor. Cell numbers were compared to DMSO vehicle control. **(B)** The corresponding PRMT5 inhibitor LD50s in the various cell lines. Mean ± SEM of 4 independent experiments are shown. *P<0.05, **P=<0.01, ***P<0.001, student's t-test comparing the overexpressing cell lines to the empty vector (EV) control.

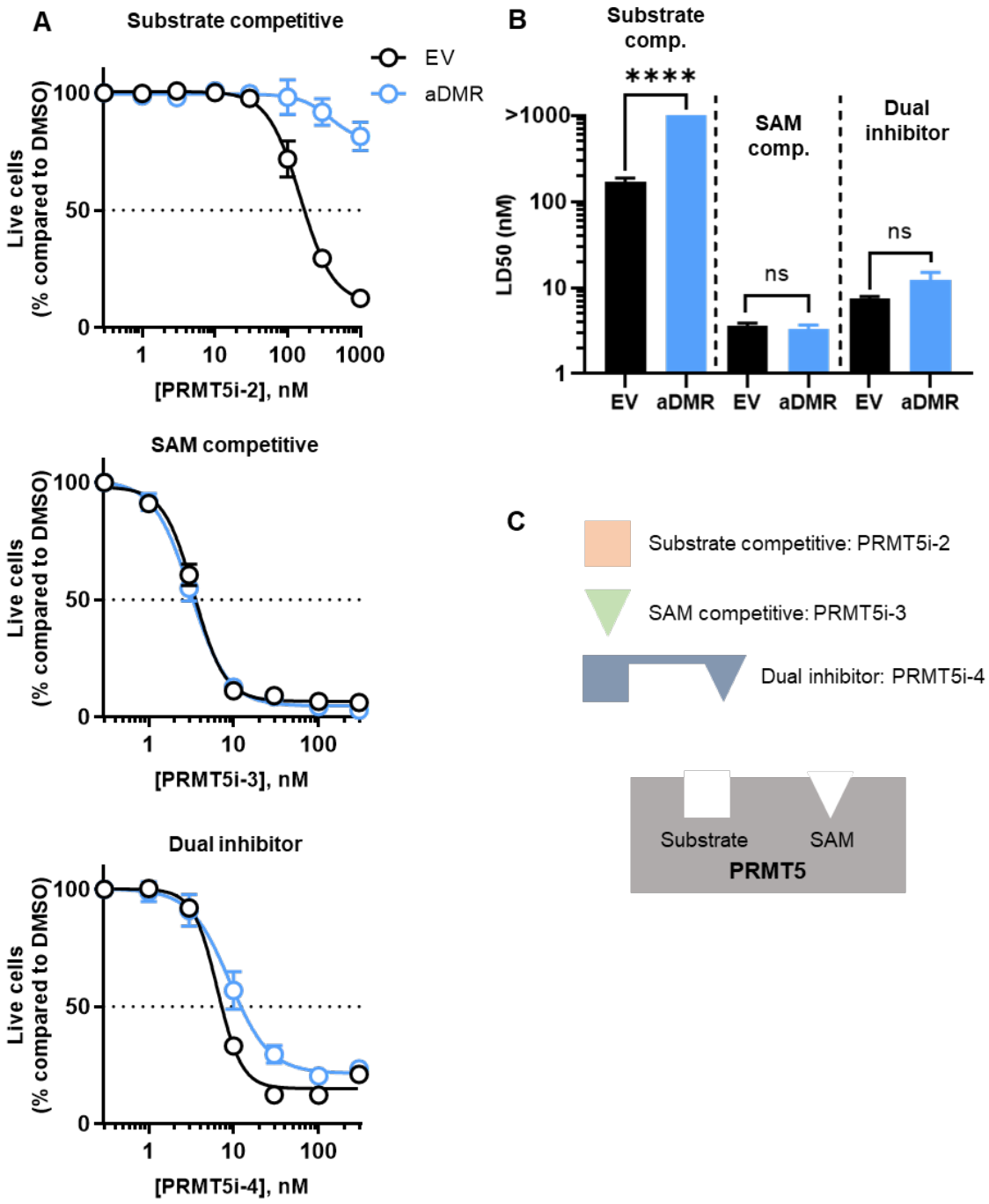

Figure 4.5 Response to substrate competitive vs. SAM competitive PRMT5 inhibitors.

(A) Growth curves following a 72 hour cell death assay in our aDMR mutant PRMT5 expressing cell lines compared to EV control with various PRMT5 inhibitors: a substrate competitive inhibitors, a SAM competitive inhibitor and an inhibitor that binds to both sites. Cell viability was compared to DMSO vehicle control. **(B)** The corresponding PRMT5 inhibitor LD50s in our aDMR mutant cell line as compared to EV control. Mean ± SEM of 4 independent experiments are shown. *P<0.05, **P=<0.01, ***P<0.001, student's t-test comparing the aDMR mutant cell line to the empty vector (EV) control. **(C)** A schematic demonstrating binding differences between the three inhibitors.

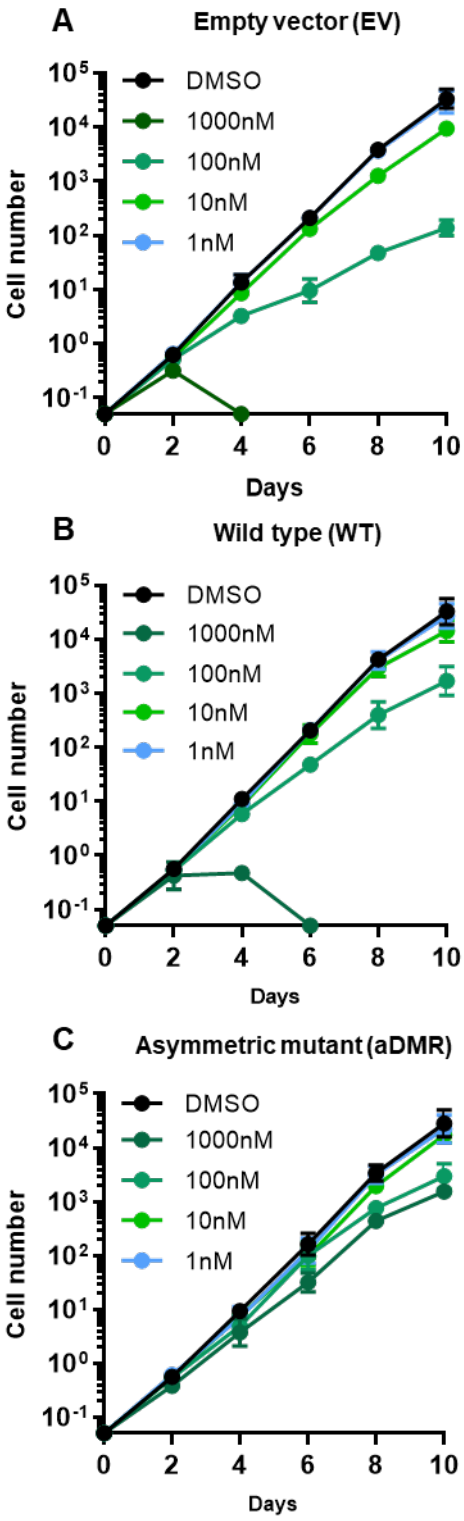

Figure 4.6 Long term treatment with a PRMT5 inhibitor
Growth curves over a 10 day cell growth assay in cells with enforced expression of WT (middle panel) and aDMR mutant (bottom panel) PRMT5 as compared to our empty vector control (top panel) when treated with a substrate competitive PRMT5 inhibitor. DMSO was used as a vehicle control. Mean cell number ± SD of 3 independent experiments are shown.

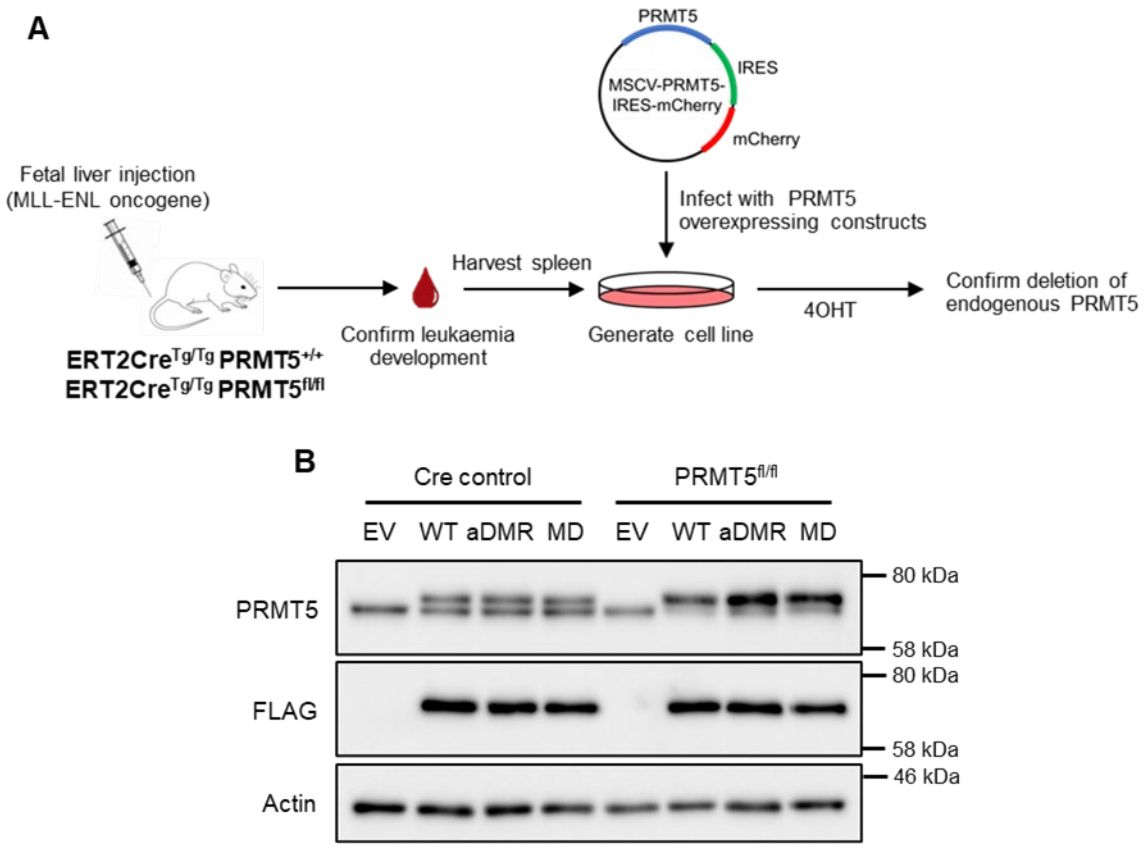

Figure 4.7 Generation of *in vitro* rescue model of PRMT5 deletion
(A) Schematic of rescue experiment where a leukaemic cell line generated in transgenic mice modelling PRMT5 deletion are infected with vectors in order to enforce PRMT5 expression. **(B)** Western blot analysis of PRMT5 and PRMT5-FLAG protein in the infected cre control and PRMT5$^{fl/fl}$ cell lines. Actin was used as a loading control.

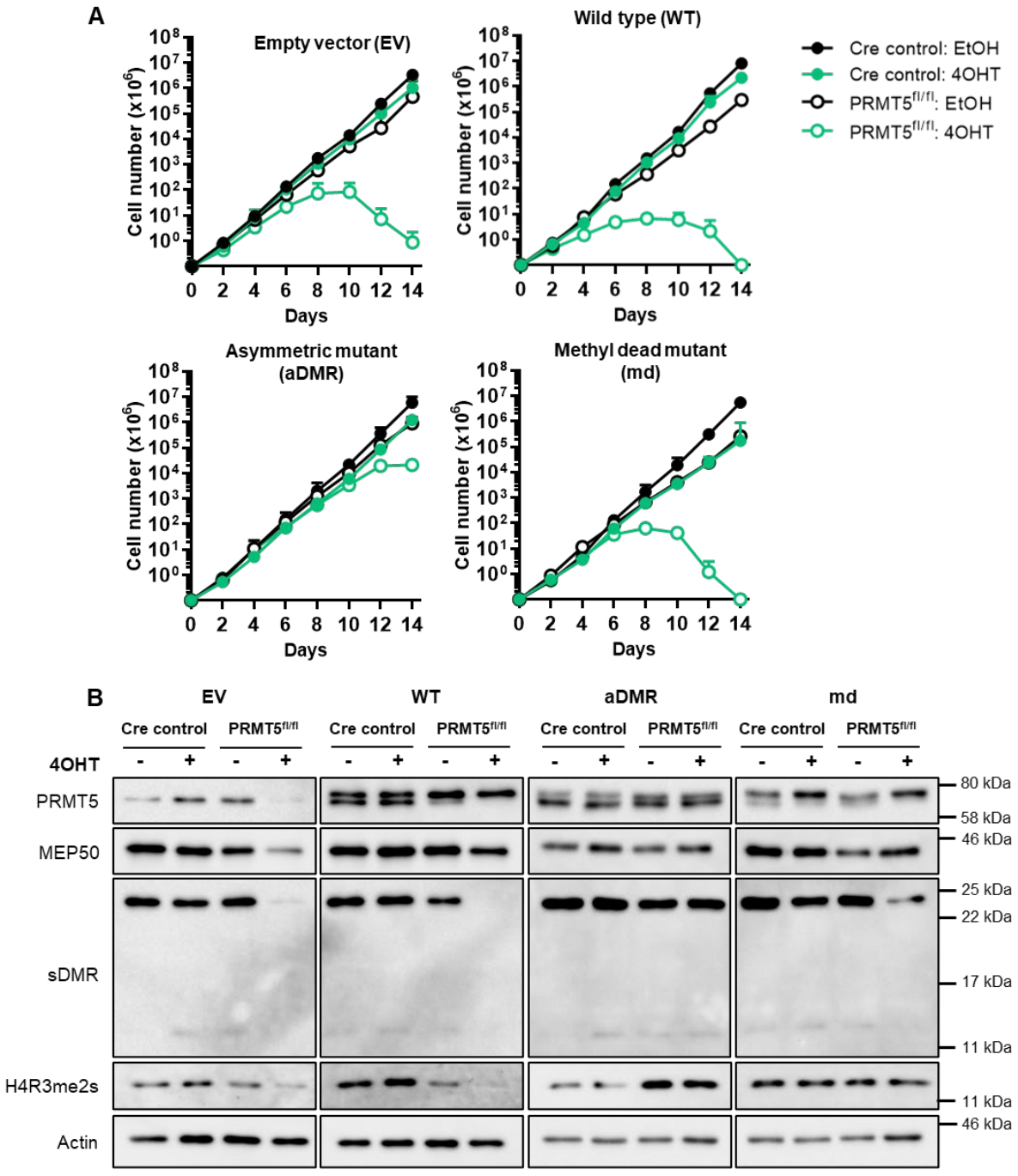
A
Empty vector (EV)
Wild type (WT)
Asymmetric mutant (aDMR)
Methyl dead mutant (md)
Cell number (x10^6)
Days
Cre control: EtOH
Cre control: 4OHT
PRMT5fl/fl: EtOH
PRMT5fl/fl: 4OHT
B
EV
WT
aDMR
md
Cre control
PRMT5fl/fl
4OHT
PRMT5
MEP50
sDMR
H4R3me2s
Actin
80 kDa
58 kDa
46 kDa
25 kDa
22 kDa
17 kDa
11 kDa
11 kDa
46 kDa

Figure 4.8 Enforcing exogenous expression of PRMT5 in the *in vitro* PRMT5 deletion model.

(A) Growth curves following a 2 week cell growth assay in PRMT5$^{fl/fl}$ cells exogenously expressing PRMT5. Cells were treated with 10nM of 4OHT to induce deletion, and response was compared to Cre control cells. EtOH was used as the vehicle control. Mean cell number ± SD of 3 independent experiments are shown. **(B)** Western blot analysis of samples taken at day 4 from the above experiment probing for PRMT5, MEP50, sDMR and the H4R3me2s methylation mark. Actin was used as a loading control.

Chapter 5:

Identifying mechanisms that confer sensitivity and resistance to PRMT5 inhibitors

5.1 Introduction

Treatment options for AML have been largely limited to cytotoxic chemotherapy for the past four decades. Through the use of NGS and other techniques, there has been a recent increase in the appreciation of the variety of genetic and epigenetic changes that contribute to AML onset and maintenance (152). With this knowledge, there has been a push for developing more targeted therapies, with the hopes of increase treatment efficacy and prolong survival, whilst reducing toxicity that is associated with chemotherapy. This has also led to an increase in the number of clinical trials that are currently being performed to assess efficacy of various drugs. This includes PRMT5 inhibitors (152, 153). However, because AML is a heterogeneous disease that involves an interplay between various genetic mutations (154), it is no surprise that monotherapies often led to eventual relapse. Because of this, there are a number of studies and trials assessing the efficacy of various drugs in combination (155, 156).

Recently, the generation of genome scale CRISPR/Cas9 knock-out (or GeCKO) libraries have been possible due to the development of a lentiviral delivery method. These libraries, which can target 10^2 to 10^4 genes allow for positive and negative selection screens to be performed on mammalian cell lines (157, 158). These phenotypic screens utilise sgRNA to knock out genes, and by applying selective pressure, can provide which genes are enriched or depleted in cells as an output. This method has been used in a publication by Gao et al. (159), where a library targeting a total of 1,016 epigenetic or cancer regulator genes, names the ‘Epigenetic regulator CRISPR’, or ‘EpiC’ was infected into a human lung cancer cell line. The experiment utilised the substrate competitive PRMT5 inhibitor, EPZ015666, and found that PRMT1 inhibition might sensitise cells to PRMT5 inhibition. Furthermore, MTAP deleted cells, which have been shown to have attenuated PRMT5 activity, are more sensitive to PRMT1 inhibition (159).

Throughout this chapter, a larger-scale CRISPR screen was performed in an AML cell line. A GeCKO library known as the ‘Brie’ library (targeting almost 20,000 genes) was utilised to perform a CRISPR screen in two MLL-ENL cell lines – a p53 wild type and a p53 null counterpart line. This was performed with the aim of identifying genes and pathways that may be involved in sensitivity or resistance to PRMT5 inhibition, the results of which may assist in generating data to support combination therapies in clinic.

5.2 Generation and validation of a Cas9 expressing cell line

As an overview, the CRISPR screen involved infecting MLL-ENL cell lines (both p53 wild type and p53 null) expressing the Cas9 endonuclease with a sgRNA library that contained 20,000 genes with 4 guides per gene that was targeted. These cells were cultured for a period of 2 weeks to cause a loss of representation of guides that were targeting cell essential genes. The cells were then split into two groups - cells that were treated with DMSO as the vehicle control, and cells that were treated with a predetermined, sublethal concentration of the PRMT5 inhibitor. These cells were treated until proliferation rates between the vehicle and PRMT5i treated groups returned to similar levels (suggesting that whatever guides remained in the treated pool represented genes that may confer resistance). NGS was then performed on DNA harvested from two different time points – one earlier time point with the hopes of catching genes that may be important for sensitivity and one later time point which would be important for catching genes that may confer resistance. The sgRNA representation in both the vehicle and PRMT5i treated groups were compared to the sgRNA library representation pre-infection. This then allows us to analyse expression changes of guides targeting specific genes between vehicle and PRMT5i treated cells (Fig. 5.1A).

As a precursor to conducting the screen, we generated cell lines that were expressing Cas9 in which Cas9 activity was validated. The two MLL-ENL cell lines were infected with a Cas9 lentivirus. After infection, cells were selected for with blasticidin. As we had trouble in the past with Cas9 validation, we further single cell sorted the cells to ensure pure populations. Protein was harvested from a number of

these populations, and Western blot was conducted probing with an α-Cas9 antibody. Although not all the populations in both the p53 wild type and p53 null cell lines expressed Cas9 – only 33% of cells in the wild type cells, and 83% in the p53 knockout cells - we were able to select a specific population to use for the screen. (Fig. 5.1B).

To validate Cas9 expression, cell lines were infected with a lentivirus known as BRD011. This construct expresses eGFP, but also expresses a sgRNA against GFP with the intention that eGFP will eventually be lost in cells that display Cas9 activity. BRD011 infected cells were selected for with puromycin. What is important to note is that the MLL-ENL oncogene also expresses eGFP, so our parental cell lines already initially expressed eGFP. In both the p53 wild type and null cell lines, as compared to uninfected parental cells, BRD011 infected parental cells (Cas9 negative) showed a slight increase in eGFP expression. However, in our clones that were expressing Cas9, we saw a loss of eGFP expressing cells 4 days after treatment with puromycin. Only 2% and 9% of cells expressed eGFP in the wild type cells and p53 null cells, respectively (Fig. 5.1C). As Cas9 activity was validated, these cells were next run through the CRISPR screen.

5.3 The CRISPR screen identified genes that confer sensitivity and resistance to PRMT5 inhibition

Both MLL-ENL Cas9 expressing cell lines were infected with the murine 'Brie' sgRNA library containing sgRNAs targeting 19,674 genes with 4 guides per gene (total of 78,637 guides). Cells were infected at a low multiplicity of infection (MOI = 0.3). Infected cells were selected for with puromycin and were cultured, untreated, for a period of 2 weeks to account for loss of cell essential genes. Both p53 wild type and p53 null MLL-ENL cell lines were then split into two groups – a group treated with DMSO as a vehicle control, and a group treated with the PRMT5i at a predetermined, suboptimal concentration. This was performed with two replicates per group. Cell count were obtained every 2-3 days to track the proliferation of the cells during treatment (Fig 5.2A and B). Initially, we observed that the concentration of the inhibitor that we initially used was not cause enough of a reduction in cell

growth, so after around 2 weeks of treatment (11 days for wild type p53 cells and 15 days for p53 null cells) we increased the dose with the intention of impacting cell proliferation in the treated cells. The increase in dose had the intended effect, and cell proliferation was reduced in the PRMT5i treated cells as compared to vehicle control. The proliferation rate of PRMT5i treated cells was compared to vehicle control in both cell lines (Fig 5.2C and D), and although by day 5 proliferation was reduced to less than 40% in both cell lines, proliferation rates in the PRMT5i treated group increased over the remaining 2 weeks of treatment. This proliferation trend was important, as it suggests that the surviving cells represent the pool of sgRNAs that may target cells that are responsible for resistance, and therefore treatment does not greatly impact proliferation in these cells.

To evaluate guide representations, DNA was harvested and analysed from two different time points after the dose was increased. DNA was harvested at the day 5 time point, with the aim that these samples might provide insight into guides that were beginning to lose representation and would therefore indicate genes that might be responsible for sensitivity. DNA was also harvested from at the day 16 time point. The representation of guides in these later samples would provide us with genes that might be responsible for resistance to treatment. The guide RNA representation was evaluated by the extraction of genomic DNA from surviving cells, PCR amplification of vector barcodes, and NGS sequencing.

After sgRNA reads were aligned to a sgRNA map, normalised and replicates were collapsed, we were able to compare the sgRNA representation changes in PRMT5i treated cells versus cells treated with DMSO. What we found, was that there were several genes that, when knockout, caused resistance or sensitivity to PRMT5i treatment. This was indicated by an increase or decrease in representation, respectively, of the sgRNAs that were targeting said genes. In the p53 wild type setting there was a higher number of both sensitivity and resistance hits in the samples taken at an earlier time point (Fig. 5.3A), most of which were lost by day 16 of increase treatment (Fig 5.3B). This would suggest that, by later time points you have complete loss of representation in many of the sensitivity hits, and any retained resistance hits would indicate genes that may be confer enhanced resistance. This was not as clear in the p53 null context, were fewer resistance hits were identified at

the earlier time point as compared to p53 wild type cells (Fig 5.4A), and there was an increase in the number of sensitivity hits at the later time point (Fig. 5.4B).

5.4 We were able to validate 'hits' in the p53 wild type, but not in the p53 null cell line

To validate the results of the CRISPR screen, we performed in house CRISPR experiments utilising only one sgRNA targeting specific resistance and sensitivity genes (2 guides per gene were used for validation) that were identified. Genes that showed significant differences in representation were selected based on their generated p-values (p-values were generated via MAGeCK analysis). Among these genes, candidate genes were selected based on their potential role in cancer and leukaemia (such as *Pten* and *Trp53*), or their reported interaction with PRMT5 (such as *Mtap)*. In the p53 wild type context, we decided to validate using guides against *Trp53* (Log2FC = 4.7, p<0.0001), *Calr* (Log2FC = 4.0, p<0.0001) and *Gata2* (Log2FC = 4.6, p<0.0001) as resistance hits (Fig 5.5A), and guides against *Pten* (Log2FC = -2.5, p<0.0001), *Mtap* (Log2FC = -4.4, p<0.0001), and *Uchl5* (Log2FC = -5.0, p<0.0001) as sensitivity hits (Fig 5.5B). In the p53 null context, we validated the resistance hits using guides against *Calr* (Log2FC = 3.8, p<0.0001), *Syvn1* (Log2FC = 3.5, p<0.0001) and *Cic* (Log2FC = 3.2, p<0.0001)(Fig 5.6A). Sensitivity hits were validated using guides against *Ezh2* (Log2FC = -3.7, p<0.001), *Suz12* (Log2FC = -3.3, p<0.05) and *Ino80* (Log2FC = -5.2, p<0.0001).

After cells were infected with the respective sgRNA and selected for with puromycin, they were treated with the PRMT5i at a range of doses for a period of 5 days, and viable cell were counted. This was done with the intention of generating GI_{50} values for each of the cell lines with the single gene knockout which could then be compared to cells that were infected with an empty vector backbone (BRD003) to assess whether there was sensitivity or resistance to inhibitor treatment.

In the p53 wild type MLL-ENL cells, we were able to validate most of the genes that we selected. When the sensitivity hits, MTAP and UCHL5 were knocked out, there was a significant reduction in GI_{50} values of around 5-fold as compared to empty vector control cells (Fig. 5.7A). When we knocked out p53, GATA2 and CALR, genes

that were responsible for resistance, we saw a significant increase of more than 2-fold in GI_{50} values as compared to empty vector control cells (Fig. 5.7B). However, validation was unsuccessful in the context of the p53 null MLL-ENL cells. When comparing the GI_{50} of each of the individual cell populations across all 6 genes that were selected as compared to empty vector controls, there was no significant difference (Fig. 5.8).

5.5 Sensitivity and resistance was specific to PRMT5 inhibition

We next aimed whether the sensitivity and resistance profiles we were seeing in the p53 wild type MLL-ENL cells was specific to PRMT5 inhibition. To elucidate this, we tested our knockout cell lines that we generated during validation with cytarabine – a common chemotherapy used in the treatment of AML. Cells were treated with varying concentrations for a period of 48 hours, and viable cell numbers were obtained. What we found, across all the resistance and sensitivity genes that we selected, there was no significant different in the GI_{50} values in any of the knockout lines as compared to empty vector control (Fig. 5.9). Resistance and sensitivity in these knockout lines was only observed when cells were treated with the PRMT5i.

5.6 Several pathways seem to be important for sensitivity and resistance.

To further interrogate the hits that we generated from the screen, a list of significantly underrepresented genes (defined as displaying a Log2FC<-2, $p<0.05$) and over represented genes (defined as displaying a Log2FC>2, $p<0.05$). Respectively, we generated a list of 166 genes that may be responsible for sensitivity when knocked out, and a list of 198 genes that may be responsible for resistance when knocked out.
These lists were uploaded to Metascape, and pathway analysis was conducted which generated a list of pathways associated with theses lists. The top 10 pathways that involved genes from the sensitivity list are listed in Fig. 5.10A – with metabolism of RNA being the top pathways. The top 10 pathways that involved genes from resistance list are shown in Fig.5.10B. In this case, histone modification came up as the strongest pathway.

5.7 Rationale drug selection.

The CRISPR screen performed throughout this chapter was conducted with the goal of providing us with data (both individual gene lists and pathway analysis data) that may assist in rationally identifying drug targets that may synergise with our PRMT5 inhibitor. For this purpose, we focused on genes that may be responsible for sensitivity to PRMT5 inhibition when knocked out, with the hopes that if we can inhibit said genes, we may be able to prime cells to cell death with PRMT5i treatment. With this in mind, we generated 4 gene lists that were utilised in drug selection. These lists consisted of 10-29 genes, and individual lists included sensitivity genes that had an FDR of <0.05, genes that were involved in RNA metabolism, genes that were involved in nucleotide excision repair (NER) and genes that were involved in negative regulation of mTOR. Each of these lists were separately uploaded to the clue.io platform (available at https://clue.io). Lists were analysed against the L1000 perturbational datasets that were generated by the NIH LINCS Consortium using gene expression assays (160). This was done with the intention of identifying compounds that may impact these pathways. Once a list of potential compounds was generated, we next sought to print these drugs at varying concentrations in 384 well plates to conduct a high throughput cell death drug screen. The screen consisted of pre-treating wild type p53 MLL-ENL cells with either a low dose of PRMT5i (determined to be 10nM) or DMSO vehicle as a control for 48 hours, before incorporating the cells into the drug plates for 72 hours. 140 different drugs were tested at three different concentrations – 3uM, 300nM and 30nM. Essentially, this allowed us to assess whether PRMT5i in combination with any of these drugs showed a synergistic, additive, or antagonistic effect. This was done by calculating a delta score. This delta score was calculated for each of the doses, and was represented by the observed effect (which was cell death) in combination treated cells minus the expected effect (expected effect was simply the effect observed in the PRMT5i alone treated cells + effect in compound alone treated cells). If a compound displayed a positive delta or a negative delta in combination, this would indicate synergism and antagonism with PRMT5 inhibition, respectively. A delta that is closer to 0 would suggest that drugs in combination are purely additive (Fig 5.11).

5.8 Synergy was observed with several drugs in combination with PRMT5 inhibition.

Delta scores were generated across all three doses that were used for each compound, and the greatest delta score was plotted as an indication of max. synergy. Based on previous data that has been generated in the lab, we know that the BCL-2 inhibitor, ABT199, and the DNA intercalator, Mitomycin, synergise with the PRMT5i, so the delta scores generated for these drugs (delta = 23.3 and 19.3, respectively) provide us with a delta score that may correlate with *in vitro* drug synergy. Other than these 2 drugs, the top 4 compounds that showed synergy include vincristine sulfate (delta = 17.9), Mocetinostat (delta = 20.4), KU-0063794 (delta = 22.5) and selumetinib (delta = 26.8) which displayed the highest synergistic delta score (Fig. 5.12A).

When observing the compounds that displayed a negative top delta score, there were far fewer compounds. We know, based on previous work, that cytarabine does not synergise with the PRMT5i, and its respective delta score was reflective of that (delta = -4.3). Ro-3306, an inhibitor of CDK1 was found to have the lowest negative delta score (delta = -41.9).

5.10 Dicussion

5.10.1 Using a CRISPR screen to identify genes that confer sensitivity or resistance to inhibition

Using the GeCKO sgRNA library, we were able to generate a list of genes that, when knocked out, conferred sensitivity or resistance to PRMT5 inhibition. However, our validation experiments suggest that reliable hits were only generated in the wild type MLL-ENL cell lines as opposed to the p53 null cells. Reassuringly, the screen identified *Trp53* as a resistance hit. *Trp53* sgRNAs were enriched both at day 5 and day 16, suggesting *Trp53* is responsible for longer term resistance. Although not shown here, our lab has previously seen increased resistance to PRMT5 inhibitor treatment in various p53 null cell lines. However, this has never been shown in an isogenic cell line. When validating with a sgRNA targeting *Trp53*, we were able to create an isogenic p53 that indeed showed resistance to PRMT5 inhibition. Data also suggests that a wild type p53 status may be crucial in ensuring sensitivity to PRMT5 inhibition *in vivo* (161). This is further supported by the literature. Gerhart et al. (162) have shown that colon cancer cell lines that are p53 null show increased resistance to PRMT5 inhibition, and they report that many of the downstream events of inhibition, such as alternate splicing and cell cycle arrest, are p53 dependent. Other reports using MLL-AF9 cell lines found that p53 null MLL-AF9 cell lines were resistance to differentiation that was induced by the EPZ015666 inhibitor (116). Another promising and validating find from the screen was that several PRMTs were identified as cell essential genes (and representation of their respective guides was subsequently lost soon after infection with the sgRNA library), including PRMT5. However, we were unable to validate the CRISPR data that we generated in the p53 null cell lines, and why this is the case is relatively unknown. Considering that many of the cell death and cell arrest effects that we see with PRMT5 inhibition seem to heavily rely on functional p53, it could be that the already intrinsic resistant status of the p53 null MLL-ENL cell line affect ‘true’ sensitivity hits. In the context of wild type p53, the number of significant resistance and sensitivity hits reduced with treatment time. When considering the resistance hits, we think this is because there are p53-independent effects of PRMT5 inhibition that seem to take time to trigger – this could explain the loss of resistance hits that were not able to overcome the combination of p53 dependant and independent effects of PRMT5 inhibition with increased

treatment time. When considering the sensitivity hits, analysis of an earlier time point is important as it is expected that you will eventually lose complete representation of these genes. In the p53 null context, there were fewer resistance hits at the earlier time point, which may be reflective of the paramount role that p53 has in the effect seen with inhibition, one that might trump other resistance mechanisms.

Furthermore, this resistance might confound any potential sensitivity hits as p53 null cells are more resistant to death generally.
Pooled CRISPR screens, like the one performed in this chapter, are restricted to simple readouts, such as cell proliferation/death (163). They do not support complex molecular readouts, such as transcriptome profiling, which is considered one of the more valuable readouts of cellular response (164). The use of arrayed CRISPR screens have allowed the possibility of using RNA-seq as a readout, however these are associated with lower throughput (165). Recently, a method to overcome this has been described, where pooled CRISPR screening is combine with single-cell RNA sequencing in a droplet-based method, known as CROP-seq. This method allows for pooled CRISPR screens with single-cell transcriptome resolution, and would allow for further understanding of more complex regulatory mechanisms and heterogenous cell populations (163). If the p53 null cells have reduced apoptosis, this method may overcome the downfalls of using apoptosis as a readout.

5.10.2 Interplay between MTAP and PRMT5

MTAP was identified and validated as a sensitivity marker in our CRISPR screen in p53 wild type cells. MTAP is ubiquitously expressed in normal tissues, and homozygous deletion of MTAP occurs frequently, due to its proximity (resides within 100kb) to one of the most commonly deleted tumour suppressor genes, CDKN2A(166-168). MTAP is responsible for the cleaving of methylthioadenosine, or MTA, into precursor substrates that play a role in the methionine and adenine salvage pathways. Studies have found that when MTAP is deleted, there is an accumulation of MTA in cells and a downregulation in basal levels of PRMT5 methyl marks in these cells. MTA is thought to act as a SAM-competitive inhibitor (169). This would explain the increased sensitivity that we see in MLL-ENL cells that have a

knockout of MTAP, as this accumulation of MTAP would further inhibit the function of PRMT5.

Literature seems to suggest that there are no feasible MTAP inhibitors, as very limited information exists on only one inhibitor – known as MT-DADMe-ImmA (170, 171), making MTAP an unlikely drug target. With that being said, MTAP deletion frequency is quite high in several cancers, including malignant peripheral nerve sheath tumour (MPNST), glioblastoma and oesophageal cancer (172). This brings to light the therapeutic potential of PRMT5 inhibition in these types of cancers, where deletion of MTA might sensitise cells to PRMT5 inhibition.

5.10.3 Pathways involved in resistance and sensitivity

PRMT5 has been described as having a role in many different cellular processes, including DNA damage repair (150), splicing (88, 145) and histone modifications (89), it is no surprise that several of these pathways were implicated as being involved in sensitivity or resistance in the pathway analysis of genes identified by the CRISPR screen. One interesting finding was the duality between sensitivity genes and resistance genes in terms of mTOR signalling. Pathway analysis revealed that several genes that were identified as a sensitivity hit were involved in negative regulation of mTOR. Considering these genes were knocked out in the CRISPR screen, this suggests that the inverse, i.e. positive regulation of mTOR may sensitise cells to PRMT5 inhibition. Conversely, knocking out genes that were responsible for positive regulation of TOR signalling seemed to be involved in PRMT5 resistance. This would suggest that PRMT5 inhibition would be most effective in cells that upregulate mTOR.

Considering that many cancers are associated with an up-regulation of the mTOR pathway, this makes the pathway an attractive target for therapies (173). Despite mTOR being described as an important regulator of AML initiation and maintenance, the efficacy of mTOR inhibitors have yielded mixed results clinically (174).

5.10.4 Combining PRMT5i with Selumetinib

Our high throughput drug-screen identified selumetinib as the highest scoring synergistic compound. Selumetinib is an inhibitor of MAPK kinase (or MEK) 1 and 2. The potential clinical efficacy of this drug is currently being investigated in neurofibromatosis type 1-related neurofibroma (175). Studies have shown that there is an interplay between PRMT5 and a downstream target of MEK1/2, known as ERK1/2. ERK1/2 is activated via phosphorylation, and inactivated by dephosphorylation (176). Phosphorylation of ERK1/2, along with other factors in the RAS-ERK pathway is crucial for cell proliferation, differentiation and survival, and it has been reported that PRMT5, through methylation of RAF proteins, limits ERK1/2 phosphorylation (177). In PC12 cells, a neural cell lines that is often used for the study of neural differentiation (178), this limitation driven by PRMT5 has been shown to induce proliferation (177, 179), and inhibition of PRMT5 in this cell lines has promoted cell differentiation as opposed to proliferation (177). Dysregulation of ERK signalling via PRMT5 inhibition has also been shown in T cells (180).

To our knowledge, this interplay between PRMT5 and MEK/ERK has not been studied in AML. The synergistic interaction observed in the drug screen suggests that this interplay may be targeted by drugs to sensitise cells to PRMT5, as data suggests that is might cause a reduction in proliferation.

5.10.5 ABT199 and Mocetinostat

ABT199, or venetoclax, is a Bcl-2 inhibitor that has gained a lot of traction in the AML clinical sphere. There are numerous ongoing clinical trials assessing the efficacy of ABT199, particularly in combination with other compounds (181). Another compound that has been investigated in AML is mocetinostat, a selective class I and IV HDAC inhibitor (182). This compound has been shown to reduce cell viability *in vitro* (183) and has exhibited anti-leukaemic activity in a phase I clinical trial in AML and MDS (184). However, like with many compounds, monotherapies often provide modest clinical efficacy, and so there is often a push to combine multiple compounds. We have previously shown, although the data was not included in this chapter, that there is synergy between ABT199 and PRMT5i. Our results also suggest that HDAC

inhibitors might synergise with PRMT5 inhibition, and the findings from the drug screen provide rationale for further testing of these combinations.

5.10.5 PRMT5s role in cell cycle

Conversely, the drug screen identified Ro-3306 as the compound that displayed the highest antagonistic relationship when combined with PRMT5 inhibitor. Ro-3306 is an inhibitor of CDK1. Treatment with Ro-3306 arrests cells at the G2/M border of the cell cycle, essentially maintaining a mitotic state (185). PRMT5 is also known to play roles in cell cycle regulation. PRMT5 correlated with increase protein expression of the G1 phase regulators, CDK4 and CDK6, an is therefore essential for cell proliferation (186). It has been shown that deficiency or inhibition of PRMT5 leads to cell cycle arrest and subsequent apoptosis (122). Our data supports the notion that Ro-3306 causes a G2/M block, and therefore G1 cell cycle arrest can not be induced by PRMT5 inhibition.

5.10.6 Validating with synergy assays

Further experiments will have to be conducted to validate the strength of the synergistic interactions that we observed. The high throughput drug screen was conducted with the understanding that drugs that will synergise with PRMT5 inhibition will most likely show synergy across all of the doses that were selected, but using only 3 doses doesn’t allow us to take into account complex drug interaction patterns that are often observed in more large-scale dose-response matrix that utilise many dose pairs (187). These larger-scale experiments, combined with a statistical method for determining synergy, such as the ZIP scoring approach, would allow us to experimentally confirm drug synergy, while keep false discovery rates (FDR) relatively low (187).

5.10.7 Conclusion

In summary, a GeCKO library was infected into the MLL-ENL cell line. The screen involved the use of a PRMT5i in order to provide a list of genes that may be important for sensitivity and resistant to PRMT5 inhibition. The screen results were validated in the wild type p53 cell line, and we showed that knockout of several genes that came up at hits for sensitivity and resistance caused a decrease and an increase in PRMT5i GI_{50}, respectively. However, we were not able to validate the screen in the context of p53 null, and this may be due to the overriding resistance mechanisms interfering with the screen readout, which is cell proliferation. Utilising the list of genes that were reported as significant hits in the sensitivity screen, as well as pathway analysis, we were able to rationally select a variety of compounds. These compounds were run through a high throughput drug screen assay, where cells were treated with these compounds as single agents, or in combination with the PRMT5i. The drug screen identified a selection of drugs that displayed synergy with our PRMT5i, including two drugs in which synergy has been confirmed in the past. Future experiments will need to confirm synergy in the other synergistic hits, and more complex CRISPR screening methods (such as CROP-seq) could be employed to overcome the lack of validation in the p53 null context.

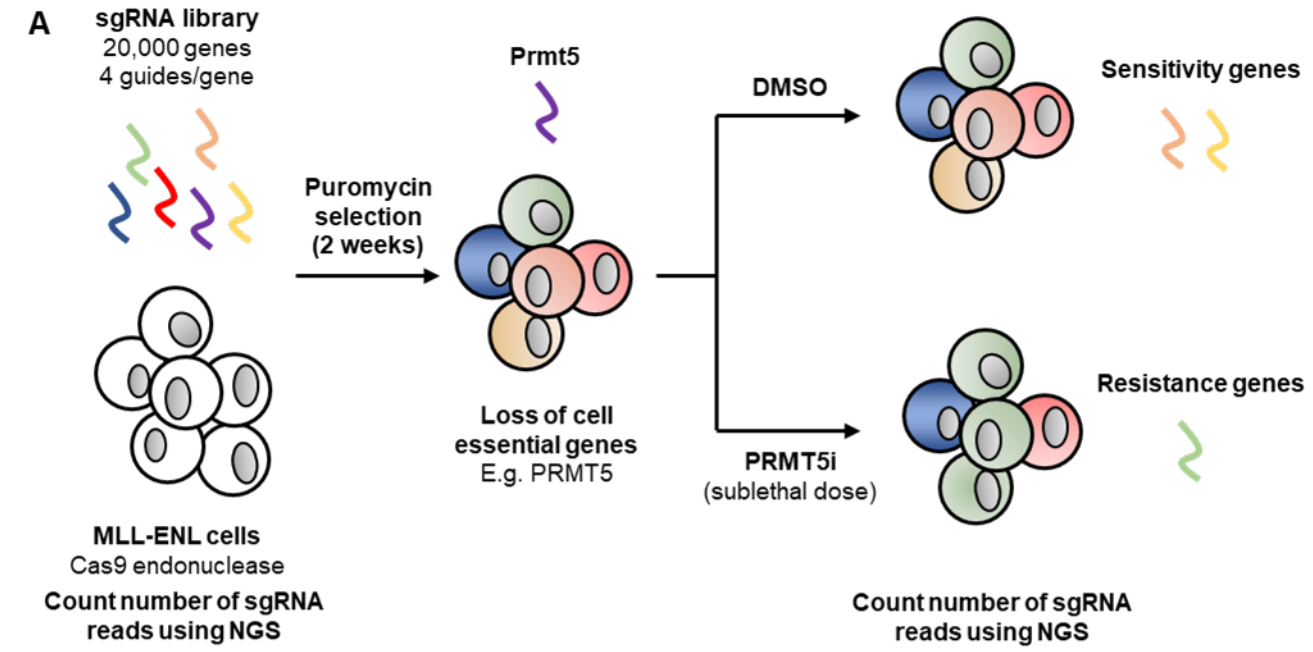
A
sgRNA library
20,000 genes
4 guides/gene
Puromycin
selection
(2 weeks)
Prmt5
Loss of cell
essential genes
E.g. PRMT5
DMSO
PRMT5i
(sublethal dose)
Sensitivity genes
Resistance genes
MLL-ENL cells
Cas9 endonuclease
Count number of sgRNA
reads using NGS
Count number of sgRNA
reads using NGS

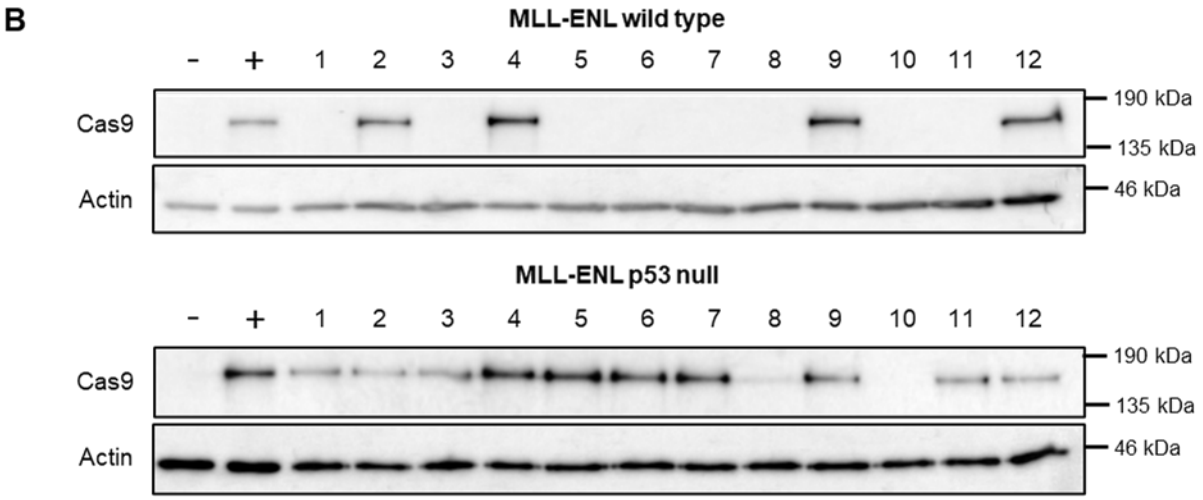
B
MLL-ENL wild type
- + 1 2 3 4 5 6 7 8 9 10 11 12
Cas9
Actin
190 kDa
135 kDa
46 kDa
MLL-ENL p53 null
- + 1 2 3 4 5 6 7 8 9 10 11 12
Cas9
Actin
190 kDa
135 kDa
46 kDa

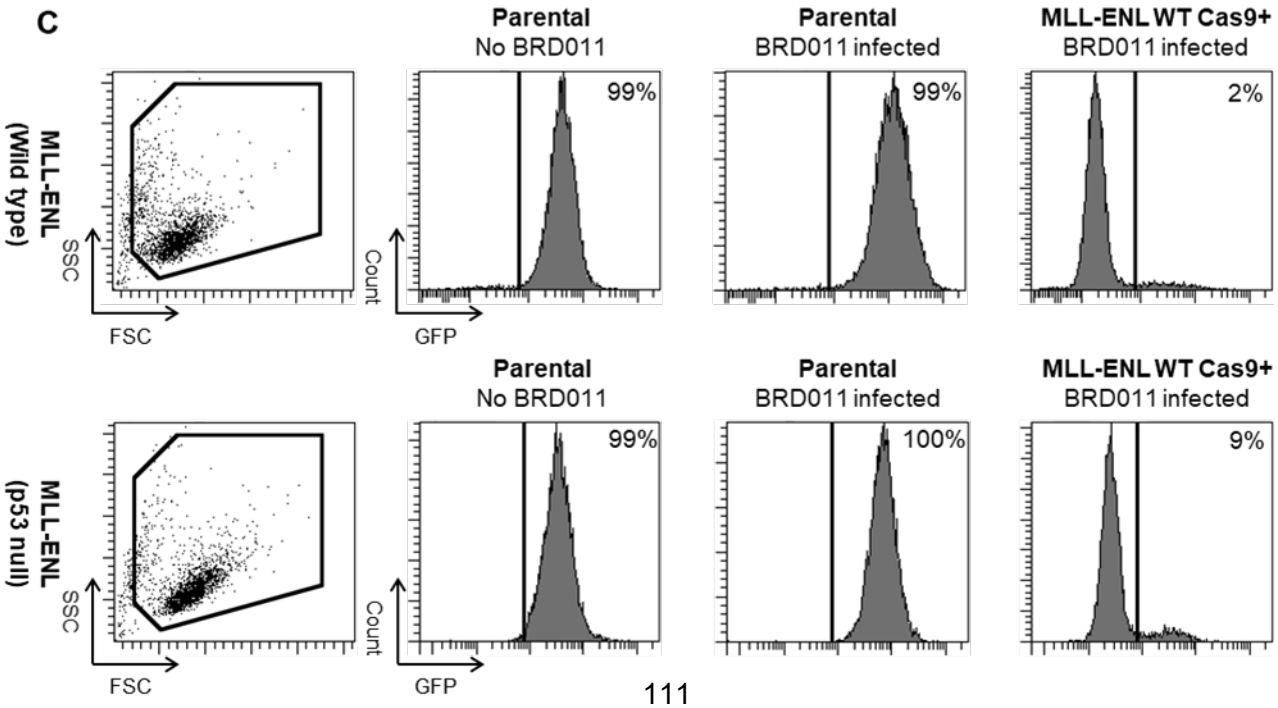
C
Parental
No BRD011
Parental
BRD011 infected
MLL-ENL WT Cas9+
BRD011 infected
MLL-ENL
(Wild type)
SSC
FSC
Count
GFP
99%
99%
2%
Parental
No BRD011
Parental
BRD011 infected
MLL-ENL WT Cas9+
BRD011 infected
MLL-ENL
(p53 null)
SSC
FSC
Count
GFP
99%
100%
9%

Figure 5.1 Strategy and validation of the CRISPR screen using sgRNA library. **(A)** Experimental strategy used for the CRISPR screen. **(B)** Western blot analysis of various clones of wild type and p53 knockout MLL-ENL cells infected with Cas9 lentivirus. Protein was probed for Cas9 protein. Actin was used as a loading control. **(C)** FACS analysis of GFP expression levels in cells expressing Cas9+, with parental cells acting as a Cas9 null control. These cells were infected with BRD011 vector to validate Cas9 expression, and infected cells were selected for by treating with puromycin for 4 days.

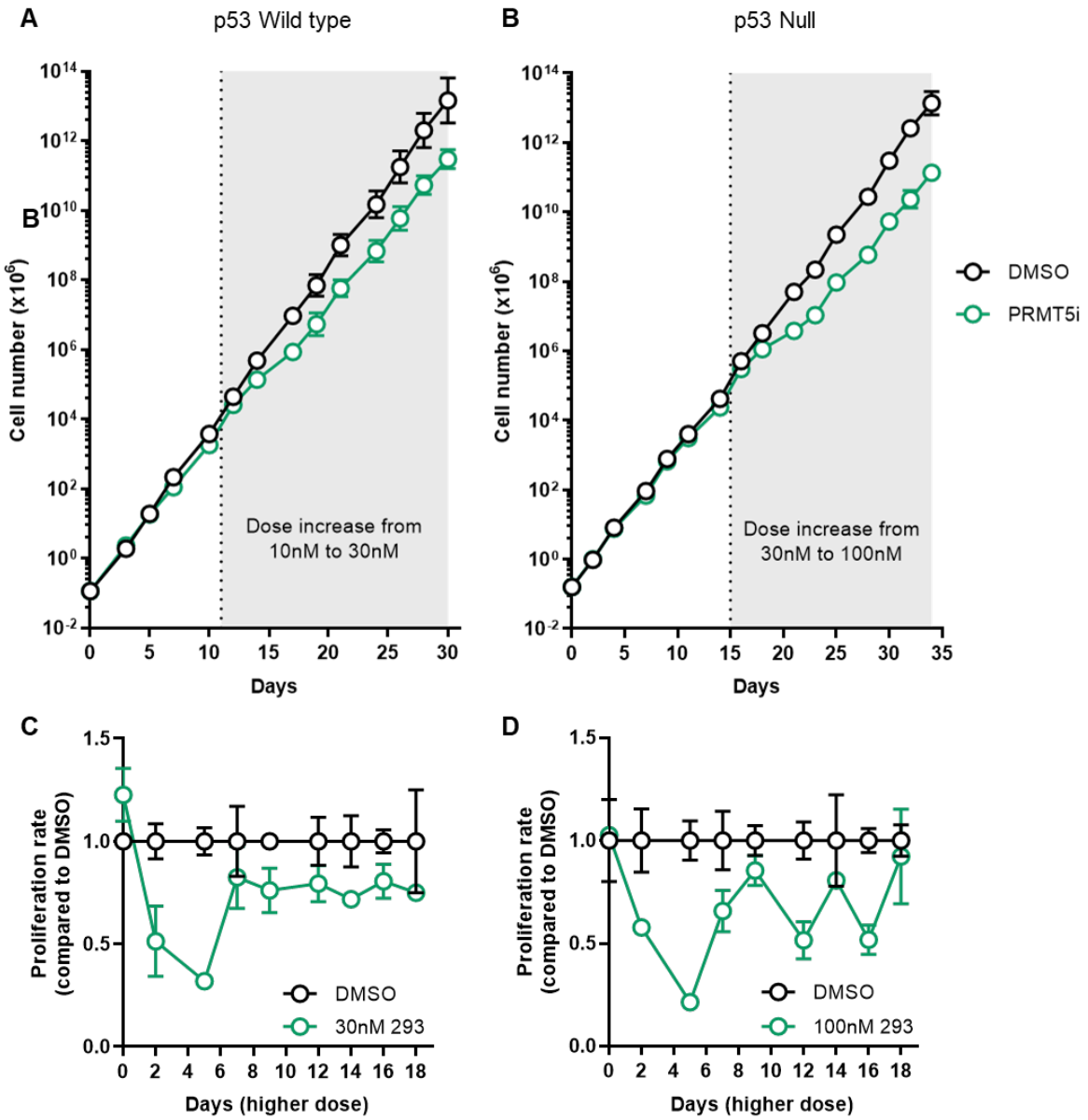

Figure 5.2 Effects of PRMT5 inhibition during the CRISPR screen
(A-B) Growth curves generated over 30 – 35 days in **(A)** wild type and **(B)** p53 null MLL-ENL Cas9 expressing cells treated with a PRMT5 inhibitor. Both cell lines were treated with a higher concentration of PRMT5 inhibitor for the last two weeks of the screen. **(C-D)** Growth curves displayed as a measure of cell proliferation as compared to vehicle (DMSO) treated cells in the **(A)** wild type and **(C)** p53 null lines. Proliferation is plotted from when the cell lines were treated with an increased dose of PRMT5i. Mean ± SEM of two replicates is shown.

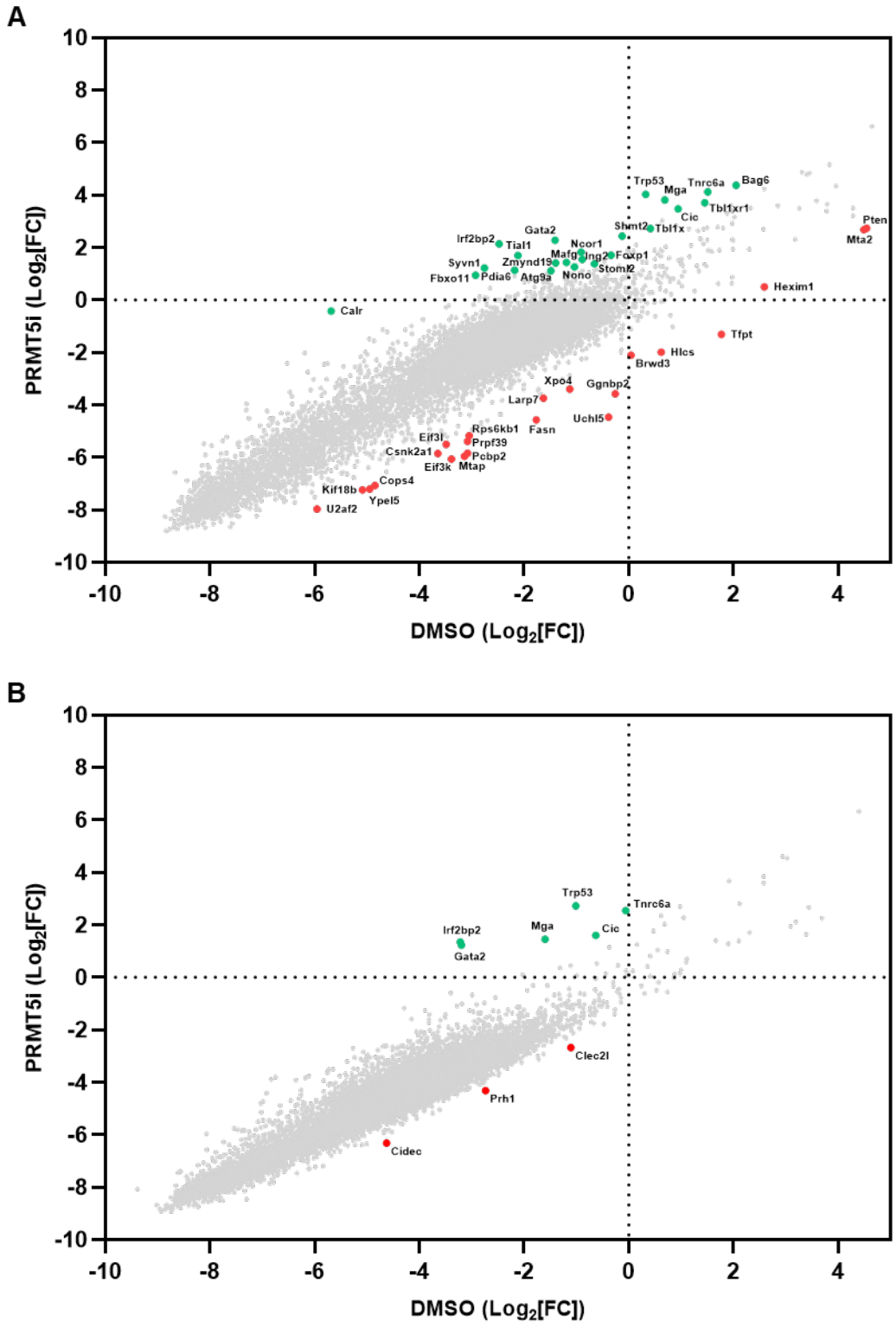

Figure 5.3 sgRNA representation in *wild type* MLL-ENL cells treated with PRMT5i. The Log_2 fold-change (as compared to the library pre-infection) of sgRNA abundance in the PRMT5 inhibitor treatment group versus DMSO control from DNA harvested at **(A)** day 5 of treatment and **(B)** day 16 of treatment. The sgRNAs identified as strong resistance 'hits' are coloured green, and sgRNAs identified as strong sensitivity 'hits' are coloured red.

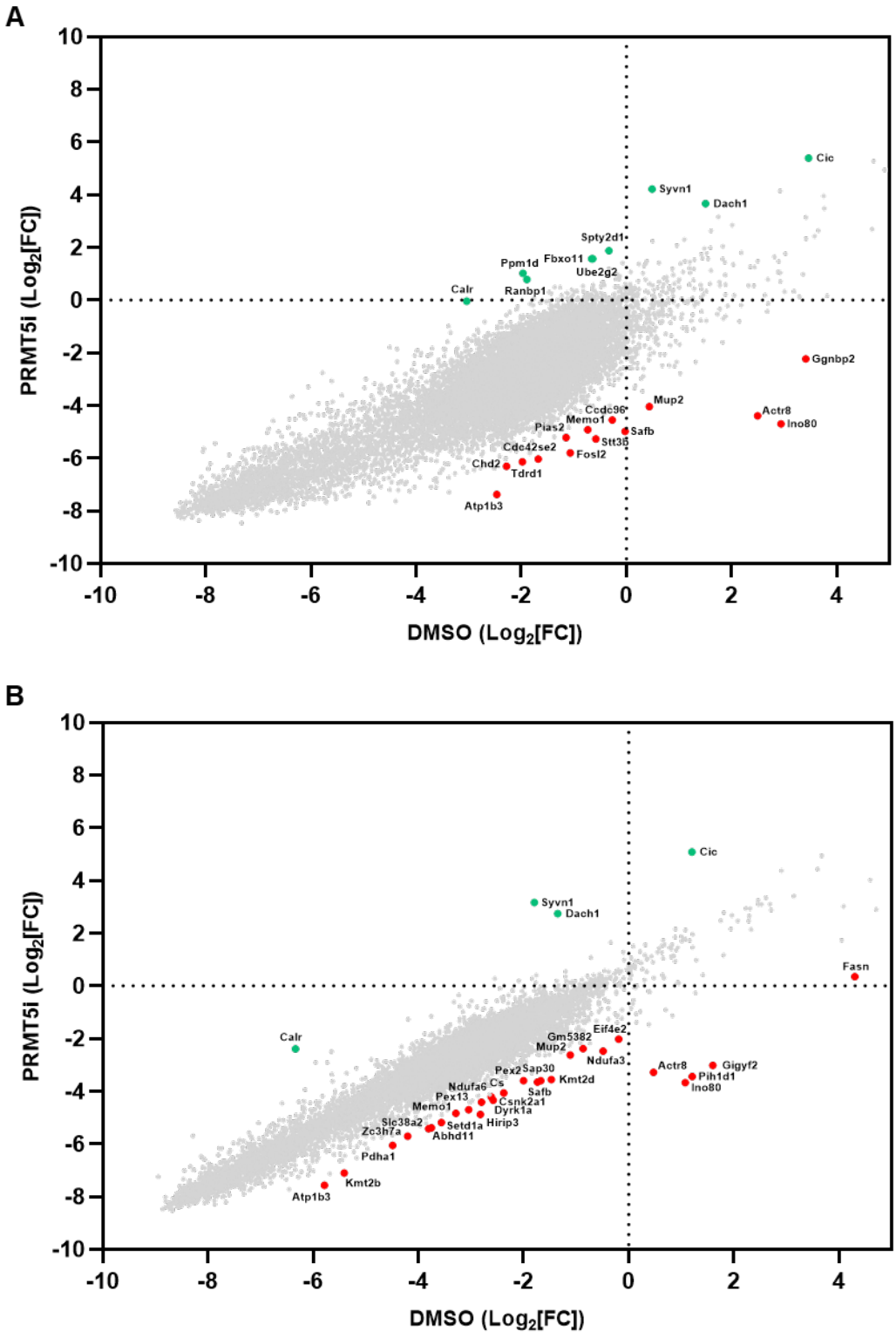

Figure 5.4 sgRNA representation in *p53 null* MLL-ENL cells treated with PRMT5i. The Log_2 fold-change (as compared to the library pre-infection) of sgRNA abundance in the PRMT5 inhibitor treatment group versus DMSO control from DNA harvested at **(A)** day 5 of treatment and **(B)** day 16 of treatment. The sgRNAs identified as strong resistance 'hits' are coloured green, and sgRNAs identified as strong sensitivity 'hits' are coloured red.

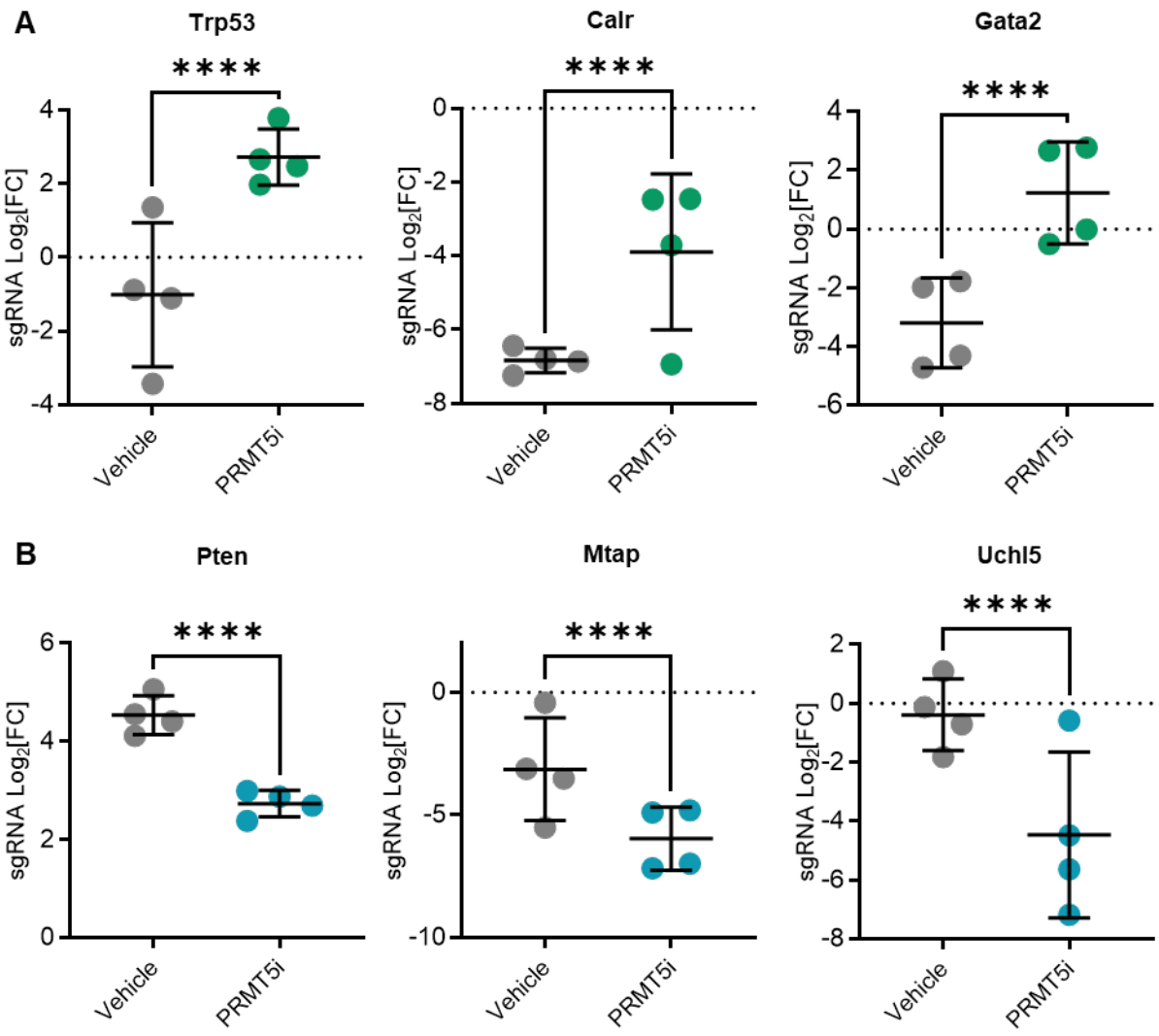

Figure 5.5 sgRNA representation changes in p53 wild type MLL-ENL cells
Changes in sgRNA representation are shown as Log_2FC expression change in the PRMT5i treated group as compared to vehicle (DMSO) control. **(A)** Selection of sgRNAs that were overrepresented targeting genes may confer resistance from cells harvested at the later treatment time point. **(B)** Selection of sgRNAs that were underrepresented targeting genes that may confer sensitivity from cells harvested at the earlier treatment time point. Mean ± SD of the 4 guides is shown. *P<0.05, **P=<0.01, ***P<0.001, ****P<0.0001, MAGeCK analysis was used to generate p-values.

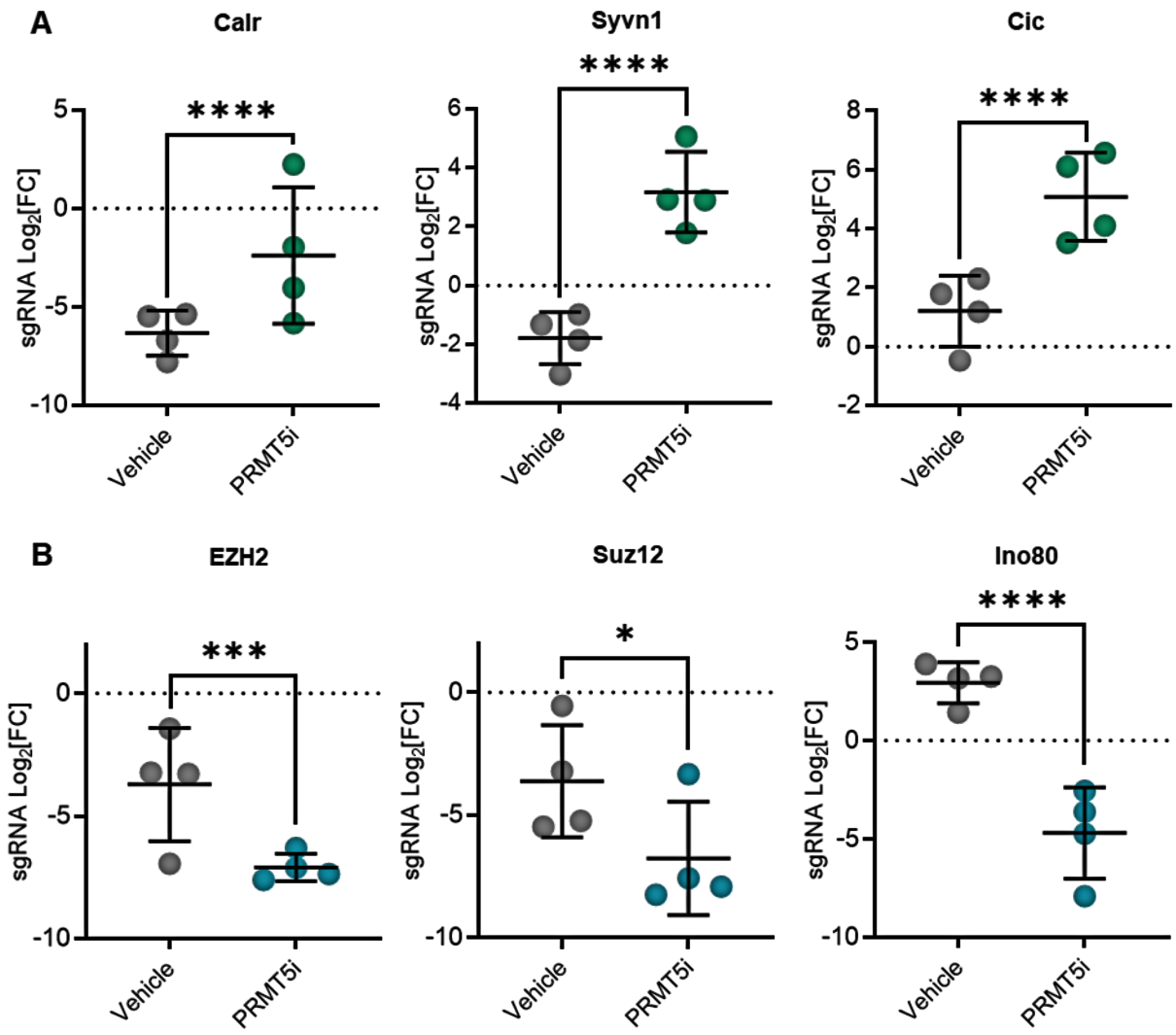

Figure 5.6 sgRNA representation changes in p53 null MLL-ENL cells
Changes in sgRNA representation are shown as Log_2FC expression change in the PRMT5i treated group as compared to vehicle (DMSO) control. **(A)** Selection of sgRNAs that were overrepresented targeting genes may confer resistance from cells harvested at the later treatment time point. **(B)** Selection of sgRNAs that were underrepresented targeting genes that may confer sensitivity from cells harvested at the earlier treatment time point. Mean ± SD of the 4 guides is shown. *P<0.05, **P=<0.01, ***P<0.001, ****P<0.0001. MAGeCK analysis was used to generate p-values.

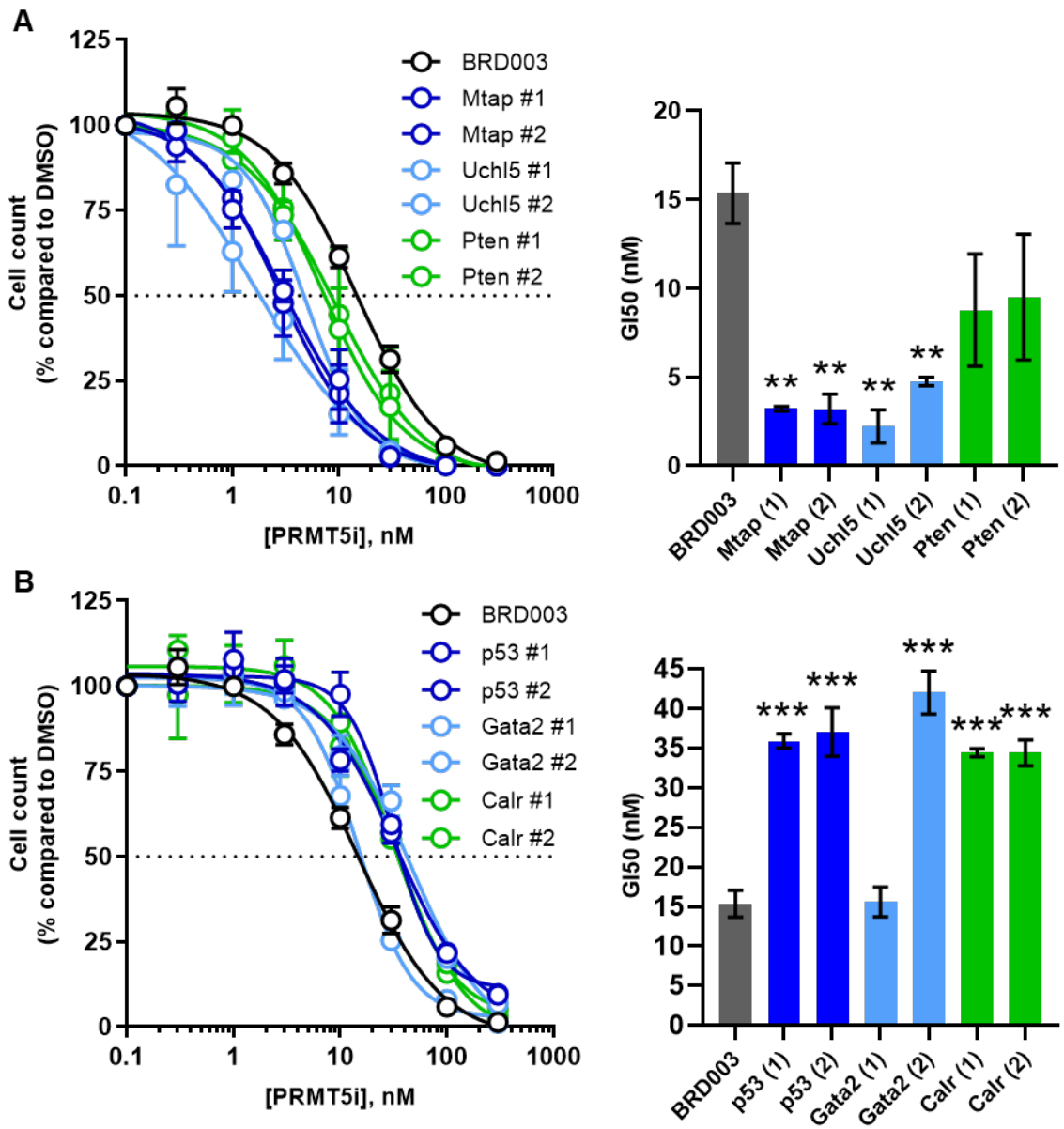

Figure 5.7 Validation of hits in p53 wild type MLL-ENL cells

A cell growth assay was conducted to generate a dose-response curve by treating MLL-ENL p53 wild type cells, infected with 1 sgRNA, with increasing concentrations of PRMT5i for 5 days (right panels). This curve was converted into an GI_{50} value (right panels). This was done in **(A)** cells that had a knockout in a gene that was identified as a sensitivity gene in the screen and in **(B)** cells that had a knockout in a gene that was identified as a resistance gene. Data is shown as Mean ± SEM of 3 independent experiments. *P<0.05, **P=<0.01, ***P<0.001, student's t-test compared to BRD003 vector controls.

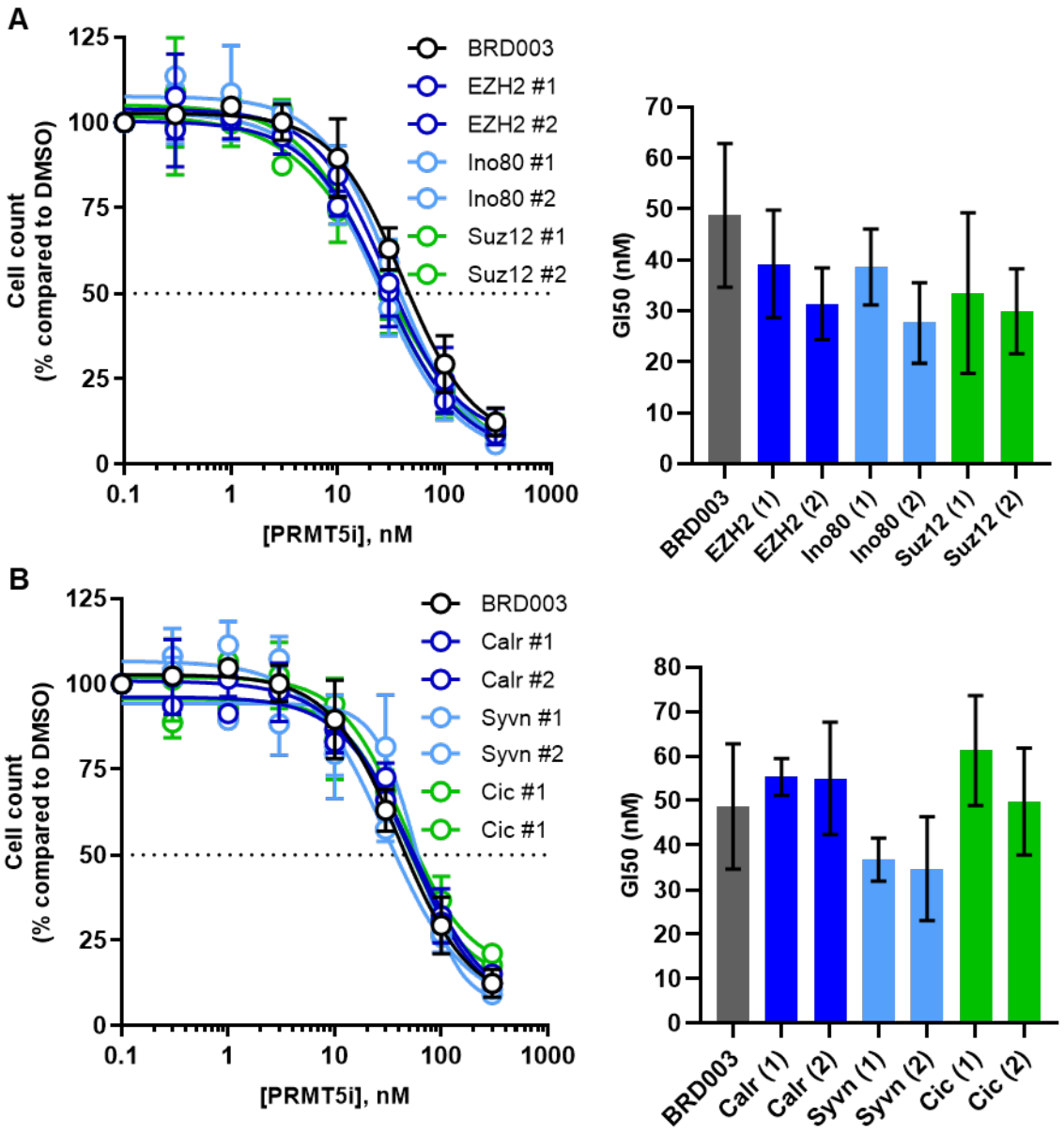

Figure 5.8 Validation of hits in p53 null MLL-ENL cells

A cell growth assay was conducted to generate a dose-response curve by treating MLL-ENL p53 null cells, infected with 1 sgRNA, with increasing concentrations of PRMT5i for 5 days (right panels). This curve was converted into an GI_{50} value (right panels). This was done in **(A)** cells that had a knockout in a gene that was identified as a sensitivity gene in the screen and in **(B)** cells that had a knockout in a gene that was identified as a resistance gene. Data is shown as Mean ± SEM of 3 independent experiments. *P<0.05, **P=<0.01, ***P<0.001, student's t-test compared to BRD003 vector controls.

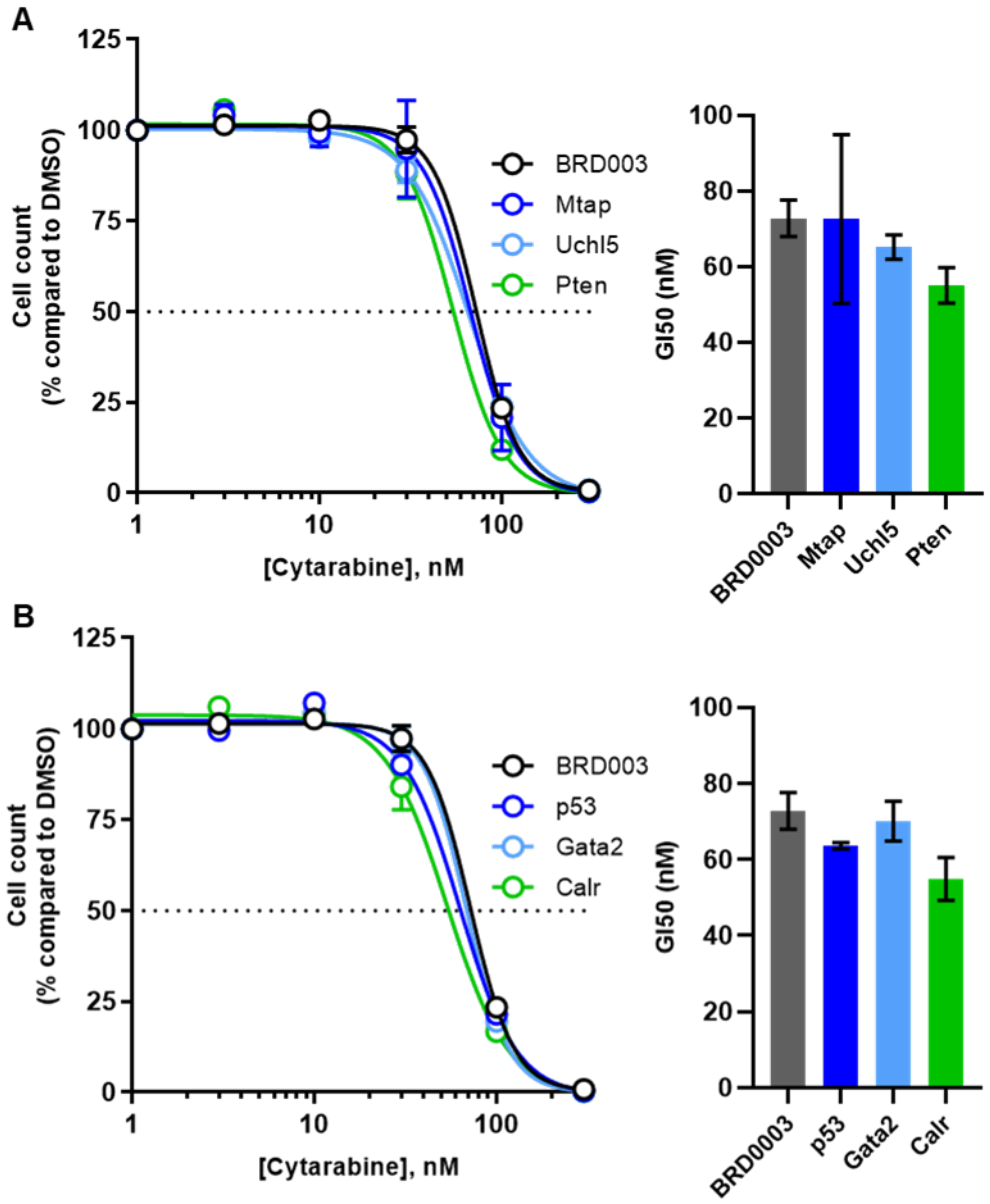

Figure 5.9 Resistance and sensitivity is PRMT5 inhibitor specific
p53 wild type MLL-ENL cells infected with 1 sgRNA were treated with varying doses of Cytarabine for 48 hours to assess the effects of single gene knockout on sensitivity or resistance to chemotherapy. Cell growth curves are shown in the left panels, and GI_{50} values are shown in the right panels in **(A)** cells that had a knockout in a gene that was identified as a sensitivity gene in the screen and **(B)** cells that had a knockout in a gene that was identified as a resistance gene. Data is shown as mean ± SEM of 3 independent experiments.

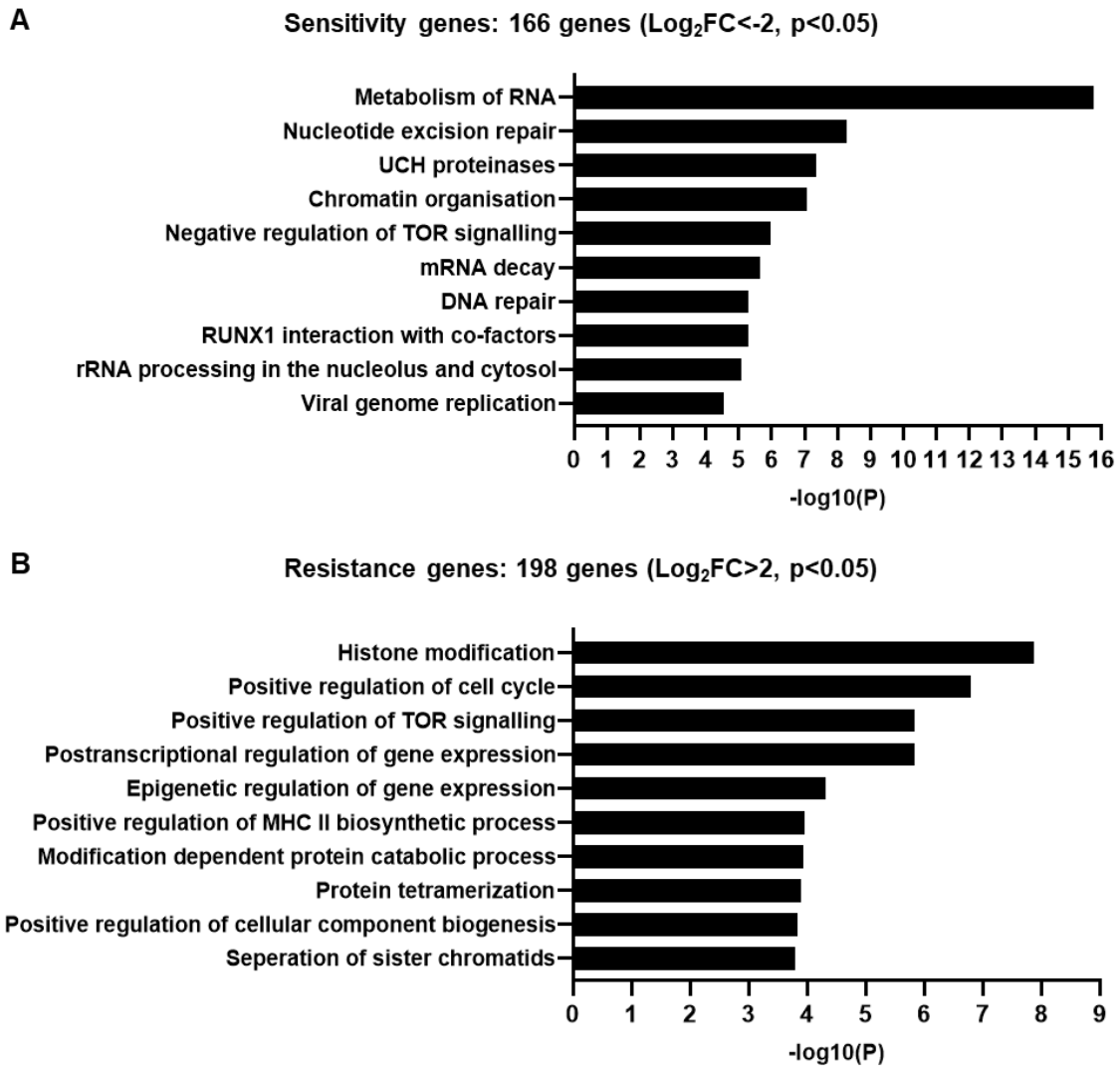

Figure 5.10 Pathways responsible for sensitivity and resistance
Pathway analysis was conducted using metascape. **(A)** The top 10 pathways that include genes that were identified as sensitivity hits. Hits were defined as showing a $Log^2FC<-2$ (with a p value<0.05) as compared to vehicle control. **(B)** The top 10 pathways that include genes that were identified as resistance hits. Hits were defines as showing a $Log_2FC>2$ (with a p-value<0.05) as compared to vehicle control.

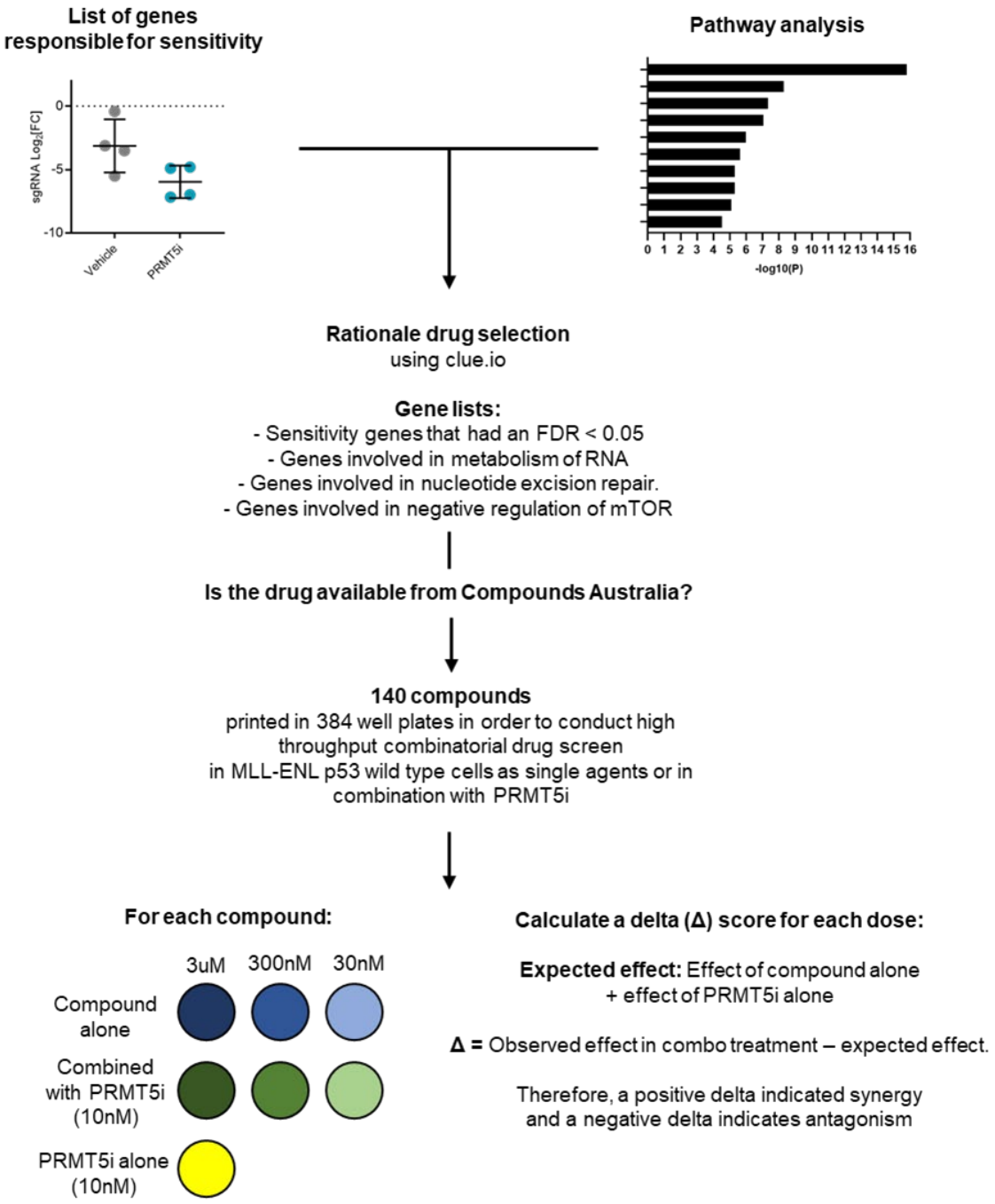

Figure 5.11 Rational drug selection and drug screen strategy
Describes the method used to select compounds rationally to test in combination with the PRMT5i. Clue.io database was employed, and several gene lists were used to aid in selection. Once selected, a drug screen was performed to assess the effects of the rationally selected compounds as single agents and in combination with PRMT5 inhibition.

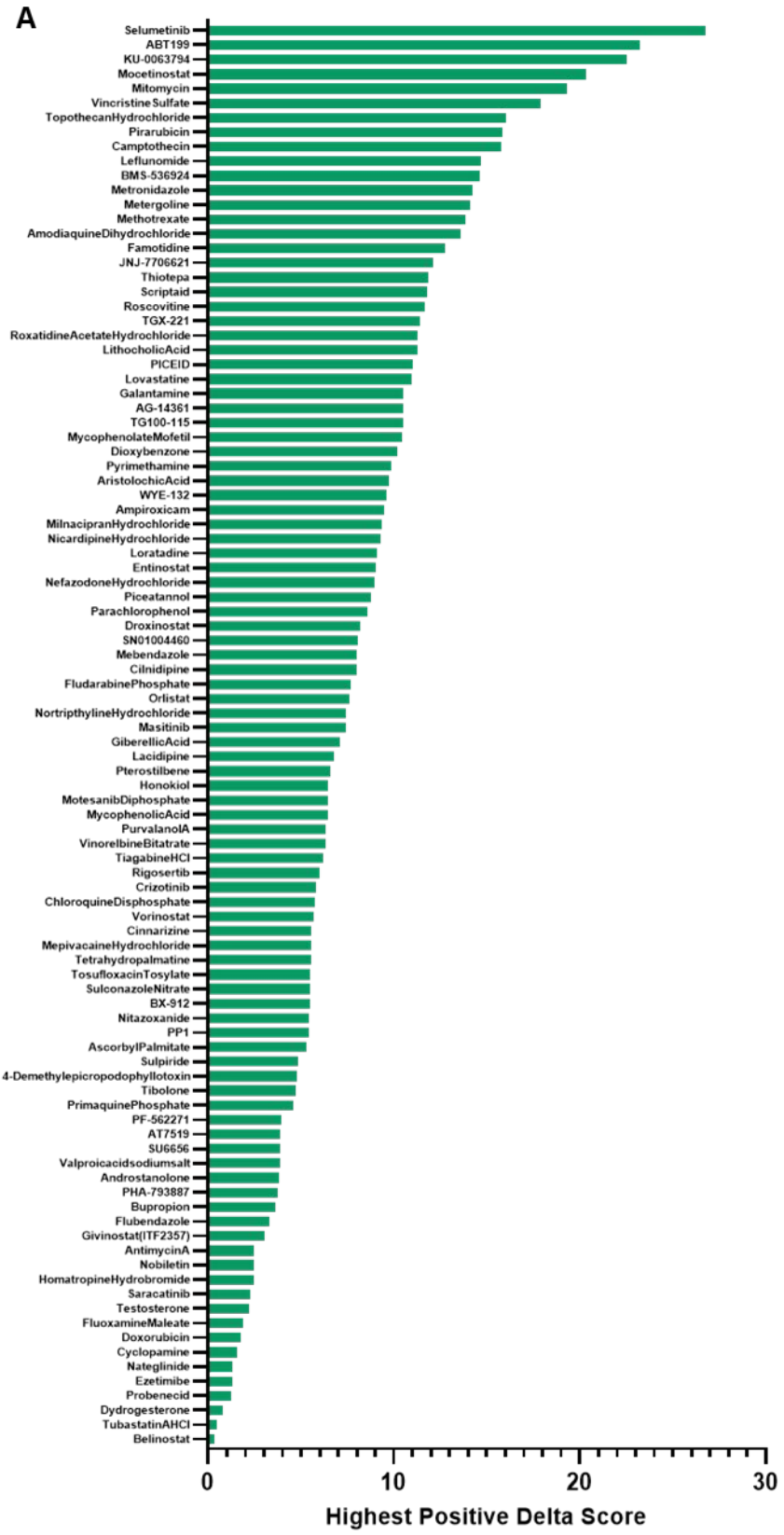
A
Selumetinib
ABT199
KU-0063794
Mocetinostat
Mitomycin
VincristineSulfate
TopothecanHydrochloride
Pirarubicin
Camptothecin
Leflunomide
BMS-536924
Metronidazole
Metergoline
Methotrexate
AmodiaquineDihydrochloride
Famotidine
JNJ-7706621
Thiotepa
Scriptaid
Roscovitine
TGX-221
RoxatidineAcetateHydrochloride
LithocholicAcid
PICEID
Lovastatine
Galantamine
AG-14361
TG100-115
MycophenolateMofetil
Dioxybenzone
Pyrimethamine
AristolochicAcid
WYE-132
Ampiroxicam
MilnacipranHydrochloride
NicardipineHydrochloride
Loratadine
Entinostat
NefazodoneHydrochloride
Piceatannol
Parachlorophenol
Droxinostat
SN01004460
Mebendazole
Cilnidipine
FludarabinePhosphate
Orlistat
NortripthylineHydrochloride
Masitinib
GiberellicAcid
Lacidipine
Pterostilbene
Honokiol
MotesanibDiphosphate
MycophenolicAcid
PurvalanolA
VinorelbineBitatrate
TiagabineHCl
Rigosertib
Crizotinib
ChloroquineDisphosphate
Vorinostat
Cinnarizine
MepivacaineHydrochloride
Tetrahydropalmatine
TosufloxacinTosylate
SulconazoleNitrate
BX-912
Nitazoxanide
PP1
AscorbylPalmitate
Sulpiride
4-Demethylepicropodophyllotoxin
Tibolone
PrimaquinePhosphate
PF-562271
AT7519
SU6656
Valproicacidsodiumsalt
Androstanolone
PHA-793887
Bupropion
Flubendazole
Givinostat(ITF2357)
AntimycinA
Nobiletin
HomatropineHydrobromide
Saracatinib
Testosterone
FluoxamineMaleate
Doxorubicin
Cyclopamine
Nateglinide
Ezetimibe
Probenecid
Dydrogesterone
TubastatinAHCl
Belinostat
0
10
20
30
Highest Positive Delta Score

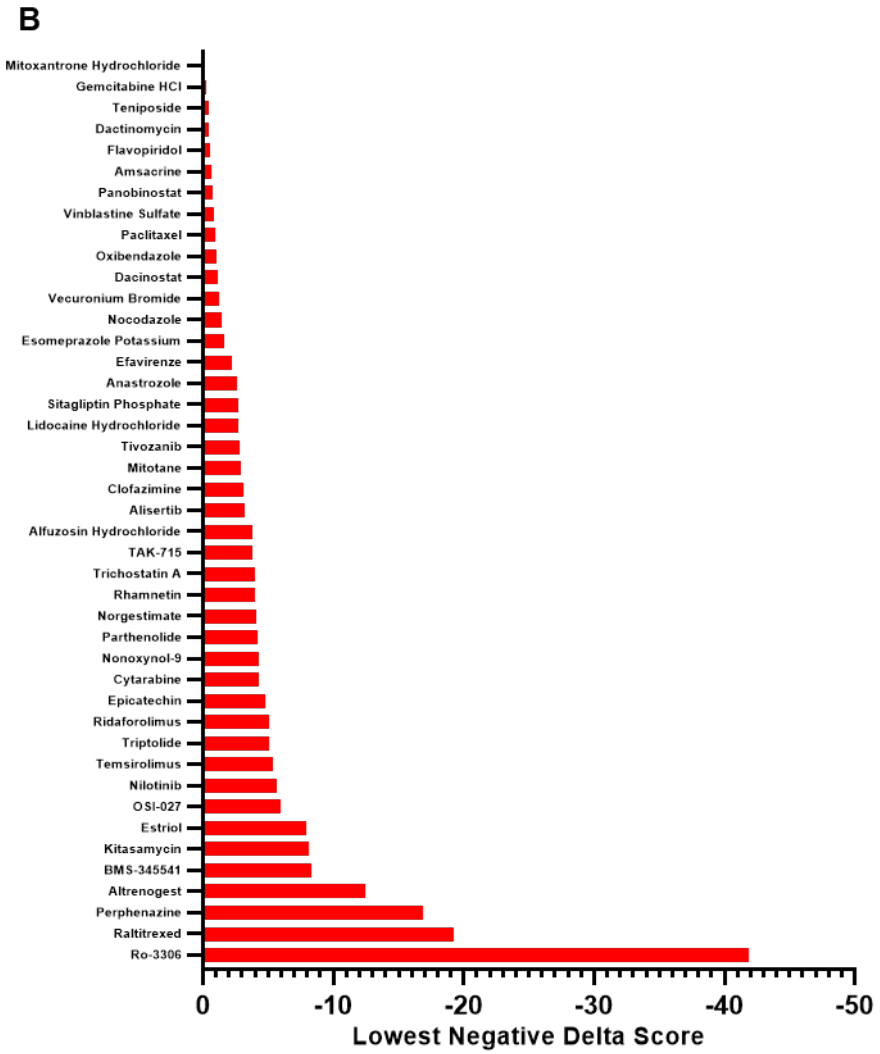

Figure 5.12 High throughput drug screen combining several compounds with PRMT5 inhibition

p53 wild-type MLL-ENL cells were treated with a variety of compounds. These cells pre-treated with either PRMT5i (at a sub-lethal dose of 10nM) or DMSO (as a vehicle control) for 2 days before being treated with various compounds at 3 ranging doses. A delta (Δ) score was generated to observe synergistic (positive Δ), antagonistic (negative Δ) and additive (Δ = 0) effects. **(A)** Shows the highest delta score that was achieved across the doses in drugs that had a positive delta score. **(B)** shows the lowest delta score that was achieved across the doses in drugs that had a negative delta score.

Chapter 6:

Conclusions and Future Directions

As PRMT5 plays a role in many cellular processes within many different systems of the body, this can make it difficult to delineate each individual role that PRMT5 may be involved in, as often PRMT5 will display interplay in different processes at the same time. Although literature suggests that there is an increase in PRMT5 expression in many cancers (188), including haematological (108, 109), how this can contribute to leukaemia onset or maintenance is still relatively unclear. This question, coupled with the understanding that PRMT5 seems to be more highly expressed in stem and progenitor like cells, leaves a lot to be uncovered. Whether PRMT5 is responsible for maintaining pluripotency or inhibiting differentiation is still yet to be elucidated.

This first aim of this thesis was to try and uncover whether there would be any effect on cell 'stemness' following enforced expression of PRMT5. To do this, we utilised a transgenic mouse model in which exogenous PRMT5 expression was driven by the Rosa26 locus. Unfortunately, we were unable to achieve any significant overexpression of PRMT5, and we postulate that this may not necessarily be a downfall of the transgenic system, but it may in fact be due to inadequate expression of MEP50 – PRMT5s critical co-factor. The regulation of the PRMT5:MEP50 complex is not yet fully understood (189), and to our knowledge there does not seem to be any significant evidence of overexpression experiments involving MEP50, so future experiments could utilise a co-overexpression system as it is believed the MEP50 is crucial to stabilise PRMT5 levels.

With the hopes of trying to increase expression of exogenous PRMT5, this project also utilised a retroviral system *in vivo* in a leukaemic cell line – MLL-ENL. Although we were able to achieve higher protein expression differences between PRMT5 overexpressing and control cells, there was still a disparity between the observed increase in mRNA levels as compared to the protein levels, just as we had seen in the previously mentioned transgenic system.

With that being said, inhibitor studies revealed some interesting findings in regard to the Phe327 amino acid. When cells were treated with a substrate competitive PRMT5 inhibitor, resistance was observed in cells that were enforcing expression of our F327M mutant form. This would suggest that this mutant form of PRMT5 is not only active but may be able to compensate for a lack of PRMT5 activity (resistance was observed even at 1uM of inhibitor). Whether the mutant form is able to bind the inhibitor is still yet to be elucidated by co-IP.

The PRMT5 deletion phenotype previously reported in the literature that leads to loss of haematopoiesis (95) was also confirmed in this thesis in an ERT2Cre model. In an attempt to rescue this phenotype, we infected a cell line that was generated from this mouse model with our PRMT5 enforcing constructs. Following deletion of endogenous PRMT5, we were not able to rescue cells, even with our wild type PRMT5 construct. Why this is remains a mystery, as sequencing confirmed correct PRMT5 sequence, and the inhibitor referred to in the previous section suggest that the exogenous PRMT5 is active as there is an increase in resistance in cells exogenous expressing wild type PRMT5, as opposed to an increase in sensitivity seen in cells exogenously expressing methylation dead PRMT5. *In vitro* methylation will need to be confirmed in these lines, as if it is indeed that PRMT5 is functional, it might uncover some interesting reasons as to why rescue is not possible in the ERT2Cre cells.

Finally, and most fruitfully, the final part of this thesis investigates the use of a genome wide murine CRISPR screen in identifying genes that may confer sensitivity or resistance to PRMT5 inhibition in our MLL-ENL cell line. This was performed in both the wild type p53 and p53 null setting, and we were able to validate the results of the screen in the wild type p53 context, but not in the p53 null setting. Interestingly, there are mixed reports including concerns around the performance of genome wide CRISPR screens in p53 wild type cells, as p53 in these cells is involved in DNA damage response, and therefore may impact the efficiency of generating viable edited cells. However, it is suggested the proper screen design can ensure robust performance in these cases (190). We know in the case of the MLL-ENL cells that p53 null status makes cells more resistant, and lack of p53 may be responsible for overcoming death in cells with a knockout of a gene that causes sensitivity, for example. It would be interesting to repeat the CRISPR screen in

another leukaemic cell line in order to compare the hits that are generated to the hits generated in the MLL-ENL cells. Any overlapping hits might suggest targets that a less specific to particular mutational statuses of cells and more pan-cancerous.

With that being said, we successfully generated a list of genes that, when knocked down, conferred sensitivity in the MLL-ENL p53 wild type cells. This list, along with information obtained from pathway analysis, allowed us to rationally select and implement a high throughput drug screen utilised a large number compounds. The drugs that showed synergy will need to be confirmed in more robust synergy assays with more powerful statistical readouts of synergy, but the screen allowed us to select candidate drugs that may be promising.

With current treatments in AML being associated with poor outcomes, the ultimate goal of these synergy assays is to provide clinical data that would support the use of PRMT5 inhibitors in clinic. Considering that there are multiple clinical trials running at the moment utilising PRMT5 inhibitors, this data, coupled with an ever increasing understanding of PRMT5s role in biology and haematopoiesis, will hopefully pave the way for more effective targeted treatments for patients suffering with this devastating disease.

References:

1. Dunn C. The differentiation of haemopoietic stem cells. Series haematologica (1968). 1971;4(4):1-71.

2. Ho MS, Medcalf RL, Livesey SA, Traianedes K. The dynamics of adult haematopoiesis in the bone and bone marrow environment. British journal of haematology. 2015;170(4):472-86.

3. Cavazzana-Calvo M, Fischer A, Bushman FD, Payen E, Hacein-Bey-Abina S, Leboulch P. Is normal hematopoiesis maintained solely by long-term multipotent stem cells? Blood, The Journal of the American Society of Hematology. 2011;117(17):4420-4.

4. Ng YY, Baert MR, de Haas EF, Pike-Overzet K, Staal FJ. Isolation of human and mouse hematopoietic stem cells. Genetic Modification of Hematopoietic Stem Cells: Springer; 2009. p. 13-21.

5. Lowenberg B, Downing JR, Burnett A. Acute myeloid leukemia. N Engl J Med. 1999;1999(341):1051-62.

6. Estey E, Döhner H. Acute myeloid leukaemia. The Lancet. 2006;368(9550):1894-907.

7. Deschler B, Lübbert M. Acute myeloid leukemia: epidemiology and etiology. Cancer. 2006;107(9):2099-107.

8. De Kouchkovsky I, Abdul-Hay M. Acute myeloid leukemia: a comprehensive review and 2016 update. Blood cancer journal. 2016;6(7):e441-e.

9. Australian Institute of Health and Welfare. Cancer in Australia 2019. 2019.

10. Thursfield V, Farrugia H. Cancer in Victoria: Statistics & Trends 2016. Cancer Council Victoria, Melbourne. 2017.

11. Walter RB, Estey EH. Management of older or unfit patients with acute myeloid leukemia. Leukemia. 2015;29(4):770.

12. Rubnitz JE, Gibson B, Smith FO. Acute myeloid leukemia. Pediatric clinics of North America. 2008;55(1):21-51.

13. Nichol JN, Kinal M, Miller WH. The etiology of acute leukemia. Neoplastic Diseases of the Blood: Springer; 2018. p. 161-77.

14. Kelly LM, Gilliland DG. Genetics of myeloid leukemias. Annual review of genomics and human genetics. 2002;3(1):179-98.

15. Takahashi S. Current findings for recurring mutations in acute myeloid leukemia. Journal of hematology & oncology. 2011;4(1):36.

16. Iliakis G, Wang Y, Guan J, Wang H. DNA damage checkpoint control in cells exposed to ionizing radiation. Oncogene. 2003;22(37):5834-47.

17. Lichtman MA. A historical perspective on the development of the cytarabine (7 days) and daunorubicin (3 days) treatment regimen for acute myelogenous leukemia: 2013 the 40th anniversary of 7+ 3. Blood Cells, Molecules, and Diseases. 2013;50(2):119-30.

18. Löwenberg B, Pabst T, Vellenga E, van Putten W, Schouten HC, Graux C, et al. Cytarabine dose for acute myeloid leukemia. New England Journal of Medicine. 2011;364(11):1027-36.

19. Burnett AK, Russell NH, Hills RK, Kell J, Cavenagh J, Kjeldsen L, et al. A randomized comparison of daunorubicin 90 mg/m2 vs 60 mg/m2 in AML induction: results from the UK NCRI AML17 trial in 1206 patients. Blood, The Journal of the American Society of Hematology. 2015;125(25):3878-85.

20. Norsworthy KJ, DeZern AE, Tsai H-L, Hand WA, Varadhan R, Gore SD, et al. Timed sequential therapy for acute myelogenous leukemia: results of a retrospective study of 301 patients and review of the literature. Leukemia research. 2017;61:25-32.

21. Lai C, Doucette K, Norsworthy K. Recent drug approvals for acute myeloid leukemia. Journal of hematology & oncology. 2019;12(1):100.

22. Jen EY, Ko C-W, Lee JE, Del Valle PL, Aydanian A, Jewell C, et al. FDA approval: gemtuzumab ozogamicin for the treatment of adults with newly diagnosed CD33-positive acute myeloid leukemia. Clinical cancer research. 2018;24(14):3242-6.

23. Flaherty KT, Infante JR, Daud A, Gonzalez R, Kefford RF, Sosman J, et al. Combined BRAF and MEK inhibition in melanoma with BRAF V600 mutations. New England Journal of Medicine. 2012;367(18):1694-703.

24. Fitzgerald JB, Schoeberl B, Nielsen UB, Sorger PK. Systems biology and combination therapy in the quest for clinical efficacy. Nature chemical biology. 2006;2(9):458-66.

25. Lehár J, Krueger AS, Avery W, Heilbut AM, Johansen LM, Price ER, et al. Synergistic drug combinations tend to improve therapeutically relevant selectivity. Nature biotechnology. 2009;27(7):659-66.

26. Burnett A, Wetzler M, Lowenberg B. Therapeutic advances in acute myeloid leukemia. J Clin Oncol. 2011;29(5):487-94.

27. Lapidot T, Sirard C, Vormoor J, Murdoch B, Hoang T, Caceres-Cortes J, et al. A cell initiating human acute myeloid leukaemia after transplantation into SCID mice. Nature. 1994;367(6464):645-8.

28. Ng SW, Mitchell A, Kennedy JA, Chen WC, McLeod J, Ibrahimova N, et al. A 17-gene stemness score for rapid determination of risk in acute leukaemia. Nature. 2016;540(7633):433.

29. Reya T, Morrison SJ, Clarke MF, Weissman IL. Stem cells, cancer, and cancer stem cells. nature. 2001;414(6859):105.

30. Thomas D, Majeti R. Biology and relevance of human acute myeloid leukemia stem cells. Blood. 2017:blood-2016-10-696054.

31. Cancer Genome Atlas Research Network. Genomic and epigenomic landscapes of adult de novo acute myeloid leukemia. New England Journal of Medicine. 2013;368(22):2059-74.

32. Corces-Zimmerman MR, Hong W-J, Weissman IL, Medeiros BC, Majeti R. Preleukemic mutations in human acute myeloid leukemia affect epigenetic regulators and persist in remission. Proceedings of the National Academy of Sciences. 2014;111(7):2548-53.

33. Jan M, Snyder TM, Corces-Zimmerman MR, Vyas P, Weissman IL, Quake SR, et al. Clonal evolution of preleukemic hematopoietic stem cells precedes human acute myeloid leukemia. Science translational medicine. 2012;4(149):149ra18-ra18.

34. Grimwade D, Mrózek K. Diagnostic and prognostic value of cytogenetics in acute myeloid leukemia. Hematology/Oncology Clinics. 2011;25(6):1135-61.

35. Döhner H, Estey E, Grimwade D, Amadori S, Appelbaum FR, Büchner T, et al. Diagnosis and management of AML in adults: 2017 ELN recommendations from an international expert panel. Blood. 2017;129(4):424-47.

36. Papaemmanuil E, Doehner H, Campbell PJ. Genomic Classification in Acute Myeloid Leukemia. The New England journal of medicine. 2016;375(9):900-1.

37. Waddington C. Preliminary notes on the development of the wings in normal and mutant strains of Drosophila. Proceedings of the National Academy of Sciences. 1939;25(7):299-307.

38. Humpherys D, Eggan K, Akutsu H, Hochedlinger K, Rideout WM, Biniszkiewicz D, et al. Epigenetic instability in ES cells and cloned mice. Science. 2001;293(5527):95-7.

39. Fraga MF, Ballestar E, Paz MF, Ropero S, Setien F, Ballestar ML, et al. Epigenetic differences arise during the lifetime of monozygotic twins. Proceedings of the National Academy of Sciences. 2005;102(30):10604-9.

40. Jones PA, Baylin SB. The epigenomics of cancer. Cell. 2007;128(4):683-92.

41. Alberts B, Johnson A, Lewis J, Raff M, Roberts K, Walter P. Molecular biology of the cell. Garland Science. New York. 2015:1227-42.

42. Grewal SI, Moazed D. Heterochromatin and epigenetic control of gene expression. science. 2003;301(5634):798-802.

43. De Majo F, Calore M. Chromatin remodelling and epigenetic state regulation by non-coding RNAs in the diseased heart. Non-coding RNA research. 2018;3(1):20-8.

44. Dai Z, Ramesh V, Locasale JW. The evolving metabolic landscape of chromatin biology and epigenetics. Nature Reviews Genetics. 2020:1-17.

45. Figueroa ME, Lugthart S, Li Y, Erpelinck-Verschueren C, Deng X, Christos PJ, et al. DNA methylation signatures identify biologically distinct subtypes in acute myeloid leukemia. Cancer cell. 2010;17(1):13-27.

46. Gröschel S, Sanders MA, Hoogenboezem R, de Wit E, Bouwman BA, Erpelinck C, et al. A single oncogenic enhancer rearrangement causes concomitant EVI1 and GATA2 deregulation in leukemia. Cell. 2014;157(2):369-81.

47. Wouters BJ, Delwel R. Epigenetics and approaches to targeted epigenetic therapy in acute myeloid leukemia. Blood. 2015:blood-2015-07-604512.

48. Jaiswal S, Fontanillas P, Flannick J, Manning A, Grauman PV, Mar BG, et al. Age-related clonal hematopoiesis associated with adverse outcomes. New England Journal of Medicine. 2014;371(26):2488-98.

49. Kahn P. From genome to proteome: looking at a cell's proteins. American Association for the Advancement of Science; 1995.

50. Walsh CT, Garneau-Tsodikova S, Gatto Jr GJ. Protein posttranslational modifications: the chemistry of proteome diversifications. Angewandte Chemie International Edition. 2005;44(45):7342-72.

51. Duan G, Walther D. The roles of post-translational modifications in the context of protein interaction networks. PLoS computational biology. 2015;11(2):e1004049.

52. Clarke SG. Protein methylation at the surface and buried deep: thinking outside the histone box. Trends in biochemical sciences. 2013;38(5):243-52.

53. Zhang L, Ma H. Complex evolutionary history and diverse domain organization of SET proteins suggest divergent regulatory interactions. New Phytologist. 2012;195(1):248-63.

54. Alban C, Tardif M, Mininno M, Brugière S, Gilgen A, Ma S, et al. Uncovering the protein lysine and arginine methylation network in Arabidopsis chloroplasts. PLoS One. 2014;9(4):e95512.

55. Bedford MT, Richard S. Arginine methylation: an emerging regulatorof protein function. Molecular cell. 2005;18(3):263-72.

56. Martin C, Zhang Y. The diverse functions of histone lysine methylation. Nature reviews Molecular cell biology. 2005;6(11):838.

57. Bedford MT, Clarke SG. Protein arginine methylation in mammals: who, what, and why. Molecular cell. 2009;33(1):1-13.

58. Yost JM, Korboukh I, Liu F, Gao C, Jin J. Targets in Epigenetics: Inhibiting the Methyl Writers of the Histone Code. Current chemical genomics. 2011;5:72.

59. Shi Y, Lan F, Matson C, Mulligan P, Whetstine JR, Cole PA, et al. Histone demethylation mediated by the nuclear amine oxidase homolog LSD1. Cell. 2004;119(7):941-53.

60. Tsukada Y-i, Fang J, Erdjument-Bromage H, Warren ME, Borchers CH, Tempst P, et al. Histone demethylation by a family of JmjC domain-containing proteins. Nature. 2006;439(7078):811.

61. Yang Y, Bedford MT. Protein arginine methyltransferases and cancer. Nature Reviews Cancer. 2013;13(1):37.

62. Walport LJ, Hopkinson RJ, Chowdhury R, Schiller R, Ge W, Kawamura A, et al. Arginine demethylation is catalysed by a subset of JmjC histone lysine demethylases. Nature communications. 2016;7:11974.

63. Blanc RS, Richard S. Arginine methylation: the coming of age. Molecular cell. 2017;65(1):8-24.

64. Lakowski TM, Frankel A. Kinetic analysis of human protein arginine N-methyltransferase 2: formation of monomethyl-and asymmetric dimethyl-arginine residues on histone H4. Biochemical Journal. 2009;421(2):253-61.

65. Raman B, Guarnaccia C, Nadassy K, Zakhariev S, Pintar A, Zanuttin F, et al. N ω-arginine dimethylation modulates the interaction between a Gly/Arg-rich peptide from human nucleolin and nucleic acids. Nucleic acids research. 2001;29(16):3377-84.

66. Schapira M, de Freitas RF. Structural biology and chemistry of protein arginine methyltransferases. MedChemComm. 2014;5(12):1779-88.

67. Wolf S. The protein arginine methyltransferase family: an update about function, new perspectives and the physiological role in humans. Cellular and molecular life sciences. 2009;66(13):2109-21.

68. Yang Y, Hadjikyriacou A, Xia Z, Gayatri S, Kim D, Zurita-Lopez C, et al. PRMT9 is a type II methyltransferase that methylates the splicing factor SAP145. Nature communications. 2015;6:6428.

69. Hadjikyriacou A, Yang Y, Espejo A, Bedford MT, Clarke SG. Unique features of human protein arginine methyltransferase 9 (PRMT9) and its substrate RNA splicing factor SF3B2. Journal of Biological Chemistry. 2015:jbc. M115. 659433.

70. Zurita-Lopez CI, Sandberg T, Kelly R, Clarke SG. Human protein arginine methyltransferase 7 (PRMT7) is a type III enzyme forming ω-NG-monomethylated arginine residues. Journal of Biological Chemistry. 2012:jbc. M111. 336271.

71. Sun L, Wang M, Lv Z, Yang N, Liu Y, Bao S, et al. Structural insights into protein arginine symmetric dimethylation by PRMT5. Proceedings of the National Academy of Sciences. 2011;108(51):20538-43.

72. Antonysamy S, Bonday Z, Campbell RM, Doyle B, Druzina Z, Gheyi T, et al. Crystal structure of the human PRMT5: MEP50 complex. Proceedings of the National Academy of Sciences. 2012;109(44):17960-5.

73. Ho M-C, Wilczek C, Bonanno JB, Xing L, Seznec J, Matsui T, et al. Structure of the arginine methyltransferase PRMT5-MEP50 reveals a mechanism for substrate specificity. PLoS One. 2013;8(2):e57008.

74. Troffer-Charlier N, Cura V, Hassenboehler P, Moras D, Cavarelli J. Functional insights from structures of coactivator-associated arginine methyltransferase 1 domains. The EMBO journal. 2007;26(20):4391-401.

75. Yue WW, Hassler M, Roe SM, Thompson-Vale V, Pearl LH. Insights into histone code syntax from structural and biochemical studies of CARM1 methyltransferase. The EMBO journal. 2007;26(20):4402-12.

76. Zhang X, Zhou L, Cheng X. Crystal structure of the conserved core of protein arginine methyltransferase PRMT3. The EMBO journal. 2000;19(14):3509-19.

77. Krapivinsky G, Pu W, Wickman K, Krapivinsky L, Clapham DE. pICln binds to a mammalian homolog of a yeast protein involved in regulation of cell morphology. Journal of Biological Chemistry. 1998;273(18):10811-4.

78. Pollack BP, Kotenko SV, He W, Izotova LS, Barnoski BL, Pestka S. The human homologue of the yeast proteins Skb1 and Hsl7p interacts with Jak kinases and contains protein methyltransferase activity. Journal of Biological Chemistry. 1999;274(44):31531-42.

79. Boulanger M-C, Miranda TB, Clarke S, Di Fruscio M, Suter B, Lasko P, et al. Characterization of the Drosophila protein arginine methyltransferases DART1 and DART4. Biochemical journal. 2004;379(2):283-9.

80. Hung C-M, Li C. Identification and phylogenetic analyses of the protein arginine methyltransferase gene family in fish and ascidians. Gene. 2004;340(2):179-87.

81. Pal S, Vishwanath SN, Erdjument-Bromage H, Tempst P, Sif S. Human SWI/SNF-associated PRMT5 methylates histone H3 arginine 8 and negatively regulates expression of ST7 and NM23 tumor suppressor genes. Molecular and cellular biology. 2004;24(21):9630-45.

82. Shin W-H, Kihara D. 55 Years of the Rossmann fold. Protein Supersecondary Structures: Springer; 2019. p. 1-13.

83. Rho J, Choi S, Seong Y, Cho W, Kim S, Im D. PRMT5, which forms distinct homo-oligomers, is a member of the protein-arginine methyltransferase family (vol 276, pg 11393, 2001). JOURNAL OF BIOLOGICAL CHEMISTRY. 2001;276(19):16592-.

84. Zhang X, Cheng X. Structure of the predominant protein arginine methyltransferase PRMT1 and analysis of its binding to substrate peptides. Structure. 2003;11(5):509-20.

85. Antonysamy S. The structure and function of the PRMT5: MEP50 complex. Macromolecular Protein Complexes: Springer; 2017. p. 185-94.

86. Pal S, Yun R, Datta A, Lacomis L, Erdjument-Bromage H, Kumar J, et al. mSin3A/histone deacetylase 2-and PRMT5-containing Brg1 complex is involved in transcriptional repression of the Myc target gene cad. Molecular and cellular biology. 2003;23(21):7475-87.

87. Zhao Q, Rank G, Tan YT, Li H, Moritz RL, Simpson RJ, et al. PRMT5-mediated methylation of histone H4R3 recruits DNMT3A, coupling histone and DNA methylation in gene silencing. Nature structural & molecular biology. 2009;16(3):304-11.

88. Bezzi M, Teo SX, Muller J, Mok WC, Sahu SK, Vardy LA, et al. Regulation of constitutive and alternative splicing by PRMT5 reveals a role for Mdm4 pre-mRNA in sensing defects in the spliceosomal machinery. Genes & development. 2013;27(17):1903-16.

89. Majumder S, Alinari L, Roy S, Miller T, Datta J, Sif S, et al. Methylation of histone H3 and H4 by PRMT5 regulates ribosomal RNA gene transcription. Journal of cellular biochemistry. 2010;109(3):553-63.

90. Zhou Z, Sun X, Zou Z, Sun L, Zhang T, Guo S, et al. PRMT5 regulates Golgi apparatus structure through methylation of the golgin GM130. Cell research. 2010;20(9):1023.

91. Tee W-W, Pardo M, Theunissen TW, Yu L, Choudhary JS, Hajkova P, et al. Prmt5 is essential for early mouse development and acts in the cytoplasm to maintain ES cell pluripotency. Genes & development. 2010;24(24):2772-7.

92. Stopa N, Krebs JE, Shechter D. The PRMT5 arginine methyltransferase: many roles in development, cancer and beyond. Cellular and molecular life sciences. 2015;72(11):2041-59.

93. Kanade SR, Eckert RL. Protein arginine methyltransferase 5 (PRMT5) signaling suppresses protein kinase Cδ-and p38δ-dependent signaling and keratinocyte differentiation. Journal of Biological Chemistry. 2012;287(10):7313-23.

94. Bagger FO, Kinalis S, Rapin N. BloodSpot: a database of healthy and malignant haematopoiesis updated with purified and single cell mRNA sequencing profiles. Nucleic acids research. 2019;47(D1):D881-D5.

95. Liu F, Cheng G, Hamard P-J, Greenblatt S, Wang L, Man N, et al. Arginine methyltransferase PRMT5 is essential for sustaining normal adult hematopoiesis. The Journal of clinical investigation. 2015;125(9):3532.

96. Liu Y, Elf SE, Miyata Y, Sashida G, Liu Y, Huang G, et al. p53 regulates hematopoietic stem cell quiescence. Cell stem cell. 2009;4(1):37-48.

97. Kanda M, Shimizu D, Fujii T, Tanaka H, Shibata M, Iwata N, et al. Protein arginine methyltransferase 5 is associated with malignant phenotype and peritoneal metastasis in gastric cancer. International journal of oncology. 2016;49(3):1195-202.

98. Han X, Li R, Zhang W, Yang X, Wheeler CG, Friedman GK, et al. Expression of PRMT5 correlates with malignant grade in gliomas and plays a pivotal role in tumor growth in vitro. Journal of neuro-oncology. 2014;118(1):61-72.

99. Bao X, Zhao S, Liu T, Liu Y, Liu Y, Yang X. Overexpression of PRMT5 promotes tumor cell growth and is associated with poor disease prognosis in epithelial ovarian cancer. Journal of Histochemistry & Cytochemistry. 2013;61(3):206-17.

100. Ibrahim R, Matsubara D, Osman W, Morikawa T, Goto A, Morita S, et al. Expression of PRMT5 in lung adenocarcinoma and its significance in epithelial-mesenchymal transition. Human pathology. 2014;45(7):1397-405.

101. Zhang H-T, Zhang D, Zha Z-G, Hu C-D. Transcriptional activation of PRMT5 by NF-Y is required for cell growth and negatively regulated by the PKC/c-Fos signaling in prostate cancer cells. Biochimica et Biophysica Acta (BBA)-Gene Regulatory Mechanisms. 2014;1839(11):1330-40.

102. Koh CM, Bezzi M, Low DH, Ang WX, Teo SX, Gay FP, et al. MYC regulates the core pre-mRNA splicing machinery as an essential step in lymphomagenesis. Nature. 2015;523(7558):96.

103. Miller DM, Thomas SD, Islam A, Muench D, Sedoris K. c-Myc and cancer metabolism. AACR; 2012.

104. Greenblatt SM, Liu F, Nimer SD. Arginine methyltransferases in normal and malignant hematopoiesis. Experimental hematology. 2016;44(6):435-41.

105. Wang L, Pal S, Sif S. Protein arginine methyltransferase 5 suppresses the transcription of the RB family of tumor suppressors in leukemia and lymphoma cells. Molecular and cellular biology. 2008;28(20):6262-77.

106. Pal S, Baiocchi RA, Byrd JC, Grever MR, Jacob ST, Sif S. Low levels of miR-92b/96 induce PRMT5 translation and H3R8/H4R3 methylation in mantle cell lymphoma. The EMBO journal. 2007;26(15):3558-69.

107. Chan-Penebre E, Kuplast KG, Majer CR, Boriack-Sjodin PA, Wigle TJ, Johnston LD, et al. A selective inhibitor of PRMT5 with in vivo and in vitro potency in MCL models. Nature chemical biology. 2015;11(6):432.

108. Jin Y, Zhou J, Xu F, Jin B, Cui L, Wang Y, et al. Targeting methyltransferase PRMT5 eliminates leukemia stem cells in chronic myelogenous leukemia. The Journal of clinical investigation. 2016;126(10):3961-80.

109. Tarighat S, Santhanam R, Frankhouser D, Radomska H, Lai H, Anghelina M, et al. The dual epigenetic role of PRMT5 in acute myeloid leukemia: gene activation and repression via histone arginine methylation. Leukemia. 2016;30(4):789-99.

110. Tsuchiya S, Yamabe M, Yamaguchi Y, Kobayashi Y, Konno T, Tada K. Establishment and characterization of a human acute monocytic leukemia cell line (THP-1). International journal of cancer. 1980;26(2):171-6.

111. Blum W, Schwind S, Tarighat SS, Geyer S, Eisfeld A-K, Whitman S, et al. Clinical and pharmacodynamic activity of bortezomib and decitabine in acute myeloid leukemia. Blood. 2012:blood-2012-03-413898.

112. Serio J, Ropa J, Chen W, Mysliwski M, Saha N, Chen L, et al. The PAF complex regulation of Prmt5 facilitates the progression and maintenance of MLL fusion leukemia. Oncogene. 2018;37(4):450.

113. Tan J, Muntean AG, Hess JL. PAFc, a key player in MLL-rearranged leukemogenesis. Oncotarget. 2010;1(6):461.

114. Moniaux N, Nemos C, Schmied B, Chauhan S, Deb S, Morikane K, et al. The human homologue of the RNA polymerase II-associated factor 1 (hPaf1), localized on the 19q13 amplicon, is associated with tumorigenesis. Oncogene. 2006;25(23):3247.

115. Zeng H, Xu W. Ctr9, a key subunit of PAFc, affects global estrogen signaling and drives ERα-positive breast tumorigenesis. Genes & Development. 2015(29):2153-67.

116. Kaushik S, Liu F, Veazey K, Gao G, Das P, Neves L, et al. Genetic deletion or small-molecule inhibition of the arginine methyltransferase PRMT5 exhibit anti-tumoral activity in mouse models of MLL-rearranged AML. Leukemia. 2018;32(2):499.

117. Kong G-M, Yu M, Gu Z, Chen Z, Xu R-M, O'Bryant D, et al. Selective small-chemical inhibitors of protein arginine methyltransferase 5 with anti-lung cancer activity. PloS one. 2017;12(8):e0181601.

118. Wang Q, Xu J, Li Y, Huang J, Jiang Z, Wang Y, et al. Identification of a Novel Protein Arginine Methyltransferase 5 Inhibitor in Non-small Cell Lung Cancer by Structure-Based Virtual Screening. Frontiers in pharmacology. 2018;9:173.

119. Chiang K, Zielinska AE, Shaaban AM, Sanchez-Bailon MP, Jarrold J, Clarke TL, et al. PRMT5 Is a Critical Regulator of Breast Cancer Stem Cell Function via Histone Methylation and FOXP1 Expression. Cell reports. 2017;21(12):3498-513.

120. Zhang B, Dong S, Zhu R, Hu C, Hou J, Li Y, et al. Targeting protein arginine methyltransferase 5 inhibits colorectal cancer growth by decreasing arginine methylation of eIF4E and FGFR3. Oncotarget. 2015;6(26):22799.

121. Zhang B, Zhang S, Zhu L, Chen X, Zhao Y, Chao L, et al. Arginine methyltransferase inhibitor 1 inhibits gastric cancer by downregulating eIF4E and targeting PRMT5. Toxicology and applied pharmacology. 2017;336:1-7.

122. Yan F, Alinari L, Lustberg ME, Martin LK, Cordero-Nieves HM, Banasavadi-Siddegowda Y, et al. Genetic validation of the protein arginine methyltransferase PRMT5 as a candidate therapeutic target in glioblastoma. Cancer research. 2014:canres. 0884.2013.

123. Park JH, Szemes M, Vieira GC, Melegh Z, Malik S, Heesom KJ, et al. Protein arginine methyltransferase 5 is a key regulator of the MYCN oncoprotein in neuroblastoma cells. Molecular oncology. 2015;9(3):617-27.

124. Chung J, Karkhanis V, Tae S, Yan F, Smith P, Ayers LW, et al. Protein arginine methyltransferase 5 inhibition induces lymphoma cell death through reactivation of the retinoblastoma tumor suppressor pathway and polycomb repressor complex 2 silencing. Journal of Biological Chemistry. 2013:jbc. M113. 510669.

125. Li X, Wang C, Jiang H, Luo C. A patent review of arginine methyltransferase inhibitors (2010–2018). Expert opinion on therapeutic patents. 2019;29(2):97-114.

126. Raposo AE, Piller SC. Protein arginine methylation: an emerging regulator of the cell cycle. Cell division. 2018;13(1):3.

127. Fulton MD, Brown T, Zheng YG. The Biological Axis of Protein Arginine Methylation and Asymmetric Dimethylarginine. International journal of molecular sciences. 2019;20(13):3322.

128. Mavrakis KJ, McDonald ER, Schlabach MR, Billy E, Hoffman GR, deWeck A, et al. Disordered methionine metabolism in MTAP/CDKN2A-deleted cancers leads to dependence on PRMT5. Science. 2016;351(6278):1208-13.

129. Yau EH, Rana TM. Next-generation sequencing of genome-wide CRISPR Screens. Next Generation Sequencing: Springer; 2018. p. 203-16.

130. Li W, Xu H, Xiao T, Cong L, Love MI, Zhang F, et al. MAGeCK enables robust identification of essential genes from genome-scale CRISPR/Cas9 knockout screens. Genome biology. 2014;15(12):554.

131. Tchorz JS, Suply T, Ksiazek I, Giachino C, Cloetta D, Danzer C-P, et al. A modified RMCE-compatible Rosa26 locus for the expression of transgenes from exogenous promoters. PloS one. 2012;7(1):e30011.

132. Soriano P. Generalized lacZ expression with the ROSA26 Cre reporter strain. Nature genetics. 1999;21(1):70-1.

133. George SH, Gertsenstein M, Vintersten K, Korets-Smith E, Murphy J, Stevens ME, et al. Developmental and adult phenotyping directly from mutant embryonic stem cells. Proceedings of the National Academy of Sciences. 2007;104(11):4455-60.

134. Srinivas S, Watanabe T, Lin C-S, William CM, Tanabe Y, Jessell TM, et al. Cre reporter strains produced by targeted insertion of EYFP and ECFP into the ROSA26 locus. BMC developmental biology. 2001;1(1):4.

135. Georgiades P, Ogilvy S, Duval H, Licence DR, Charnock-Jones DS, Smith SK. VavCre transgenic mice: a tool for mutagenesis in hematopoietic and endothelial lineages. genesis. 2002;34(4):251-6.

136. de Boer J, Williams A, Skavdis G, Harker N, Coles M, Tolaini M, et al. Transgenic mice with hematopoietic and lymphoid specific expression of Cre. European journal of immunology. 2003;33(2):314-25.

137. Perez-Cunningham J, Boyer SW, Landon M, Forsberg EC. Hematopoietic stem cell-specific GFP-expressing transgenic mice generated by genetic excision of a pan-hematopoietic reporter gene. Experimental hematology. 2016;44(8):755-64. e1.

138. Nyabi O, Naessens M, Haigh K, Gembarska A, Goossens S, Maetens M, et al. Efficient mouse transgenesis using Gateway-compatible ROSA26 locus targeting vectors and F1 hybrid ES cells. Nucleic acids research. 2009;37(7):e55-e.

139. Hohenstein P, Slight J, Ozdemir DD, Burn SF, Berry R, Hastie ND. High-efficiency Rosa26 knock-in vector construction for Cre-regulated overexpression and RNAi. Pathogenetics. 2008;1(1):3.

140. Wu Y, Zhou BP. Snail: more than EMT. Cell adhesion & migration. 2010;4(2):199-203.

141. Xu C, Min J. Structure and function of WD40 domain proteins. Protein & cell. 2011;2(3):202-14.

142. Boyer SW, Schroeder AV, Smith-Berdan S, Forsberg EC. All hematopoietic cells develop from hematopoietic stem cells through Flk2/Flt3-positive progenitor cells. Cell stem cell. 2011;9(1):64-73.

143. Shin JY, Hu W, Naramura M, Park CY. High c-Kit expression identifies hematopoietic stem cells with impaired self-renewal and megakaryocytic bias. Journal of Experimental Medicine. 2014;211(2):217-31.

144. Braun CJ, Stanciu M, Boutz PL, Patterson JC, Calligaris D, Higuchi F, et al. Coordinated splicing of regulatory detained introns within oncogenic transcripts creates an exploitable vulnerability in malignant glioma. Cancer cell. 2017;32(4):411-26. e11.

145. Tan DQ, Li Y, Yang C, Li J, Tan SH, Chin DWL, et al. PRMT5 modulates splicing for genome integrity and preserves proteostasis of hematopoietic stem cells. Cell reports. 2019;26(9):2316-28. e6.

146. Hess GT, Frésard L, Han K, Lee CH, Li A, Cimprich KA, et al. Directed evolution using dCas9-targeted somatic hypermutation in mammalian cells. Nature methods. 2016;13(12):1036.

147. Rajewsky K, Forster I, Cumano A. Evolutionary and somatic selection of the antibody repertoire in the mouse. Science. 1987;238(4830):1088-94.

148. Musiani D, Bok J, Massignani E, Wu L, Tabaglio T, Ippolito MR, et al. Proteomics profiling of arginine methylation defines PRMT5 substrate specificity. Science signaling. 2019;12(575):eaat8388.

149. Larsen SC, Sylvestersen KB, Mund A, Lyon D, Mullari M, Madsen MV, et al. Proteome-wide analysis of arginine monomethylation reveals widespread occurrence in human cells. Sci Signal. 2016;9(443):rs9-rs.

150. Hamard P-J, Santiago GE, Liu F, Karl DL, Martinez C, Man N, et al. PRMT5 regulates DNA repair by controlling the alternative splicing of histone-modifying enzymes. Cell reports. 2018;24(10):2643-57.

151. Mamane Y, Petroulakis E, Rong L, Yoshida K, Ler LW, Sonenberg N. eIF4E–from translation to transformation. Oncogene. 2004;23(18):3172-9.

152. Somervaille T, Wingelhofer B. Emerging epigenetic therapeutic targets in acute myeloid leukemia. Frontiers in oncology. 2019;9:850.

153. Watts JM, Bradley TJ, Thomassen A, Brunner AM, Minden MD, Papadantonakis N, et al. A Phase I/II Study to Investigate the Safety and Clinical Activity of the Protein Arginine Methyltransferase 5 Inhibitor GSK3326595 in Subjects with Myelodysplastic Syndrome and Acute Myeloid Leukemia. American Society of Hematology Washington, DC; 2019.

154. Chen S-J, Shen Y, Chen Z. A panoramic view of acute myeloid leukemia. Nature genetics. 2013;45(6):586.

155. Onec B, Okutan H, Albayrak M, Can ES, Aslan V, Koluman BU, et al. Combination therapy with azacitidine, etoposide, and cytarabine in the treatment of elderly acute myeloid leukemia patients: A single center experience. Journal of cancer research and therapeutics. 2018;14(5):1105.

156. Winer ES, Stone RM. Novel therapy in acute myeloid leukemia (AML): moving toward targeted approaches. Therapeutic advances in hematology. 2019;10:2040620719860645.

157. Zhou Y, Zhu S, Cai C, Yuan P, Li C, Huang Y, et al. High-throughput screening of a CRISPR/Cas9 library for functional genomics in human cells. Nature. 2014;509(7501):487-91.

158. Wang T, Wei JJ, Sabatini DM, Lander ES. Genetic screens in human cells using the CRISPR-Cas9 system. Science. 2014;343(6166):80-4.

159. Gao G, Zhang L, Villarreal OD, He W, Su D, Bedford E, et al. PRMT1 loss sensitizes cells to PRMT5 inhibition. Nucleic acids research. 2019;47(10):5038-48.

160. Subramanian A, Narayan R, Corsello SM, Peck DD, Natoli TE, Lu X, et al. A next generation connectivity map: L1000 platform and the first 1,000,000 profiles. Cell. 2017;171(6):1437-52. e17.

161. Toulmin E, Sonderegger S, Cerruti L, Terzic A, Yan F, Wong N, et al. PRMT5 Inhibition Selectively Targets Acute Myeloid Leukemia Stem Cells Though a p53-Dependent Mechanism. Blood. 2018;132(Supplement 1):4061-.

162. Gerhart SV, Kellner WA, Thompson C, Pappalardi MB, Zhang X-P, de Oca RM, et al. Activation of the p53-MDM4 regulatory axis defines the anti-tumour response to PRMT5 inhibition through its role in regulating cellular splicing. Scientific reports. 2018;8(1):1-15.

163. Datlinger P, Rendeiro AF, Schmidl C, Krausgruber T, Traxler P, Klughammer J, et al. Pooled CRISPR screening with single-cell transcriptome readout. Nature methods. 2017;14(3):297.

164. Lamb J. The Connectivity Map: a new tool for biomedical research. Nature reviews cancer. 2007;7(1):54-60.

165. Gapp BV, Konopka T, Penz T, Dalal V, Bürckstümmer T, Bock C, et al. Parallel reverse genetic screening in mutant human cells using transcriptomics. Molecular systems biology. 2016;12(8).

166. Illei PB, Rusch VW, Zakowski MF, Ladanyi M. Homozygous deletion of CDKN2A and codeletion of the methylthioadenosine phosphorylase gene in the majority of pleural mesotheliomas. Clinical Cancer Research. 2003;9(6):2108-13.

167. Powell EL, Leoni LM, Canto MI, Forastiere AA, Iocobuzio-Donahue CA, Wang JS, et al. Concordant loss of MTAP and p16/CDKN2A expression in gastroesophageal carcinogenesis: evidence of homozygous deletion in esophageal noninvasive precursor lesions and therapeutic implications. The American journal of surgical pathology. 2005;29(11):1497-504.

168. Christopher SA, Diegelman P, Porter CW, Kruger WD. Methylthioadenosine phosphorylase, a gene frequently codeleted with p16cdkN2a/ARF, acts as a tumor suppressor in a breast cancer cell line. Cancer research. 2002;62(22):6639-44.

169. Marjon K, Cameron MJ, Quang P, Clasquin MF, Mandley E, Kunii K, et al. MTAP deletions in cancer create vulnerability to targeting of the MAT2A/PRMT5/RIOK1 axis. Cell reports. 2016;15(3):574-87.

170. Basu I, Cordovano G, Das I, Belbin TJ, Guha C, Schramm VL. A transition state analogue of 5′-methylthioadenosine phosphorylase induces apoptosis in head and neck cancers. Journal of Biological Chemistry. 2007;282(29):21477-86.

171. Basu I, Locker J, Cassera MB, Belbin TJ, Merino EF, Dong X, et al. Growth and metastases of human lung cancer are inhibited in mouse xenografts by a transition state analogue of 5′-methylthioadenosine phosphorylase. Journal of Biological Chemistry. 2011;286(6):4902-11.

172. Kryukov GV, Wilson FH, Ruth JR, Paulk J, Tsherniak A, Marlow SE, et al. MTAP deletion confers enhanced dependency on the PRMT5 arginine methyltransferase in cancer cells. Science. 2016;351(6278):1214-8.

173. Siddiqui N, Sonenberg N. Signalling to eIF4E in cancer. Biochemical Society Transactions. 2015;43(5):763-72.

174. Ghosh J, Kapur R. Role of mTORC1–S6K1 signaling pathway in regulation of hematopoietic stem cell and acute myeloid leukemia. Experimental hematology. 2017;50:13-21.

175. Dombi E, Baldwin A, Marcus LJ, Fisher MJ, Weiss B, Kim A, et al. Activity of selumetinib in neurofibromatosis type 1–related plexiform neurofibromas. New England Journal of Medicine. 2016;375(26):2550-60.

176. Canagarajah BJ, Khokhlatchev A, Cobb MH, Goldsmith EJ. Activation mechanism of the MAP kinase ERK2 by dual phosphorylation. Cell. 1997;90(5):859-69.

177. Andreu-Perez P, Esteve-Puig R, de Torre-Minguela C, López-Fauqued M, Bech-Serra JJ, Tenbaum S, et al. Protein arginine methyltransferase 5 regulates ERK1/2 signal transduction amplitude and cell fate through CRAF. Science signaling. 2011;4(190):ra58-ra.

178. Westerink R, Ewing AG. The PC12 cell as model for neurosecretion. Acta Physiologica. 2008;192(2):273-85.

179. Jiang H, Zhu Y, Zhou Z, Xu J, Jin S, Xu K, et al. PRMT 5 promotes cell proliferation by inhibiting BTG 2 expression via the ERK signaling pathway in hepatocellular carcinoma. Cancer medicine. 2018;7(3):869-82.

180. Snyder KJ, Zitzer NC, Gao Y, Choe HK, Sell NE, Neidemire-Colley L, et al. PRMT5 regulates T cell interferon response and is a target for acute graft-versus-host disease. JCI insight. 2020;5(8).

181. Konopleva M, Letai A. BCL-2 inhibition in AML: an unexpected bonus? Blood. 2018;132(10):1007-12.

182. San José-Enériz E, Gimenez-Camino N, Agirre X, Prosper F. HDAC Inhibitors in Acute Myeloid Leukemia. Cancers (Basel). 2019;11(11):1794.

183. Lillico R, Lawrence CK, Lakowski TM. Selective DOT1L, LSD1, and HDAC Class i inhibitors reduce HOXA9 expression in MLL-AF9 rearranged leukemia cells, but dysregulate the expression of many histone-modifying enzymes. Journal of proteome research. 2018;17(8):2657-67.

184. Garcia-Manero G, Assouline S, Cortes J, Estrov Z, Kantarjian H, Yang H, et al. Phase 1 study of the oral isotype specific histone deacetylase inhibitor MGCD0103 in leukemia. Blood, The Journal of the American Society of Hematology. 2008;112(4):981-9.

185. Vassilev LT, Tovar C, Chen S, Knezevic D, Zhao X, Sun H, et al. Selective small-molecule inhibitor reveals critical mitotic functions of human CDK1. Proceedings of the National Academy of Sciences. 2006;103(28):10660-5.

186. Wei TYW, Juan CC, Hisa JY, Su LJ, Lee YCG, Chou HY, et al. Protein arginine methyltransferase 5 is a potential oncoprotein that upregulates G1 cyclins/cyclin-dependent kinases and the phosphoinositide 3-kinase/AKT signaling cascade. Cancer science. 2012;103(9):1640-50.

187. Yadav B, Wennerberg K, Aittokallio T, Tang J. Searching for drug synergy in complex dose–response landscapes using an interaction potency model. Computational and structural biotechnology journal. 2015;13:504-13.

188. Lattouf H, Kassem L, Jacquemetton J, Choucair A, Poulard C, Trédan O, et al. LKB1 regulates PRMT5 activity in breast cancer. International journal of cancer. 2019;144(3):595-606.

189. Qi H, Shi X, Yu M, Liu B, Liu M, Song S, et al. Sirtuin 7–mediated deacetylation of WD repeat domain 77 (WDR77) suppresses cancer cell growth by reducing WDR77/PRMT5 transmethylase complex activity. Journal of Biological Chemistry. 2018;293(46):17769-79.

190. Bowden AR, Morales-Juarez DA, Sczaniecka-Clift M, Agudo MM, Lukashchuk N, Thomas JC, et al. Parallel CRISPR-Cas9 screens clarify impacts of p53 on screen performance. Elife. 2020;9:e55325.